Chapter 3

POSSIBLE SOLUTIONS TO THE RIDE COMFORT VS. HANDLING COMPROMISE

Possible concepts for the improvement or elimination of the ride comfort *vs.* handling compromise are investigated in this chapter. Current literature is reviewed, firstly to determine possible hardware concepts for controllable suspension systems and secondly to obtain a global view of the technical requirements involved in the development and implementation of control methodologies. Fully active suspension systems are not considered mainly due to their large power requirements, especially when applied to heavy off-road vehicles. For this reason, the literature review is therefore not concerned with fully active suspension systems in particular, but instead focuses on semi-active and adaptive systems where spring and damper characteristics can be changed either continuously or switched between different discrete characteristics. Some active suspension concepts and control methods are however discussed, as many of these might be adapted to semi-active suspension systems. In some cases it might be possible to control a semi-active damper with the same strategy as a fully active suspension system, but it will only dissipate energy as no energy can be supplied. The damper will therefore be switched to the low damping state when energy supply is demanded by the control system. Active suspension systems dissipate energy for a large amount of the time in any case and semi-active dampers can therefore often approach the results obtainable with fully active systems.

After briefly discussing published literature on advanced suspension systems, this chapter deals more thoroughly with the subjects of semi-active dampers, semi-active springs and active suspension systems, followed by control techniques and algorithms. The chapter closes with a proposed controllable suspension solution to the ride comfort *vs.* handling compromise.

3.1 Published literature surveys on controllable suspension systems

Six published literature surveys concerning advanced suspension systems were found. Although these surveys do not provide sufficient detail on each topic to be really useful for the purposes of the current study, they provide a valuable source of references and a general overview on the specific subject.

Tomizuka and Hedrick (1995) discuss advanced control methods for automotive applications in general and include a paragraph on suspension systems. Various control methods are mentioned for fully active systems as well as semi-active dampers. No mention is made of the existence or control of controllable spring systems.

Sharp and Crolla (1987) discuss suspension system design in general and include aspects such as road surfaces, tyres, vehicle models and performance criteria. Passive, active, semi-active and slow active suspension systems are also included in the survey. Mention is made of slow active (3 Hz bandwidth) controllable pneumatic and hydropneumatic systems.

Active suspensions for ground transport vehicles are reviewed by **Hedrick and Wormley (1975)**. The article does not include semi-active suspension systems and no mention is made of semi-active or variable springs.

The application of neural networks and fuzzy logic to vehicle systems is reviewed by **Ghazi Zadeh, Fahim and El-Gindy (1997).** An introduction to neural networks and fuzzy logic is given. The techniques have been applied to active and semi-active suspension systems by various authors.

Elbeheiry *et. al.* (1995b) give a classified bibliography of advanced ground vehicle suspension systems. A reference list of 71 papers concerned with semi-active suspensions and 58 papers concerned with adaptive, actively damped and load-levelling suspensions is given but not discussed.

Applications of optimal control techniques to the design of active suspension systems are surveyed by **Hrovat (1997).** The main emphasis of the survey is on Linear Quadratic Optimal (LQO) control and active suspension systems, but related subjects such as semi-active suspensions and related control topics are also discussed. Some 256 papers are included in the list of references.

3.2 Controllable suspension system hardware

Vehicle suspension system configurations vary over a wide spectrum. The most important variations on the theme will now be discussed.

3.2.1 Semi-active dampers

Semi-active dampers vary from two-state (on/off) to continuously variable. Both linear and non-linear damper characteristics are considered. The majority of semi-active dampers are based on either magneto-rheological (MR) fluids or hydraulic dampers with controllable valves.

3.2.1.1 Magneto-Rheological (MR) fluids

A Magneto-rheological (MR) fluid is used as the damping medium inside a hydraulic damper and replaces the conventional damper oil. A MR fluid is a dense suspension of micrometer-sized magnetisable particles in a carrier fluid that solidify to a pasty consistency in the presence of a magnetic field (**Lord Corporation, 2005; Ouellette, 2005**). When the magnetic field is removed the fluid returns to its liquid state. Altering the strength of the applied magnetic field will proportionally control the consistency or yield strength of the fluid and therefore the pressure required to force the fluid through a magnetized orifice. MR fluids offer a very fast response time (order of 10 milliseconds) and have been commercially applied in continuously variable semi-active dampers (see

Lord Corporation 2005 for a description of MagneRide as fitted to some General Motors products).

Researchers at the Advanced Vehicle Dynamics Laboratory at Virginia Polytechnic Institute and State University used controllable MR dampers to control the roll dynamics of a Ford Expedition SUV. Results of vehicle tests indicated that a velocity based skyhook control, augmented with steering wheel feedback, outperformed the passive stock dampers (**Simon, 2001**).

3.2.1.2 Hydraulic bypass system

Semi-active dampers based on the by-pass principle use a hydraulic valve (mostly electrically operated) in parallel with a conventional damper orifice and valve assembly. A two-stage (open-closed) valve is indicated in Figure 3.1. If the bypass valve is closed, all the flow goes through the conventional damper orifice and valve assembly, giving high damping or the "on" characteristic. If the bypass valve is open, most of the flow will pass through the bypass valve due to the lower flow resistance. This results in the low damping or "off" characteristic. During valve switching some transient response will result between the "on" and "off" characteristics. The bypass valve can have several discrete stages, or it can be a servo valve giving continuously variable damping characteristics.

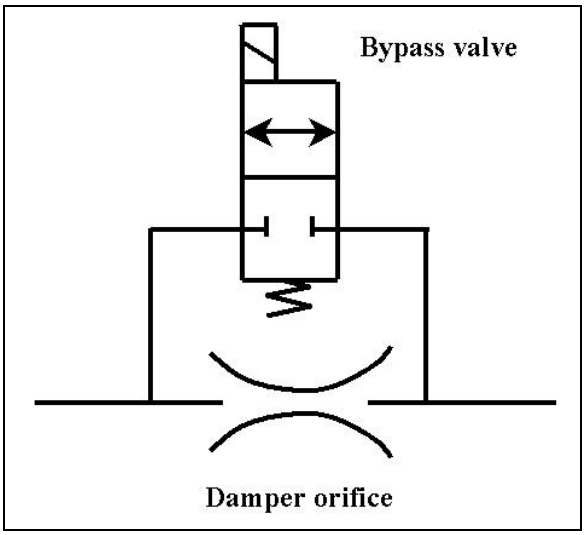

Figure 3.1 - Hydraulic two-state semi-active damper with bypass valve

The choice of valve is based on the pressure drop and flow rate characteristic, as well as the required response time.

Examples of two-state semi-active dampers, using the bypass valve principle, are discussed by **Nell (1993)** and **Nell and Steyn (1994)**. A picture of their first prototype can be seen in Figure 3.2 with the bypass valve indicated. This damper was designed for a maximum flow rate of 1000 l/min, a static wheel load of 3 ton and a response time in the region of 50 milliseconds. The largest semi-active damper for a wheeled vehicle, developed by **Els and Holman (1999), i**s indicated in Figure 3.3. This damper has a maximum damping torque of 150 kN.m and was used on a 46-ton 6x6 vehicle. These dampers are all applied to off-road military vehicles.

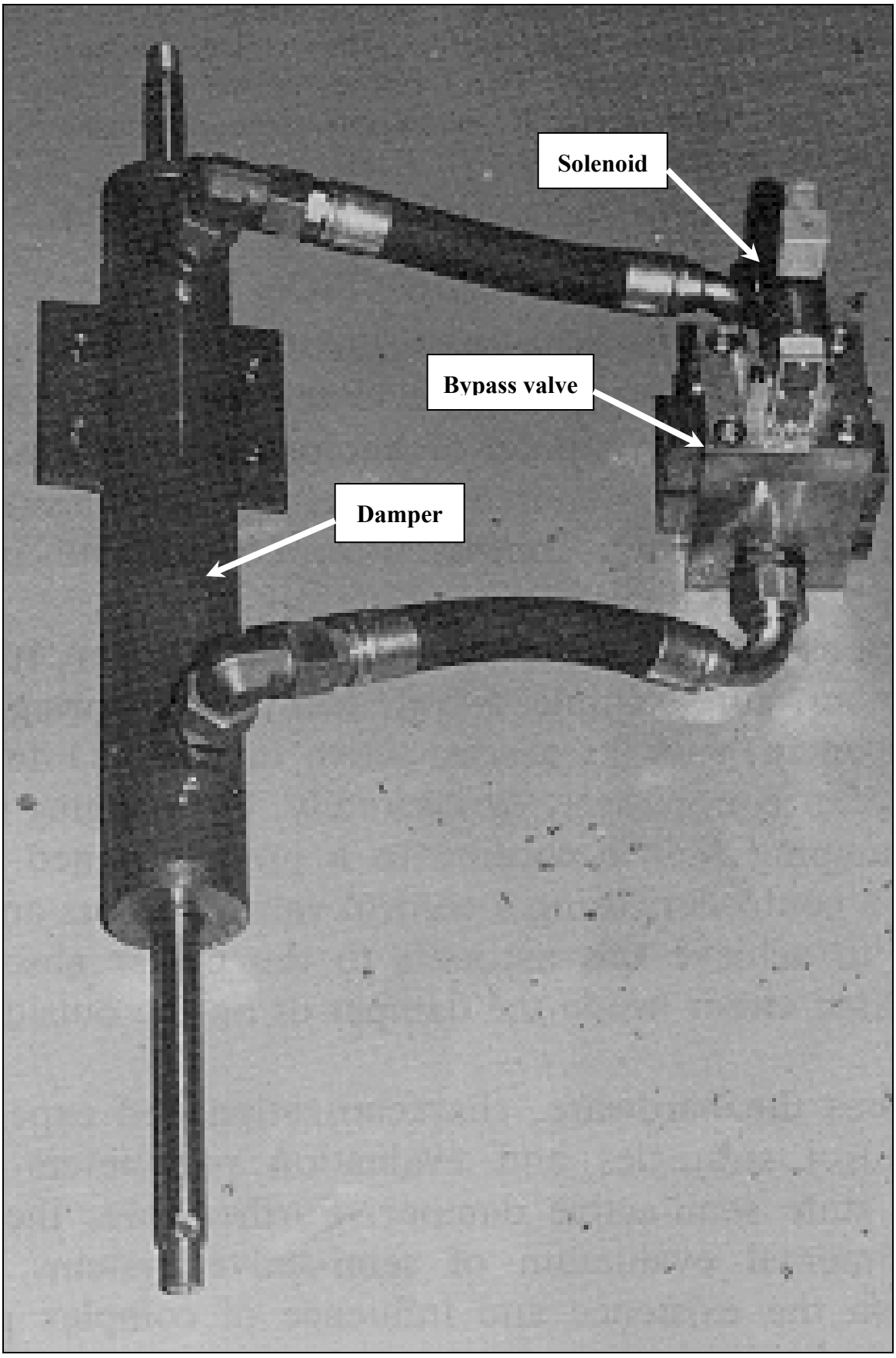

Figure 3.2 – Semi-active damper developed by **Nell (1993)**

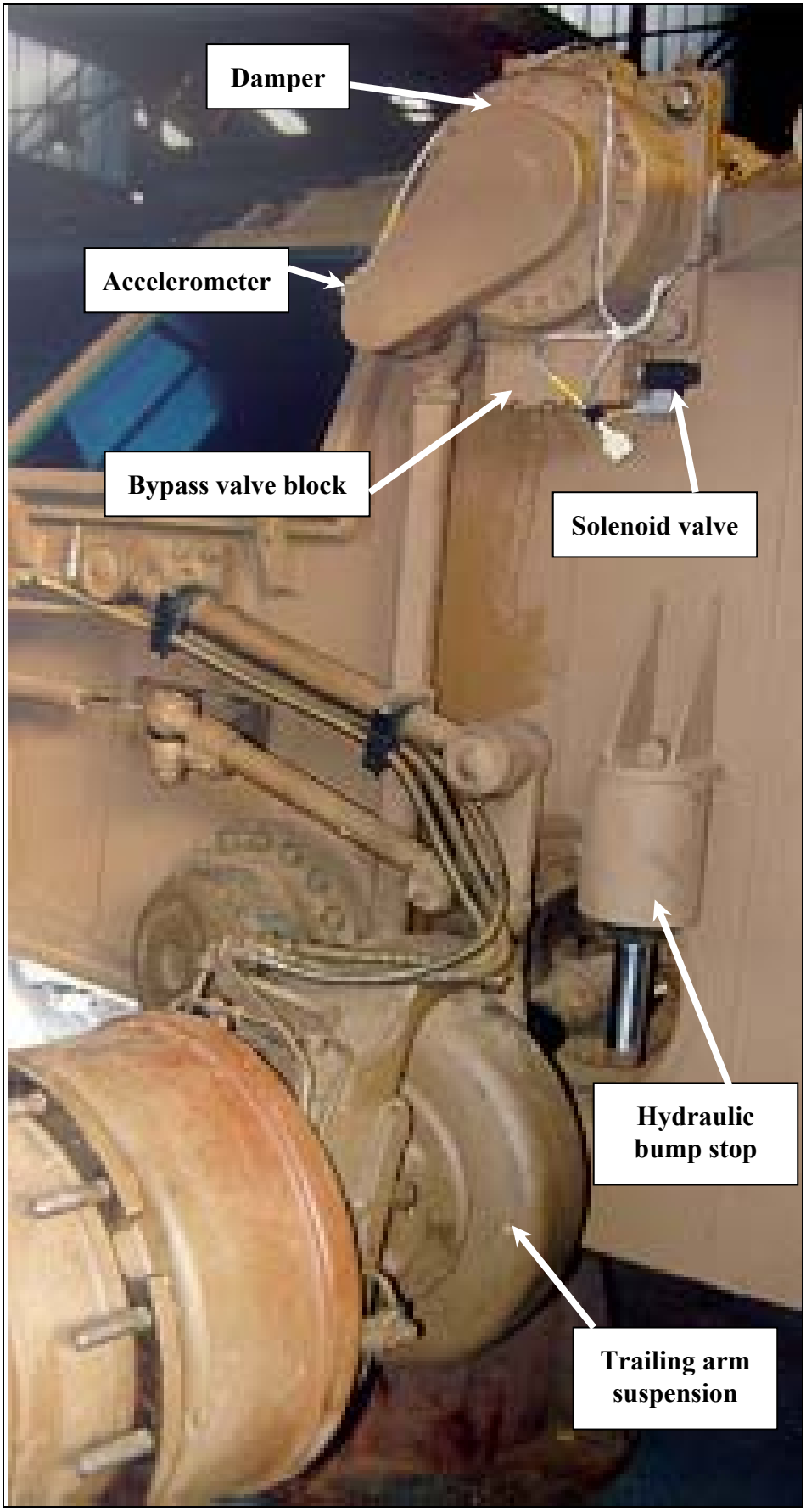

Figure 3.3 - Semi-active rotary damper developed by **Els and Holman (1999)**

3.2.2 Semi-active springs

Semi-active springs are based on either air or hydropneumatic springs that are mostly non-linear due to their operating principles. Hydropneumatic and air springs frequently incorporate some kind of slow active ride height correcting device. Cases also exist where an air spring is combined with a normal passive coil spring.

3.2.2.1 Air springs

Decker, Schramm and Kallenbach (1988) describe a prototype adjustable air spring developed by BOSCH, where the spring characteristic can be changed between several values by fast (25 milliseconds) switching of different air volumes. The adjustable spring is used in conjunction with a fast (4 milliseconds) semi-active damper. Very limited simulation results are included. A closed loop control strategy, of which no details are provided, is used to switch both the spring and damper during simulation. An improvement potential of 36% in ride comfort is obtainable from simulation results. The skyhook control strategy as proposed by Karnopp is also investigated although no further details are presented. No experimental work concerning evaluation of control strategies is presented.

An industrialised version of a semi-active suspension developed by Armstrong is discussed by **Hine and Pearce (1988).** A two or three state adjustable damper is combined with an air or oleo-pneumatic spring that is said to offer both height and spring rate control. It is not clear how the spring rate is changed but it appears as if the spring rate changes because of the ride height adjustment. The oleo-pneumatic damper can be pressurised to a maximum pressure of 200 bar (20 MPa) supplied by an oil pump. The unit is fitted with an external reservoir. The control strategy can be separated into five components namely ride, handling, acceleration, deceleration (dive), ride frequency control and vehicle levelling (if required). The system is commercially applied to the 1986 GM Corvette (5.7 litre) and Ford Granada 2.8 Ghia.

Pollard (1983) describes a fully active air actuator fitted to a railway couch. Where most conventional air suspensions have an auxiliary reservoir to provide the desirable spring and damping characteristics, the air pump actuator replaces the fixed volume reservoir with one of continuously variable volume. An electric motor is attached to the diaphragm via a nut and a lead screw. Operating the lead screw can change the volume. A prototype has been tested with good success and power consumption is found to be low.

A performance air suspension developed by Bridgestone/Firestone is described by **Alexander (2004a)**. The system is cockpit adjustable by the driver. Ride height can be lowered to improve handling or increased to improve ground clearance. Spring rate may also be reduced to improve isolation or increased for handling. The spring rate can be changed either with, or independent of height. Roll stiffness distribution between front and rear can seemingly also be altered.

The suspension system used on the 1986 model Toyota Soarer is described by **Hirose *et. al.* (1988)**. This system changes both spring and damper characteristics using direct current electric motors. The air spring uses main and supplementary air chambers connected by a disc valve to change the gas volume and therefore the spring characteristic. Height control is also implemented for which air pressure is supplied by a

compressor. System response time is 70 milliseconds. The spring and damper rates are changed simultaneously by a single electric motor. The four struts on the vehicle are also controlled together. Vehicle speed, throttle position, steering angle, height and other factors related to vehicle attitude are used to determine the suspension state.

An Electronic Controlled Suspension (ECS) as fitted to the 1984 Mitsubishi Galant is discussed by **Mizuguchi *et. al.* (1984)**. A two-stage spring is constructed using an air spring in parallel with a conventional metal coil spring. The air spring consists of two chambers connected by a valve. The valve is closed to activate the stiff spring rate. Vehicle speed, steering wheel speed, sprung mass acceleration, throttle speed and suspension stroke are used as control parameters. A methodology to determine the spring and damper rate for the two-state suspension systems is described. The suspension is either set to "off" (soft spring and soft damper) or "on" (hard spring and damper). The normal suspension state is soft for good ride comfort but is switched to hard for high vehicle speeds or during handling manoeuvres.

Karnopp and Margolis (1984) discuss the effects of a change in spring and damper rates on the transfer function of a single degree of freedom suspension system. It is said that changing the damping alone is not a very good way of stiffening or softening a suspension system. A system with two air volumes separated by control valves is proposed that enables both the spring and damper rates to be adjusted. Air can also be slowly added to or subtracted from the air volume to enable ride height adjustment. The proposed system can be adaptively controlled using brake and steering inputs as well as angular acceleration. Manual overrides can be included to suit personal preference.

Wallentowitz and Holdman (1997) give a frequency domain analysis of the effect of spring and damper constants on the transfer function of the suspension. It is concluded that two spring stages are sufficient to overcome the compromise associated with passive systems. The two-stage spring can be realised in hardware by using two air springs connected by a pipe and orifice arrangement. The orifice is designed so that the second air spring is effectively closed off at suspension frequencies higher than 5 Hz. A valve in series with the orifice can be closed to achieve a high spring rate during handling manoeuvres. No hardware seems to be available. The study is theoretical only and includes a suggestion for a possible control strategy based on the frequency response of a quarter car system.

3.2.2.2 Hydropneumatic springs

Citroën has been applying hydropneumatic suspension systems to their passenger cars for many years. **Nastasić and Jahn (2005)** describe the suspension systems fitted to different models in detail. On the XM model, both the front and rear suspensions consist of three spheres (bladder accumulators) and four dampers. The system can be switched to a low spring and low damping state (3 spheres and 4 dampers) or high spring and high damping rate (2 spheres and 2 dampers). The system reacts in less than 50 milliseconds and is computer controlled. Inputs to the controller include the angle and angular speed of the steering wheel, speed of movement of the accelerator pedal, braking effort, rotation of the front anti-rollbar and vehicle speed. A switch on the centre console enables the driver to permanently select the high spring and damper state. Another system fitted to Citroën's Activa 2 research prototype car is described by **Birch, Yamaguchi and Demmler (1990)**. The system is an upgrade of that used for the XM and ads an active anti-roll system that

can double the roll stiffness almost instantly to counter body roll. Roll control is implemented by adding a fourth sphere and a roll control strategy. Roll is reduced when this fourth sphere is disconnected from the system. The system absorbs less than 0.375 kW through a fast corner and double that amount for violent emergency avoidance action.

One of the oldest references found for a switchable hydropneumatic spring system is that described by **Eberle and Steele (1975)**. Their system is indicated in Figure 3.4 and was intended as an operator controlled system. The operator could choose the spring constant to suit the vehicle speed and the type of terrain by opening or closing two valves. Four discrete characteristics are possible namely rigid, firm, medium and soft depending on valves 1 and 2. The placing of the damping units in the branches to the accumulators permits matching of the damping to the selected spring constant.

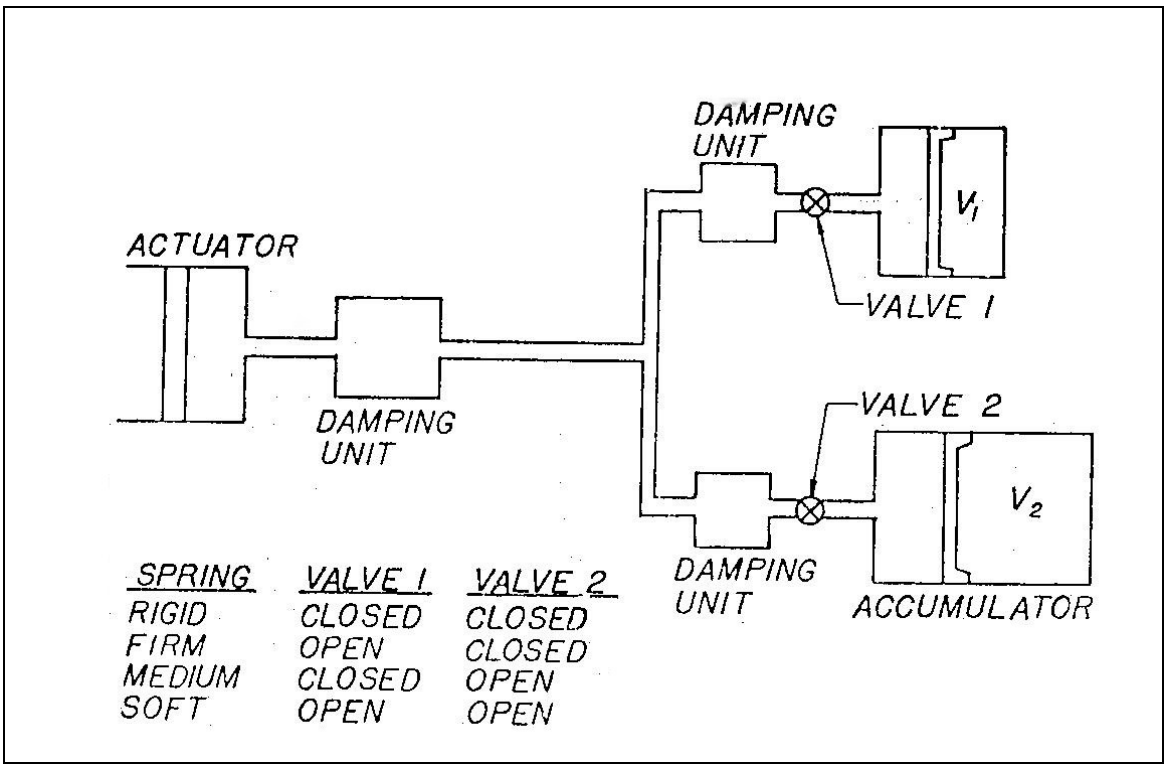

Figure 3.4 – Operator controlled variable spring as proposed by **Eberle and Steele (1975)**

3.2.2.3 Other semi-active spring concepts

Semi-active springs may be realized using other methods *e.g.*:

- Metal springs in combination with air or hydropneumatic springs
- Accumulators with adjustable volume *e.g.* lead screw connected to an electric motor
- Compressible fluid suspension systems
- Piezo-electric actuators
- Smart materials

These ideas were not given further consideration for the purposes of the present study.

3.2.3 Active suspension systems

Active suspension systems have been applied to off-road vehicles with limited success. Apart from the high cost, power requirements and bandwidth restrictions seem to be the major obstacles. Both electric and hydraulic actuators have been used.

3.2.3.1 Electric actuators

The design of an electromagnetic linear actuator for active suspension application is described by **Weeks *et. al.* (1999)** and **Buckner *et. al.* (2000)**. The actuator consists of an electric motor driving a rack-and-pinion. The actuator was designed to be used in parallel with an air spring that carries the static wheel load. The actuator was designed for retrofit to a high mobility multi-purpose wheeled vehicle (HMMWV). It produces a maximum force of 8896 N, a stroke of 127 mm and a maximum velocity if 1 m/s. The performance of the actuator was evaluated on a quarter-car test rig and found to meet and even exceed the design specifications. Very reasonable peak power requirements of about 12 kW were recorded during some rig tests.

Bose Corporation developed a prototype linear magnetic actuator that was installed at each wheel of a vehicle in a modified McPherson strut configuration (**Anon, 2005b**). A belt-driven alternator and a 12 Volt battery power the system. It is said to improve both comfort and handling and eliminates the need for anti-rollbars. No quantification of performance improvements or power requirements is given.

3.2.3.2 Hydraulic actuators

Lotus was one of the pioneers of hydraulic fully-active suspension systems. A concise summary of the development of the Lotus active suspension system is given by **Wright (2001)**. The technology was initially developed for use in Formula 1 and quickly banned. It was used later in various prototype applications to passenger cars as well as military vehicles (both wheeled and tracked).

Scientists in the Tactical Vehicle Section of the Canadian Army built an active suspension prototype based on the Iltis truck (**Anon, 2005a**). The test vehicle has been in operation since 1995 at the Royal Military College at Kingston, Ontario for it's training and testing programmes. The system uses Moog-Lotus servo-controlled actuators with a 20 Hz system response. Power requirements are low (5-10 HP) over moderate cross-country terrain. Vertical acceleration of the driver is reduced by 10% over discrete bumps while slalom speed is increased by 20%. The driver is said to feel increased control with reduced steering effort while rollover is less likely to occur.

Researchers at the University of California (Berkeley) have been involved in research on the control of fully active, hydraulic suspension systems for many years (**Hedrick and Wormley, 1975 and Hedrick et.al. 1994**).

3.3 Control techniques and algorithms

It seems that the possibilities concerning control strategies are limitless although the majority of papers use the "Skyhook" strategy proposed by **Karnopp *et. al.* (1974)** that was derived using Linear Quadratic Optimal (LQO) control theory. Other methods include neural networks, fuzzy logic, H_∞ and PD control. Preview control is often considered.

Control strategies can broadly be classified in two main categories namely **input driven** and **reaction driven** strategies. The control parameters for **input driven strategies** usually consist of parameters such as vehicle speed, steering angle and brake pressure. These strategies therefore react on inputs from the driver or vehicle before the dynamics of the vehicle changes. **Reaction driven strategies** react to the vehicle's dynamic reaction due to terrain roughness or driver input. Take as an example a vehicle driving in a straight line, when the driver gives a sudden step input on the steering wheel in order to avoid an accident. An **input driven** strategy might use steering angle as input and switch the dampers to the high damping state as soon as the steering angle or steering velocity exceeds a predetermined level, while a **reaction driven** strategy might use lateral acceleration or yaw rate as input and the dampers will only be switched to the high damping state after the tyres developed enough side force so that the vehicle will turn. In this instance it can be seen that the input driven strategy will respond earlier.

Further discrimination must also be made between the terms **adaptive**, **semi-active** and **active** suspension systems. These terms, as they are used in this study, are defined in Table 1.1. **Adaptive control** on the other hand is used for systems where the controller gains are changed (adapted) according to certain measured parameters i.e. wheel acceleration as a measure of terrain roughness.

3.3.1 Combination of input and reaction driven strategies

Hine and Pearce (1988) discuss a strategy for obtaining optimum ride comfort and handling control. The control strategy is separated into six components namely ride, handling, acceleration, deceleration (dive) as well as ride frequency control and vehicle levelling (if required). **Ride control** is initiated by the relative wheel to body displacement in combination with the vehicle speed. For any particular speed, displacement limits are established, outside of which the damper is switched to a higher level. This enables maximum use of available suspension working space while keeping the damper in the soft state for most of the time. The steering sensor together with the speed sensor is used to determine when dampers should be switched to a higher state to improve **handling**. Dampers are also switched to a higher state during **acceleration** and **deceleration** caused by throttle and brake applications. **Levelling** is effected by measurement of relative suspension displacement and compensates for mass and aerodynamic load changes. It is said that significant improvements in ride comfort have been achieved while handling is also improved. The system is commercialised and put into production on the GM Corvette (1986) and Ford Granada 2.8 Ghia.

The hydractive suspension introduced by Citroën in its XM passenger car, and featured in various other Citroën models, is described by **Nastasić and Jahn (2005)**. The angle and angular rate of the steering wheel are used together with the car's speed and the suspension is switched to firm whenever certain threshold values are exceeded to enable

handling control. The speed of movement of the throttle, as well as braking effort is measured and the suspension switched to the firm state when thresholds are exceeded to enable **acceleration** and **braking** control. **Roll** and **yaw** control is achieved by measuring the rotation angle of the front anti-rollbar. Adoption of this control strategy ensures that the system always works in advance of the dynamic reaction of the car (*i.e.* input driven control). This anticipation is said to be of particular advantage during fast driving on winding roads where it reduces body movement and greatly enhances road holding and handling, providing the driver with a unique sensation of control. The system is taken one step further in the Activa 2 concept car (**Birch *et. al.*, 1990)** by the introduction of an additional roll control program.

Mizuguchi *et. al.* (1984) discuss the control system fitted to the Mitsubishi Galant. Control inputs include steering wheel speed, lateral, longitudinal and vertical acceleration, vehicle speed and suspension stroke. Test results indicate a significant improvement in ride comfort, handling and stability. A very similar system is fitted to the Toyota Soarer (**Hirose *et. al.* 1988)**. A driver's selector switch is also included. The system includes control for anti-dive, anti-roll, anti-squat, anti-bump, response to speed and response to rough road. Very good ride comfort and stability are achieved while vehicle attitude changes are remarkably reduced.

Wallentowitz and Holdman (1997) investigate the effect of different spring and damper characteristics. They suggest that vehicle velocity and steering wheel angle be used to switch the suspension to the hard characteristics during ambitious driving situations. Otherwise damper software analyses the excitation frequency and load based on a quarter car model and switches the damper accordingly. No validation is given.

Hennecke and Zieglmeier (1988) discuss a three-state variable damping system fitted to the BMW 635 CSi. Sensors used include steering wheel angle, loading condition, travelling speed, brake pressure, throttle position and vertical body acceleration.

Poyser (1987) describes a system designed by Armstrong incorporating a ride levelling hydropneumatic spring and a 3-stage controllable damper. Steering wheel angle, vehicle speed, body roll angle, and suspension travel are used to switch the dampers. For ride comfort control the dampers are switched to the intermediate and high states when certain pre-set limits (vehicle speed dependant) are reached.

Pinkos *et. al.* (1993) investigates the feasibility of a continuously variable semi-active Electro-Rheological Magnetic (ERM) fluid damper through mathematical analysis, computer simulation and actual vehicle testing. The control strategy employed is based on adaptive gain control and vector summation of weighted sensor measurements. Each corner of the vehicle is treated independently, but the total control output is calculated from information on vehicle behaviour. Separate calculations are produced for ride comfort, roll, dive, squat, pitch, heave and yaw. The vector summation of these calculations produces an output signal to each damper. Algorithm calculations are prioritised based on safety related vehicle behaviour i.e. any calculations related to vehicle handling are completed first. Thirteen sensors are used namely vehicle speed, braking and acceleration, vertical accelerometers on the sprung mass, angular position between the body and the wheel, lateral acceleration and absolute steering wheel position. Both analogue (hardware) and digital (software) filters are employed. Quarter car and half

car models are examined while full-scale vehicle tests are also performed. Good theoretical and experimental results are obtained.

3.3.2 Linear optimal, skyhook and on-off control

These three control methods are discussed together because skyhook control was derived using linear optimal control theory and is used for a continuously variable damper. The on-off strategy is a simplification of the skyhook strategy, adapted for a two stage (on-off) semi-active damper.

Krasnicki (1981) investigates the "skyhook" damping principle applied to a two-stage (on-off) semi-active damper.

Karnopp (1990) points out that optimal control systems generally require the feedback of all state variables while passive vibration control elements generate forces related to only a subset of the system state variables. A quarter car model is used for simulation (four state variables). Modern control theory suggests that the suspension force should consist of a weighted sum of any four suitable state variables such as positions and velocities. An optimum linear active system can thus be designed using Linear Quadratic Gaussian control theory. According to the author, several other researchers report very similar results. These control methods result in significantly better control of the body (sprung mass) natural frequency. Partial state feedback is also shown to offer nearly the same results as full state feedback. It is concluded that as far as body movement due to terrain inputs is concerned, semi-active systems can approach the performance of fully active systems with state variable feedback. It is however necessary to know the sprung mass absolute velocity in order to apply state variable feedback control. (This cannot easily be measured and might not be practical for vehicle implementation. It might not even be possible to accurately estimate (see **Hedrick *et. al.*, 1994**))

Sharp and Hassan (1987) study two alternative forms of control law. A quarter car model is used for simulation. The semi-active damper is assumed to be capable of producing a force that is a linear combination of state variables as long as such a force opposes the relative motion of the damper. Otherwise it is set to produce no force. The control laws are derived using stochastic linear optimal control theory. The constants used in the control laws are obtained by minimising a performance index using two weighting parameters, one for dynamic tyre load variations and the other for suspension working space. The results given are for only one road surface roughness and one vehicle speed but cover a range of suspension working space. It is concluded that semi-active damping can improve ride comfort significantly but that the constants in the control laws must be adapted according to the terrain roughness (or available suspension working space). It is suggested that this adaptation of the coefficients can be achieved by keeping a running average of the relative suspension displacement or monitoring the number of bump stop contacts. The maximum use must be made of the available suspension travel while hitting the bump stops must be avoided.

Margolis (1982a) uses a vehicle model that includes the heave (vertical) and pitching motions of a vehicle. Controllers are designed for the fully active case and then modified to be semi-active. Two control strategies are investigated namely the familiar "skyhook" control (feedback of body absolute velocity and relative damper velocity) as well as complete state variable feedback (SVFB). It is concluded that SVFB and "skyhook"

control both give excellent results compared to that of the passive system. Results are not sufficiently strong in favour of SVFB to justify the increased complexity of measuring all four state variables.

Margolis (1982b) presents the expected response of a simple vehicle (single degree of freedom) fitted with an active and semi-active suspension when the control system is presented with non-ideal feedback information. The control strategies evaluated need feedback of the absolute velocity of the sprung mass. Determination of this velocity is quite difficult in a realistic environment where the vehicle has many degrees of freedom, for example roll, pitch, yaw and heave. This problem is intensified because all measurements are corrupted by noise. The absolute velocity can be determined by integrating an accelerometer signal by analog or digital means. It is however very difficult to produce a drift free pure integrator. A low pass filter is used instead of a pure integrator with a break frequency much lower than the frequency of interest. This is also very difficult to realise because huge capacitor and resistor values are needed. Furthermore the long time constants involved give rise to DC drift. The DC drift is exaggerated by the fact that an accelerometer that can measure at the very low frequencies is also sensitive to vehicle orientation (for example driving up a long incline). This necessitates the inclusion of a high pass filter to eliminate the DC drift or steady state bias. The high pass filter suffers from the same drawback of an extremely low break frequency. It is indicated that the provision of acceleration feedback can provide some compensation for the non-ideal velocity measurement. Significant improvements over the passive system are still achieved although degraded by non-ideal velocity measurements.

Nell and Steyn (1994) discuss the experimental evaluation of a two-state semi-active damper for off-road vehicles. Three control strategies available from literature are tested. The first strategy used is the on-off strategy proposed by Karnopp (see **Rakheja and Sankar, 1985)** that switches the damper according to the sign of the product of absolute body velocity and relative damper velocity. The second strategy uses absolute body acceleration and relative damper velocity. The third strategy proposed by **Rakheja and Sankar (1985)** uses the product of relative damper displacement and relative damper velocity. Unweighted RMS values of body acceleration, relative displacement and velocity, absolute velocity and force indicate that the biggest improvement is achieved using acceleration feedback followed by relative displacement and velocity (Rakheja and Sankar). The on-off strategy proposed by Karnopp returns unsatisfactory results without any significant improvements.

Experimental verification of theoretical work is discussed by **Rajamani and Hedrick (1991)**. A full-scale half-car suspension test rig is used to evaluate semi-active dampers. High bandwidth (10 ms) 12 state semi-active dampers as well as low bandwidth 3-state dampers are used. Conventional on-off, optimal on-off, optimal multi-state control and a robust form of multi-state control are implemented and compared to predicted results. Good correlation between predicted and measured results is achieved. The semi-active suspension is found to behave as well as the best of all passive states at every frequency.

Lizell (1988) describes semi-active damper hardware and software that is tested in the laboratory and on a vehicle. The aim of the control strategy employed is to switch the two-stage damper to the high damping state in the region of the body resonance and wheel hop frequencies, while the soft state is used for all other frequencies. This is said to improve both handling and ride comfort throughout the frequency range. Damping of the

body resonance frequency is controlled using the Karnopp strategy. The wheel hop frequency is controlled by calculating a discrete Fourier transform (DFT) around the wheel hop frequency. The value obtained is compared to a threshold level to determine damper switching. The damper is switched to the low damping state under all other conditions. The absolute body velocity is determined from integrating an acceleration signal after analog low-pass filtering. A digital high pass filter is implemented and drift in the integration process is controlled by "leakage". Preliminary test data is promising.

Ivers and Miller (1989) compare experimental results obtained from a quarter car test rig with simulation data. A semi-active damper with 25 discrete states is used. The control algorithms used are based on the simple analogy of the skyhook damper. Absolute body velocity is determined by pseudo-integrating an acceleration signal. Three cases are investigated namely passive, two stage (on-off) semi-active and continuous (25 stages) semi-active control. Test results confirm the trends indicated by simulation, but there are discrepancies due to the fact that valve response times, time delays in the control system, hysteresis, friction in the test rig and non-linear damper characteristics are ignored in the simulation.

Miller and Nobles (1988) describes the development and testing of a semi-active suspension on an M551 military tank. The article gives a good overview of the development history of controllable suspension systems and presents the basic theory concerned with optimal control, resulting in the skyhook damper and on-off strategy. The on-off strategy is implemented for vehicle trials. The determination of absolute velocity is considered a challenge and is estimated (pseudo integrated) by filtering an accelerometer signal. The valve configuration in the damper is designed so as to eliminate the need to measure relative velocity. The control system therefore only has absolute velocity as input while valve logic takes care of the rest. Vehicle testing is performed on a 10-axis vertical road simulator. Average absorbed power was used as evaluation parameter and indicated a measured performance gain between 13 and 43% depending on vehicle speed.

Miller (1988a) investigates the effect of hardware limitations on an on-off semi-active suspension using a single degree of freedom simulation model and the familiar on-off control strategy. The effects of non-zero off-state damping, valve dynamics and digital filter dynamics (used to determine the absolute velocity) are investigated. Results indicate that the off-state damping ratio should be less than 0.2. Valve response times should be less than 14 milliseconds and sampling time less than 4 milliseconds. Digital filters should have a break frequency of approximately 0.1 Hz and a damping ratio of between 0.3 and 1.0.

Temple and Hoogterp (1992) describe simulation and vehicle test results obtained for the Mobility Technology Test Bed (MTTB) vehicle. The adaptive dampers employ an on-off strategy based on hull and damper dynamics. The damper is turned on only when it will help to reduce the pitch and roll velocities. Whenever the anticipated jounce or rebound damping would tend to increase the hull pitch and roll velocities, the dampers are switched to the low damping state. No further details of the control strategy or implementation thereof are given. Nearly a 1000 mobility and agility tests were conducted on 10 vehicle configurations, all indicating noteworthy improvements in ride comfort, reaction to discrete obstacles, reductions in body roll and reductions in pitching.

Besinger, Cebon and Cole (1991) tests an on-off semi-active damper in a hardware-in-the-loop (HiL) test setup where a quarter car model is solved by computer simulation while the damper force is measured directly in real time from the experimental setup. On-off skyhook control is implemented.

Hrovat and Margolis (1981) describe an experimental heave model of a tracked air cushion vehicle incorporating an on-off semi-active damper. The control is performed using a simple analog circuit with operation amplifiers and NAND gates implementing the on-off strategy. Sinusoidal ground inputs in the range of 2 to 5.5 Hz are used. Results indicate that significant improvements can be realised using semi-active damping compared to passive damping. Absolute and relative damper velocities are obtained by analog differentiation of displacements measured by LVDT's. It is not possible to implement this strategy in a real vehicle application.

Soliman *et. al.* (1996a and 1996b) extend previous work (where linear stochastic optimal control theory was used to formulate a limited state feedback scheme) to include adaptive control based on a gain scheduling approach. Results are determined theoretically and experimentally using a quarter car model and test rig. Two strategies are investigated using RMS wheel acceleration and RMS of the suspension working space (relative displacement) respectively. Road surfaces of varying roughness are generated using Gaussian random distributions and a road roughness number. Based on linear optimal control theory, the absolute displacements and velocities of the wheel and body are still required. A look-up table is used to determine the "optimum" gains for the specific road input conditions as measured by the sensors. Theoretical and experimental results indicate that the scheme based on the RMS vertical acceleration results in the highest improvements in body acceleration, suspension working space and dynamic tyre loads.

Abd El-Tawwab and Crolla (1996) include component limitations in the theoretical and experimental investigation of a three state semi-active damper in a quarter car model and test rig. The ideal actuator force is determined from optimal control theory and involves feedback of absolute displacements and velocities for both the sprung and unsprung mass, each associated with a control gain. The gains are determined using a gradient search method. A random road input and a constant vehicle speed of 20 m/s is used. Results indicate an improvement of between 13 and 17% for sprung mass acceleration and 7 to 8% for dynamic tyre load.

Lieh (1996) studies the application of velocity feedback active suspension systems. No results are presented.

Petek *et. al.* (1995) performs vehicle tests using fast, continuously variable, electro-rheological (ER) dampers. A modified skyhook algorithm is implemented which include roll, pitch and heave motion. Accelerometers and LVDT's are used to determine body acceleration and relative displacement respectively. Accelerations are integrated (to obtain absolute roll, pitch and heave velocities) and relative displacements differentiated to obtain relative velocities. Four gain constants are used to determine the relative importance of roll, pitch and heave motion. Test results indicate significant improvements in ride comfort and stability compared to the standard passive suspension.

3.3.3 Neural networks and Fuzzy logic

An extensive literature survey on the applications of fuzzy logic and neural networks to vehicle systems, including suspension control, is given by **Ghazi Zadeh *et. al.* (1997)**.

Chou *et. al.* (1998) present a new control scheme referred to as the grey-fuzzy control method that consists of two parts namely the grey predictors and the fuzzy logic controller. The system is said to be able to control excessive tyre deflection and improve ride comfort. The Taguchi method is employed to search for the optimal control parameters and the results, obtained by computer simulation of a quarter car model, is said to be satisfactory.

Hashiyama *et. al.* (1995) presents a new method to generate fuzzy controllers through the use of a genetic algorithm (GA). Appropriate combinations of input variables, number of fuzzy rules and parameters for membership functions are determined automatically through the GA operations. A fuzzified version of Karnop's law of suspension control was incorporated as the initial fuzzy rules. These initial rules are not modified by the GA but the GA with a new local improvement mechanism is applied to find additional fuzzy rules for better performance. The performance index is improved but no comparisons are given to the passive suspension performance.

Yoshimura *et. al.* (1997) presents a semi-active suspension controlled by fuzzy reasoning. The input variables to the fuzzy control rules are the suspension travel and its derivative. The aim is to minimise body vertical and roll acceleration at the centre of gravity under the constraints of suspension travel and tyre deflection. A half car simulation model is used. Simulation results show that the proposed system is very effective in improving the vertical and rotary accelerations of the vehicle body as well as tyre deflections.

3.3.4 H_∞ control

Palmeri *et. al.* (1995) describes the application of H_∞ optimal control theory to the design of a fully active suspension system for an experimental Lancia Thema sedan car. The system functions as a Multiple Input Single Output (MISO) regulator with hub acceleration, actuator force and actuator position as inputs. The H_∞ control strategy has been chosen to take advantage of the possibility to design a competitive MISO controller as well as exploit robust disturbance rejection which the H_∞ theory grants. Each corner of the vehicle is modelled as a seventh order state-space model. The H_∞ regulator is a model-based compensator, which means that it contains the system's state-space model that is observed and the control compensates for the error. Vehicle tests on a laboratory test setup indicate that H_∞ performs significantly better at all speeds than the skyhook baseline, especially at low frequencies around the body roll frequency.

3.3.5 Proportional Derivative (PD) control

Esmailzadeh (1979) uses a linear model of a suspension system employing a pneumatic isolator and a three-way servo valve. Simulation is performed on an analogue computer and compared to experimental measurements of a quarter car model. Proportional and derivative feedback control is used.

3.3.6 Preview control

Currently no feasible mass production preview sensors are available for suspension control purposes and even if such sensors become available in the near future, it is doubtful whether they will be of much use on off-road vehicles travelling over rough, vegetation covered and deformable terrain. Preview control is not discussed in depth due to this reason.

Soliman and Crolla (1996b) investigate the use of preview or "look-ahead" information for semi-active damper systems using a quarter car theoretical model. The system is said to achieve the same performance as a fully active system without preview.

Youn (1991) derives a preview control strategy using optimal control theory with jerk included in the performance index. Simulation is performed using a two-degree of freedom quarter car model. The proposed control method is said to improve handling and ride comfort simultaneously. The jerk controller can determine the damping coefficient or spring stiffness of the semi-active system.

Crolla and Abdel-Hady (1991) investigates the effect of wheelbase preview (i.e. that the rear suspension input is just a delayed version of the input at the front) on the performance of semi-active and fully active suspension systems. A continuous semi-active damper is used which is modelled as having a maximum and minimum damping constant. Damper response time is modelled as a first order time lag. A simple full vehicle model with vertical, pitch and roll degrees of freedom is used for simulation. The control law is based on full state feedback. The conclusion is drawn that semi-active systems with wheelbase preview can perform better than fully active systems without wheelbase preview.

3.3.7 Model following

Pollard (1983) adopts a strategy first developed for a maglev train, to control the active suspension of a normal train. The control system consists of two complementary parts. At low frequencies the vehicle must follow the tracks and displacements must be maintained within certain limits. The actuator is then controlled so as to minimise relative displacements over the secondary suspension. At high frequencies, the acceleration of the body is fed back to the control system and the system tries to minimise acceleration. The control system is said to model the ideal suspension while the actuator tries to correct the error. The bounce and pitch modes of the body are controlled separately.

3.3.8 Frequency domain analysis

Hamilton (1985) proposes to use a Discrete Fourier Transform (DFT) to calculate the magnitude of vibration levels in different frequency bands in order to control body resonances.

Kojima *et. al.* (1991) implement a frequency detection method that changes the dampers to high damping when suspension inputs are predominantly in the low frequency range. Low damping is used for suspension movements that are predominantly in the high frequency range. It is found that the low frequency region is accompanied by large suspension stroke variation and large variations in distance between the vehicle body and

ground while damping force variation ratio and bounce down acceleration is small. The magnitude of these parameters is reversed in the high frequency region, enabling discrimination between frequency ranges on the basis of the amplitude of these parameters. A relative position sensor measures suspension movement and piezo-electric ceramic sensor is used to detect the damping force variation ratio. The suspension movement sensor does not have an absolute neutral position signal but determines the neutral position by compensation with learning control. Additional sensors, for example vehicle speed, steering, brake application and throttle angle are also used.

3.3.9 "Relative" control

Rakheja and Sankar (1985) and **Alanoly and Sankar (1987)** present an "original" control strategy employing only directly measurable variables in vehicle applications. A continuously modulated damper is controlled using only relative damper displacement and relative velocity as feedback signals. A condition function based on the sign of the product of relative velocity and relative displacement determines whether the high (on) or low (off) damping state have to be used. The origin of, or reasoning behind, this strategy appears to be determined from a thought experiment. There is very little variation between this scheme and the "skyhook" damping algorithm. Performance approaching that of a fully active suspension system is achieved from simulation results on a single degree of freedom system. This system avoids the problem of measuring the sprung mass absolute velocity, that is said to be a near impossible task, and has never been implemented on a vehicle (at the time of writing). The same strategy is proposed by **Jolly and Miller (1989)** and is termed "relative control". It is developed by means of intuitive reasoning. Relative control is found to perform better than the passive system but slightly worse than skyhook control. At high frequencies, relative control gives results very similar to skyhook damping, but at low frequencies, relative control performs worse than the passive system. It is likely that relative control will provide better performance in applications where most of the disturbance energy is transmitted at higher frequencies.

3.3.10 Traditional controller design on the s-plane

Hall and Gill (1987) depart from the approach of using optimal control theory. Instead they try to relate the position of the closed loop poles of the system on the s-plane to the poles of a well-designed "skyhook" system. Not much success is achieved with this method. The authors then revert to scanning of the s-plane in order to find optimum pole locations. It is concluded that, although the transmissibility indicates significant improvements, the phase relationships need to be taken into account.

3.3.11 Minimum product (MP) strategy

Nell and Steyn (1998) develop an alternative control strategy (called the minimum product or MP strategy) for semi-active dampers on off-road vehicles that takes into account the pitch and roll degrees of freedom. The strategy selects a combination of damper settings (all dampers on vehicle taken into account) that minimises roll and/or pitch acceleration. Both simulation and experimental results, that indicate that this strategy performs better over off-road terrain in comparison with both the passive and on-off skyhook systems, are given. The damper state that will give the lowest acceleration in the present direction of movement, or the highest acceleration in the opposite direction, is selected. Input variables to the control system are relative velocity of each damper as well

as the roll and pitch accelerations of the vehicle body (calculated from three vertical acceleration measurements by assuming that the vehicle body is rigid).

3.3.12 Roll and pitch velocity

Salemka and Beck (1975) formulate and test a strategy based on the roll and pitch velocities of the vehicle body. Terrain parameters, for example the relative amount of roll and pitch velocities and vertical acceleration generated by the terrain, severely influence the success of any control strategy.

3.3.13 Resistance control

Fodor and Redfield (1996) implement resistance control semi-active damping on a 1/30th-scale quarter car test rig. Test results are compared to simulation results and good correlation is found.

3.3.14 Mechanical control

Speckhart and Harrison (1968) perform an analytical and experimental investigation of a hydraulic damper having internal inertially controlled valves. The valve is purely mechanical and no “control system” is used. The system claims to improve ride comfort by reducing jerk. System performance is evaluated by simulation and laboratory testing of a two degree of freedom system.

3.3.15 Steepest gradient method

Tseng and Hedrick (1994) investigate the optimal semi-active suspension that will minimise a deterministic quadratic performance index. The optimal control law is a time-varying solution that involves three related Ricatti equations. The constant Ricatti equation (so-called “clipped optimal” solution) is not optimal. They develop a new semi-active algorithm called the “steepest gradient” algorithm. Performance is shown to be superior to that of the “clipped optimal” solution.

3.3.16 Use of estimators and observers

Hedrick *et. al.* (1994) propose a new method for designing observers for automotive suspensions. The methodology guarantees exponentially convergent state estimation using easily accessible and inexpensive measurements. It is also demonstrated that the sprung mass absolute velocity cannot be estimated in an exponentially stable manner with such measurements. The estimation error is merely bounded and would not converge to zero. Results are verified on the Berkely Active Suspension Test Rig with excellent results. The sprung mass velocity is, however, not estimated, but determined by integrating the body acceleration after passing it through a high pass filter.

3.3.17 Control of handling

No literature proposing any control strategies for specifically improving vehicle handling was found. In cases where handling is considered, it seems that the authors opted for the stiffest possible setting when encountering handling manoeuvres.

3.3.18 Control of rollover

A genetic algorithm predictor for vehicle rollover was developed by **Trent and Greene (2002)**. They modelled a 1997 model Jeep Cherokee SUV. Their preliminary results indicate rollover prediction of 400 milliseconds in advance of the actual event. They suggest that this early warning could be used to prevent rollover by activating other vehicle systems such as differential braking or suspension control.

3.3.19 Ride height adjustment

A decrease in ride height is generally beneficial for handling as the centre of gravity height will be decreased. This improves the static stability factor (SSF) and should therefore reduce the rollover propensity of the vehicle. Care should however be taken not to change the suspension geometry in a manner that will adversely affect the handling. On the other hand an increase in ride height might benefit ride comfort over rough terrain because suspension travel in bump will be increased, thereby reducing the number of bump-stop contacts. In many vehicles, the ability to maintain constant ride height independent of load is a major advantage, without necessarily adding the capability to increase or decrease ride height. The success of ride height control can be judged by it's numerous commercial applications.

3.3.20 Comparison of semi-active control strategies for ride comfort improvement

Voigt (2006) studied several control strategies proposed in literature during the last 20 years with the objective of improving ride comfort. The study focussed on on-off control ideas. The aim of the study was to develop and implement an appropriate ride comfort control strategy for a 4-state semi-active hydropneumatic suspension system, consisting of a two-state semi-active hydropneumatic spring and a two-state semi-active damper.

Simulation models of both ¼ car and ½ car (pitch and bounce) vehicles were developed in Simulink. Typical values for a Land Rover Defender 110 SUV were used in the models. The suspension model developed by **Theron and Els (2005),** as described in paragraph 4.8, was used in the simulation. Hardware-in-the-loop (HiL) testing of a prototype suspension system was also performed using the techniques developed by Misselhorn**, Theron and Els (2006).** The suspension used in the HiL test rig was Prototype 2 discussed in chapter 4 of the present study. Simulation results and HiL results were found to correlate very well (within 10%). In order to simulate ride comfort for both on- and off-road conditions, road inputs included:

i) sine waves with frequencies between 0 and 30 Hz and amplitudes of 0.001 to 0.015 m.
ii) Belgian paving (Figure 2.21)
iii) APG bump (Figure 2.22)
iv) typical random road profiles ranging from a "smooth runway" to a "ploughed field" generated from road roughness information obtained from literature.

The following control ideas were evaluated:

i) ADD – Acceleration driven damper as proposed by **Silane *et. al.* (2004)**. This proposed strategy is the same as the strategy proposed by **Holsher and Huang (1991)**.

ii) Skyhook – The familiar skyhook damper strategy proposed by **Karnopp *et. al.* (1973)**.
iii) ReS – The strategy proposed by **Rakheja and Sankar (1985)**.
iv) MP – The minimum product strategy proposed by **Nell (1993)**.

Table 3.1 indicates all the proposed ideas that were evaluated. No useful semi-active spring control ideas were found. The springs were controlled using appropriately modified versions of the damper control ideas. As a comparison, the passive "ride comfort" mode (soft spring and low damping) of the semi-active hydropneumatic spring-damper system was also simulated.

Simulation results indicated that "Spring ADD" performed marginally better than the passive "ride comfort" mode. No control strategy was able to outperform the passive "ride comfort" mode by more than 2%, which is within expected simulation error. The "ride comfort" mode outperformed all control strategies for all HiL tests.

Voigt also investigated why the skyhook strategy performed unsatisfactory. The non-linearity of the system affects performance. Skyhook performs well at low frequencies but performance deteriorates at higher frequencies. This indicates that the valve response time is too slow. Better ride comfort is also achieved by controlling the spring rather than the damper.

The effect of limited suspension working space was also adressed by including bump stops in the model. This had the biggest effect on the ride comfort of the passive suspension. Again the "ride comfort" mode performed the best of all the possibilities. It seems that the suspension system under consideration exhibits the same useful characteristic of the twin-accumulator system described by **Abd El-Tawwab (1997)** amongst others. Due to the dampers between the accumulators, the large accumulator is progressively "sealed off" by the increased flow through the damper, *i.e.* spring stiffness increases automatically when terrain gets rougher (higher flow rate of oil) thereby eliminating bumpstop contact. This change is not discrete but happens gradually in relationship to the suspension velocity.

It is concluded from **Voigt's** study that it is not possible to improve ride comfort to any worthwhile extent by controlling the spring and damper characteristics when the characteristics have been optimised for ride comfort.

A similar study for handling has not yet been performed.

3.4 Conclusion

The following conclusions are made with respect to possible solutions for the ride comfort *vs.* handling compromise:

i) The ride comfort vs. handling compromise can be eliminated using active suspension systems. These systems are very expensive and require significant amounts of engine power. This option is disregarded for these reasons.
ii) Semi-active suspension systems have the potential to approximate the performance of fully active systems, but at a considerable reduction in cost and complexity.

Table 3.1 – Control strategies evaluated by **Voigt (2006)**

Control Strategy Description	Damper Strategy	Damper	Spring strategy	Spring
ADD	$\ddot{x}_1(\dot{x}_1-\dot{x}_2)>0$ $\ddot{x}_1(\dot{x}_1-\dot{x}_2)<0$	Hard Soft	Soft spring	
Skyhook	$\dot{x}_1(\dot{x}_1-\dot{x}_2)>0$ $\dot{x}_1(\dot{x}_1-\dot{x}_2)<0$	Hard Soft	Soft spring	
ReS	$(\dot{x}_1-\dot{x}_2)(x_1-x_2)<0$ $(\dot{x}_1-\dot{x}_2)(x_1-x_2)>0$	Hard Soft	Soft spring	
Spring ADD	Hard damping		$\ddot{x}_1(\dot{x}_1-\dot{x}_2)>0$ $\ddot{x}_1(\dot{x}_1-\dot{x}_2)<0$	Hard Soft
Spring Skyhook1	Hard damping		$\dot{x}_1(\dot{x}_1-\dot{x}_2)<0$ $\dot{x}_1(\dot{x}_1-\dot{x}_2)>0$	Hard Soft
Spring Skyhook2	Hard damping		$x_1(x_1-x_2)<0$ $x_1(x_1-x_2)>0$	Hard Soft
Spring Skyhook3	Hard damping		$\ddot{x}_1(x_1-x_2)>0$ $\ddot{x}_1(x_1-x_2)<0$	Hard Soft
Spring ReS	Hard damping		$(\dot{x}_1-\dot{x}_2)(x_1-x_2)>0$ $(\dot{x}_1-\dot{x}_2)(x_1-x_2)<0$	Hard Soft
Combo ADD1	$\ddot{x}_1(\dot{x}_1-\dot{x}_2)>0$ $\ddot{x}_1(\dot{x}_1-\dot{x}_2)<0$	Hard Soft	$\ddot{x}_1(\dot{x}_1-\dot{x}_2)>0$ $\ddot{x}_1(\dot{x}_1-\dot{x}_2)<0$	Hard Soft
Combo ADD2	$\ddot{x}_1(\dot{x}_1-\dot{x}_2)>0$ $\ddot{x}_1(\dot{x}_1-\dot{x}_2)<0$	Hard Soft	$\ddot{x}_1(x_1-x_2)>0$ $\ddot{x}_1(x_1-x_2)<0$	Hard Soft
Combo ADD3	$\ddot{x}_1(\dot{x}_1-\dot{x}_2)>0$ $\ddot{x}_1(\dot{x}_1-\dot{x}_2)<0$	Hard Soft	$x_1(x_1-x_2)<0$ $x_1(x_1-x_2)>0$	Hard Soft
Combo Skyhook1	$\dot{x}_1(\dot{x}_1-\dot{x}_2)>0$ $\dot{x}_1(\dot{x}_1-\dot{x}_2)<0$	Hard Soft	$\dot{x}_1(\dot{x}_1-\dot{x}_2)>0$ $\dot{x}_1(\dot{x}_1-\dot{x}_2)<0$	Hard Soft
Combo Skyhook2	$\dot{x}_1(\dot{x}_1-\dot{x}_2)>0$ $\dot{x}_1(\dot{x}_1-\dot{x}_2)<0$	Hard Soft	$x_1(x_1-x_2)<0$ $x_1(x_1-x_2)>0$	Hard Soft
Combo Skyhook3	$\dot{x}_1(\dot{x}_1-\dot{x}_2)>0$ $\dot{x}_1(\dot{x}_1-\dot{x}_2)<0$	Hard Soft	$\ddot{x}_1(x_1-x_2)>0$ $\ddot{x}_1(x_1-x_2)<0$	Hard Soft
Combo ReS1	$(\dot{x}_1-\dot{x}_2)(x_1-x_2)<0$ $(\dot{x}_1-\dot{x}_2)(x_1-x_2)>0$	Hard Soft	$(\dot{x}_1-\dot{x}_2)(x_1-x_2)>0$ $(\dot{x}_1-\dot{x}_2)(x_1-x_2)<0$	Hard Soft
Combo ReS2	$(\dot{x}_1-\dot{x}_2)(x_1-x_2)<0$ $(\dot{x}_1-\dot{x}_2)(x_1-x_2)>0$	Hard Soft	$\ddot{x}_1(x_1-x_2)<0$ $\ddot{x}_1(x_1-x_2)>0$	Hard Soft
Combo KP	$\ddot{z}_w.\ddot{z}_{b(2)}<\ddot{z}_w.\ddot{z}_{b(1)}$ $\ddot{z}_w.\ddot{z}_{b(2)}>\ddot{z}_w.\ddot{z}_{b(1)}$	Hard Soft	$\ddot{z}_w.\ddot{z}_{b(2)}<\ddot{z}_w.\ddot{z}_{b(1)}$ $\ddot{z}_w.\ddot{z}_{b(2)}>\ddot{z}_w.\ddot{z}_{b(1)}$	Hard Soft

iii) There are two viable concepts for a semi-active damper namely: Magneto-rheological (MR) fluids and hydraulic dampers with bypass valves. Designs can be continuously variable or discrete.
iv) There are basically two viable concepts for a semi-active spring namely air springs and hydropneumatic springs.
v) As far as control is concerned, a myriad of possibilities exist. All ideas can however not be easily implemented in the vehicle *e.g.* measurement of absolute body velocity for full-state feedback.
vi) Ride height adjustment is widely used and offers many possibilities.
vii) Reaction speed needs to be taken into account to determine potential system performance.
viii) Very little literature exists on semi-active springs.
ix) Most control ideas are developed using ¼ car linear models that do not sufficiently represent actual vehicle dynamics.
x) Very limited hardware has been implemented and documented.
xi) Almost no work has been performed on off-road vehicles.
xii) The majority of studies focus on ride comfort, and handling is often neglected.
xiii) Preview is a popular research topic, although hardware implementation is problematic.

3.5 Proposed solutions to the ride comfort *vs.* handling compromise

Based on the ideas and research described in chapters 2 and 3, the proposed solution to the "ride comfort *vs.* handling compromise" is to use a twin accumulator hydropneumatic (two-state) spring combined with an on-off (two-state) semi-active hydraulic damper (achieved with a by-pass valve), based loosely on idea by **Eberle and Steele (1975)**. Although more than two spring and/or damper characteristics can be incorporated, two is considered sufficient based on the simulation results presented in Chapter 2.

Based on the results, presented by **Voigt (2006)**, for ride comfort control, and assuming that the same trends will be found for handling, if studied, the best practical solution would be no "control" other than switching between the "ride comfort" and "handling" modes. The pre-requisite is however that a successfull ride comfort *vs*. handling decision-making strategy can be developed that will automatically switch between the "ride comfort" and "handling" modes. The switching must be safe and quick enough to prevent accidents, using only easily measurable parameters.

The proposed suspension system will now be called the **4**-**S**tate **S**emi-active **S**uspension **S**ystem or **4S$_4$**.

Chapter 4

THE FOUR-STATE SEMI-ACTIVE SUSPENSION SYSTEM ($4S_4$)

The development of a prototype **4**-**S**tate **S**emi-active **S**uspension **S**ystem (**$4S_4$**) is described in this chapter. Literature appropriate to the development of the suspension system, and the working principle of the system is discussed. Two prototype suspension systems (from now on referred to as Prototype 1 and Prototype 2 respectively) were designed, manufactured, tested on a laboratory test rig and modelled mathematically.

After determination of the space envelope on the proposed test vehicle, Prototype 1 was designed and manufactured by Hytec, a specialist hydraulic equipment manufacturer. Prototype 1 suffered from several drawbacks that necessitated a redesign. Prototype 2 is an in-house design and solved all the problems experienced on Prototype 1.

Detailed test results for Prototype 2 are discussed and interpreted. Test results for Prototype 1 are only discussed where necessary to motivate some of the decisions made during development of Prototype 2. Test results include spring and damper characteristics as well as several parameters required for mathematical modelling of the suspension system. These parameters include the bulk modulus of the oil, thermal time constant of the accumulators, valve response times and pressure drops over the valves.

4.1 Literature

4.1.1 Hydropneumatic springs

Hydropneumatic springs are often modelled as polytropic gas compression processes. With the assumption that the ideal gas law is applicable, this approach gives satisfactory first order results. The static spring force can be calculated accurately using isothermal compression. The dynamic force is however time and temperature dependent and requires a more advanced model to achieve accurate results.

A detailed hydropneumatic spring model is developed and validated by **Els (1993)** and **Els and Grobbelaar (1993)**. This model is based on the solution of the energy equation of a gas in a closed container and therefore takes time- and temperature dependency of the spring characteristic into account. It is based on a thermal time constant approach and uses the Benedict-Webb-Rubin (BWR) equation for real gas behaviour (**Cooper and Goldfrank, 1976**). The model is verified against experimental results and good correlation is achieved between measured and predicted spring characteristics. The model is further developed to include heat transfer effects from the damper that is usually an

integral part of a hydropneumatic suspension system **(Els and Grobbelaar, 1999).** This model was used to predict the $4S_4$ spring characteristics in paragraph 4.8.

Another approach that can be used to model hydropneumatic springs is by making use of the so-called anelastic model **(Kornhauser, 1994** and **Giliomee *et. al*, 2005).**

4.1.2 Variable spring concepts

The concept of making a semi-active spring using accumulators is not new. The fundamental idea was proposed by **Eberle and Steele (1975)** as discussed in par 3.2.2.2. **Decker *et. al.* (1988)** also implemented an air spring with various discrete volumes that can be switched. The design was made for a passenger car, but no quantitative results or design guidelines are given.

A passive twin-accumulator suspension system is proposed by **Abd El-Tawwab (1997)**. Two accumulators are connected via an orifice. As the flow rate of oil in the system increases, damping through the orifices increases thereby resulting in different amounts of fluid flowing into each accumulator. This results in a speed or frequency dependant spring characteristic. The $4S_4$ system incorporates this capability as a function of its design.

First attempts by the candidate to develop a two-state semi-active spring combined with a two-state semi-active damper are discussed by **Giliomee and Els (1998)**. The design was for a heavy off-road wheeled vehicle with a static wheel load of 3 000 kg. Experimental results included testing the system in a single degree of freedom test rig using various control methods. Initial results were very promising and warranted further development of the $4S_4$ system.

4.1.3 Hydraulic semi-active dampers

Semi-active dampers have been applied widely in prototypes and production vehicles. The work of **Nell (1993)**, **Nell and Steyn (1994, 1998 and 2003)** as well as **Els and Holman (1999)** is of particular significance to the development of the $4S_4$ due to the applications to heavy off-road military vehicles. The applications varied from two-state translational semi-active dampers for a 12-ton 4x4 vehicle up to a two-state semi-active rotary damper for a 46-ton self-propelled gun. In all these cases simulation results are validated using vehicle tests with prototype dampers and control systems fitted. The results are generally very satisfactory.

All these dampers operate on the bypass valve principle and have valve response times of between 40 and 200 milliseconds. Large flow rates of up to 1000 l/min can be accommodated with acceptable pressure drops over the valves.

4.2 $4S_4$ Working principle

The concept behind the $4S_4$ system is to achieve switching between two discrete spring characteristics, and between two discrete damper characteristics. The high and low characteristics for both spring and damper are possible by alternate channeling of hydraulic fluid with solenoid valves. The basic circuit diagram of the proposed suspension system is given in Figure 4.1. The strut is fixed between the vehicle body and

the unsprung mass, replacing both the spring and damper. The strut is connected to two accumulators via the control valves and hydraulic damper valves. The two-state hydropneumatic spring can also be used on its own in parallel with an additional semi-active damper *e.g.* a continuously variable MR fluid based damper, but then some of the elegance and packaging possibilities of the $4S_4$ unit will be sacrificed.

The low spring rate is achieved by compressing the combined volume of gas in the two accumulators. By sealing off accumulator 2 with valve 3, a smaller gas volume is compressed and a higher spring rate is achieved. Spring rates can be individually tailored by changing the two gas volumes. For low damping, the hydraulic dampers (dampers 1 and 2) are short circuited by opening the bypass valves (valves 1 and 2). For high damping these valves are closed and the hydraulic fluid is forced through the dampers resulting in high damping force. The proposed system therefore achieves its aim to provide switching between two discrete spring characteristics, as well as switching between two discrete damper characteristics using solenoid valves.

The concept can easily be extended to more spring characteristics by adding more accumulators and valves. The two-state dampers can also be upgraded by fitting proportional or servo valves, thereby achieving continuously variable semi-active damping. Although these improvements are possible, they will add considerable complexity and cost and are therefore not considered at present. Adding or extracting oil from the unit results in ride height adjustment.

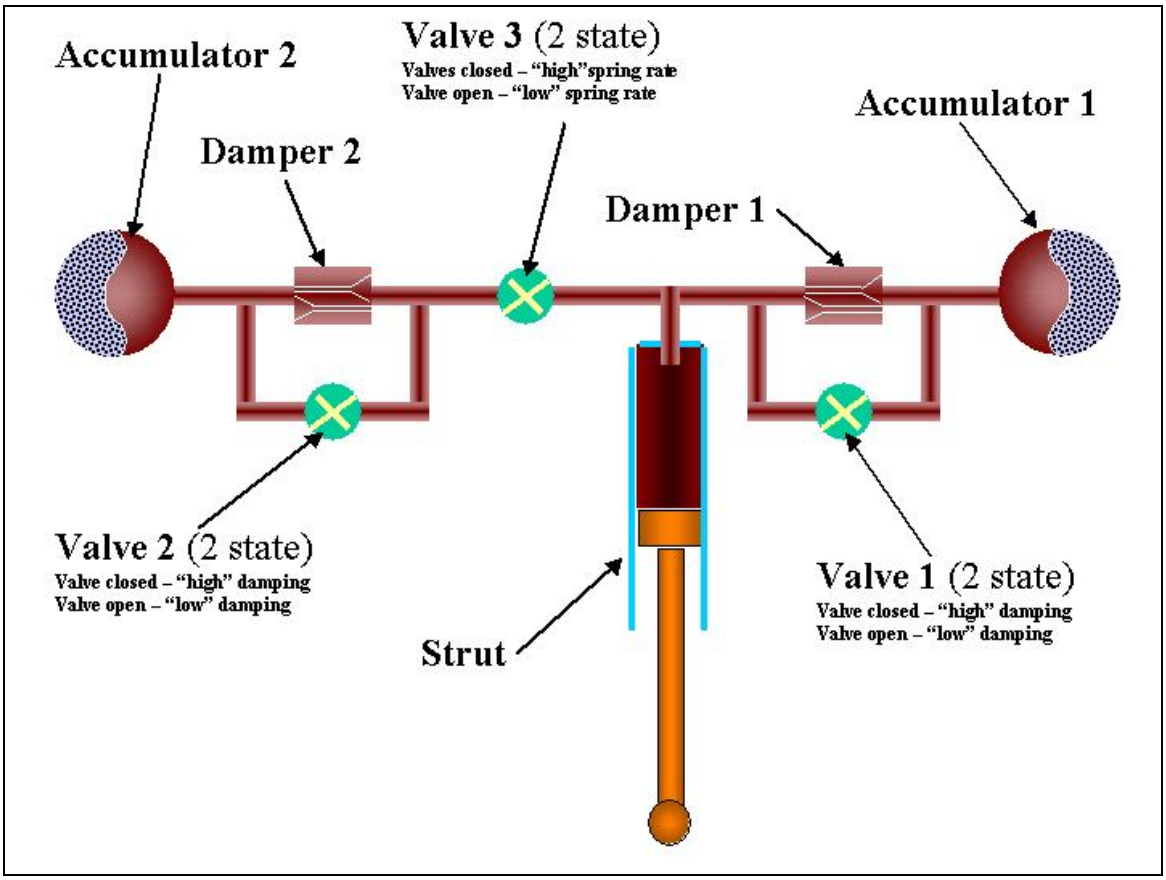

Figure 4.1 – $4S_4$ circuit diagram

4.3 Design requirements

Before designing the new suspension system, it is necessary to obtain the specifications for the existing baseline system in terms of wheel load, maximum suspension deflection and space envelope available.

The maximum static vertical wheel load for the fully laden Land Rover Defender 110 test vehicle is 800 kg and occurs on the rear wheels. The prototype suspension system is therefore designed for a static load of 8000 N and a dynamic load of 40 000 N (five times the static wheel load). Provision is made for a total suspension travel of 300 mm (maximum compression to maximum rebound). The baseline rear suspension system has a total travel of 290 mm (170 mm compression and 120 mm rebound). The required suspension characteristics for the springs and dampers are obtained from the analysis in chapter 2. Gas volumes of 0.1 litre (Accumulator 1) and 0.4 litre (Accumulator 2) are used as design values. Provision is made for fitment of a wide range of available hydraulic damper packs so that the damper characteristics can be fine-tuned before final vehicle implementation. To enable the use of standard hydraulic seals, valves and fittings, the system is designed not to exceed a maximum pressure of 20 MPa. A maximum relative suspension velocity of 2 m/s is assumed to be sufficient for extreme events. This was determined from simulation results as well as measurements on the baseline vehicle. It is envisaged that the suspension system must be able to control the body's natural frequencies in the region of one to two Hz. This requires a valve reaction of 10 to 20 Hz or 50 to 100 milliseconds. This was also found to be the case by **Nell (1993)** and **Nell and Steyn (1994).**

The main design specifications for the prototype controllable suspension system are summarized as follows:

i) Suspension travel of 300 mm (same as for baseline suspension)
ii) Soft suspension static gas volume of 0.5 litre
iii) Hard suspension static gas volume of 0.1 litre
iv) Maximum system pressure at full bump of 20 MPa
v) Maximum relative suspension velocity of 2 m/s
vi) Maximum suspension force of 40 kN (5x static force)
vii) Valve response time of the order of 50 milliseconds
viii) Must fit into available space envelope without major modifications to vehicle
ix) Low damper characteristic < 0.5 of baseline value
x) High damper characteristics between 2 and 3 times the baseline value

These specifications are for the rear suspension and represent the worst-case scenario. The only changes required for fitment of the prototype to the front suspension of the Land Rover 110, is to reduce the total suspension travel to 250 mm.

The piston diameter required to give a maximum pressure of 20 MPa at 40 kN is 50.5 mm. A piston diameter of 50 mm will be used for the design of the prototype. Figure 4.2 indicates the relative suspension velocity over the left rear spring of a standard Land Rover Defender 110 when driven on the Gerotek Test Facility's rough track. This velocity was calculated by differentiating the measured relative displacement. The maximum extreme event velocity over this type of terrain at representative speeds is 2 m/s. The 50 mm piston diameter will therefore result in a flow rate of 236 litre/min at 2 m/s relative suspension velocity.

Selection of an appropriate valve was based on the response time of 50 milliseconds, maximum system pressure of 20 MPa and maximum extreme event flow rate of 236 litre/min. Choice and availability of valves is problematic as a valve with a fast switching time is required. Standard valves, available off-the-shelf, can meet either the flow or the time response requirements, but not both. For this flow rate requirement logic element valves operated by a pilot solenoid valves are usually employed **(Nell (1993), Nell and Steyn (1994), Janse van Rensburg, Steyn and Els (2002), Els and Holman (1999))**. This solution is bulky and expensive, and above all results in response times that are strongly pressure dependent and very slow at small pressure differences. The design has therefore been modified to use two smaller, fast switching valves in parallel to handle the required flow and meet the switching time requirement.

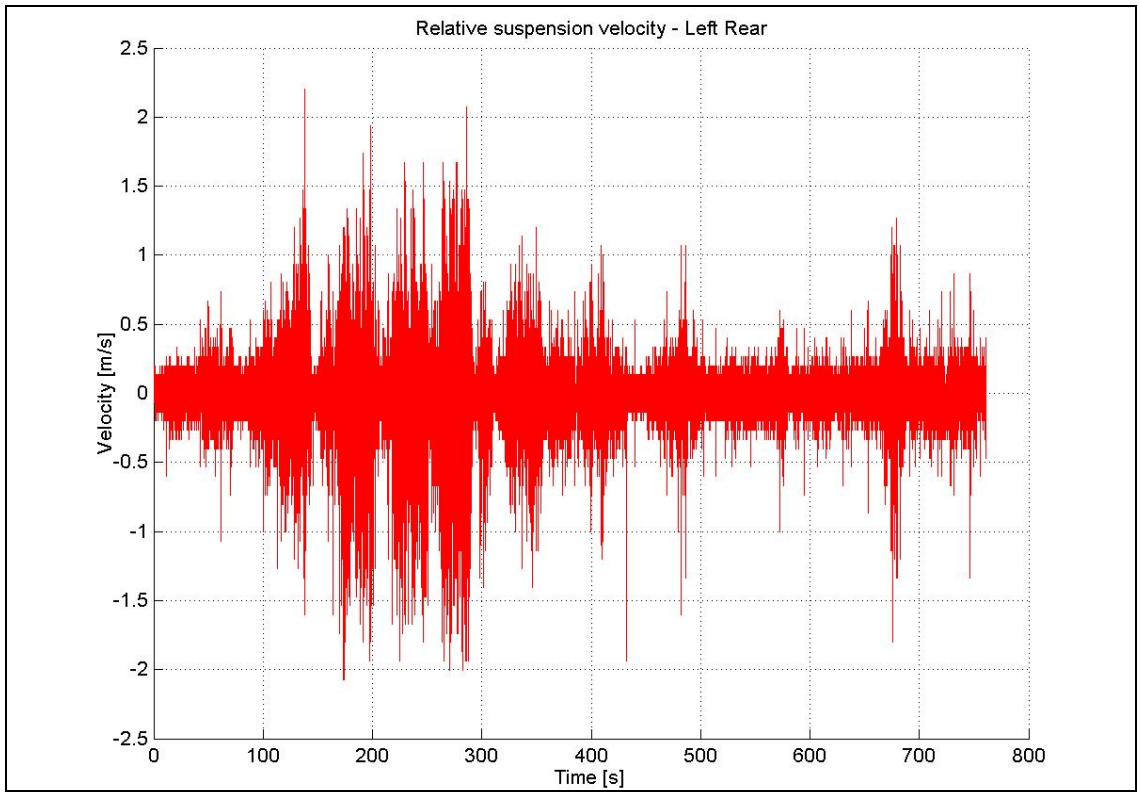

Figure 4.2 – Relative suspension velocity over Gerotek Rough track

The valve selected for the current application is the SV10-24 2-way normally closed spool valve from HydraForce (**Anon, 1998**). This valve has previously been characterized for a different project at the University of Pretoria and information on response times and pressure drops are available (**De Wet, 2000).** The valve is actuated by a solenoid that is available in different voltage ratings. The response time (initial delay) is quoted to be 30 milliseconds when energised (i.e. opening) and 25 milliseconds when de-energised (i.e. closing). This is the time from the switch signal to the first indication of the change of state, called the initial delay (see par 4.7.6 for definitions). This response time is quoted at a flow rate of 80% of the nominal flow rate when the valve is fully open. The valve is designed for a maximum operating pressure of 20.1 MPa and proof pressure of 35 MPa. The valve can handle a flow of 113.6 litre/min at a pressure of 6.9 MPa and 37.9 litre/min at 20.7 MPa (see Figures 4.3 and 4.4). When valve 3 in the proposed concept (see Figure 4.1) is open, the flow will be split between accumulators 1 and 2 but with the higher portion of the flow going into the bigger accumulator 2. The expected flow is however

still higher than the maximum capacity of the valve. It was therefore decided to use two valves in parallel for V_3.

Eight standard Land Rover Defender rear dampers were stripped, the damper packs removed and mounted in the $4S_4$ units (two damper packs per unit). Due to the difference in bore size, and thus flow rate, as well as the pressure difference now acting on a larger area, use of the standard damper packs resulted in the required hard damper characteristics (see discussion in paragraph 4.7.5 and Figure 4.27).

4.4 Space envelope

The space envelope available for the new suspension was determined by physical measurement on a Land Rover Defender 110 vehicle. The controllable suspension system, with the required characteristics, has to fit in the space envelope. The left front and left rear axle portions and wheel well details were measured and modelled in Solid Edge for this purpose as indicated in Figures 4.5 and 4.6.

4.5 Detail design of $4S_4$

The height of the space envelope is the major restricting parameter, followed by the distance between the fenders and the inside of the wheel arches. Length should not pose any limitations, as the full tyre diameter is available. To comply with the height restriction, the two accumulators are mounted to the front and rear of the main strut respectively as indicated in Figure 4.7. The strut is connected to the two accumulators via a valve block. All the control valves, hydraulic damper valves, control ports and channels are accommodated inside the valve block. Piston accumulators are used mainly for two reasons:

i) It can be made long and thin compared to bladder accumulators, thereby resulting in more freedom of packaging
ii) The gas volume can be controlled much more precisely (see paragraph 4.7.1 – charging of unit).

The choice as far as sealing arrangements are concerned is between sealing in the cylinder bore and sealing on the piston rod. The rod sealing arrangement was chosen instead of the more conventional cylinder sealing because it was much easier to finish the rod to the correct tolerances and surface finish required than the cylinder bore. The options considered for surface coatings at this stage is the normal hard chroming as well as a tungsten-carbide-cobalt coating applied with a high velocity oxygen fuel (HVOF) process. The latter is very resistant to flaking and has extremely good wear resistance. For both Prototypes 1 and 2, the tungsten-carbide-cobalt coating was used because it is suggested for the application by one of the world's biggest seal manufacturers, Greene Tweede. After coating the rod was ground and superfinished with diamond tape to obtain a hard, corrosion resistant component with the required surface finish to ensure durability and low friction. During the design phase, attention was given to minimise friction and stick-slip. Standard seals from the Busak and Shamban catalogue (**Anon, 2005d**) were used throughout the design of the $4S_4$. A Turcon AQ Seal 5 and two Glydring wear rings were used on the floating pistons in the accumulators. The main cylinder pressure was sealed

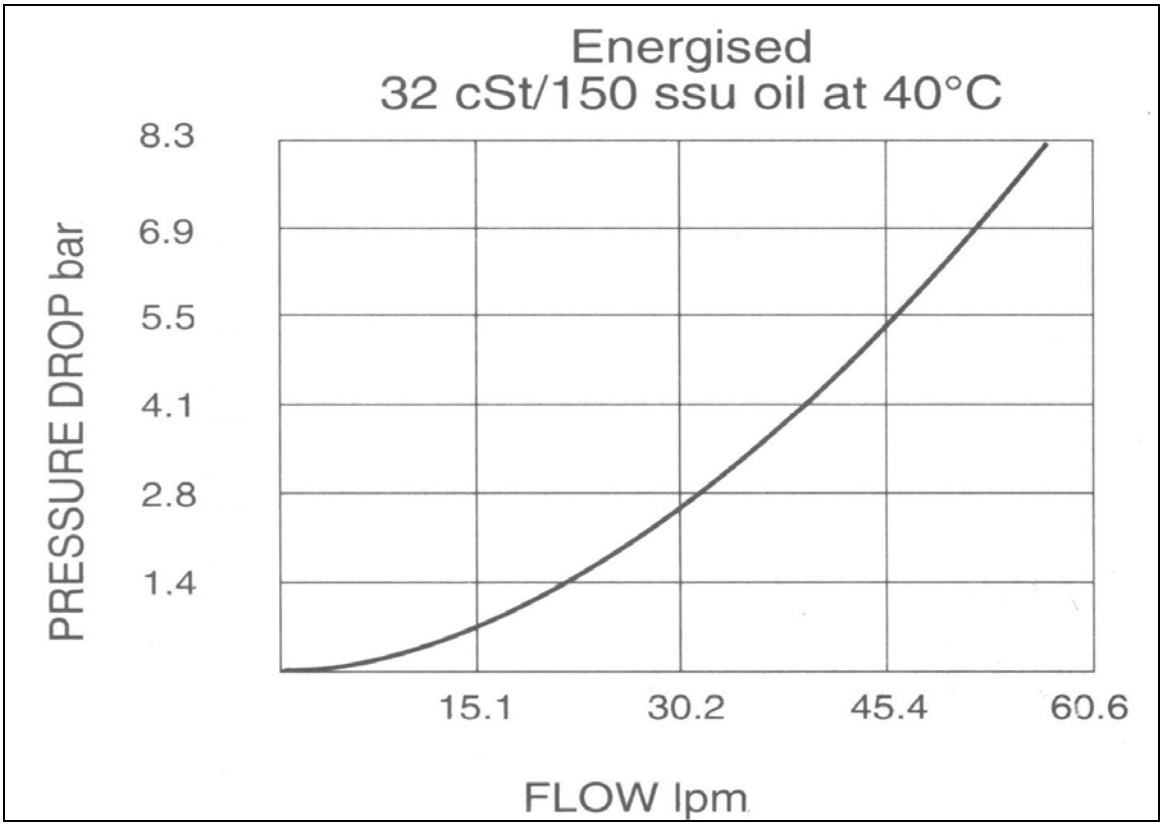

Figure 4.3 – Pressure drop vs. flow rate for SV10-24 valve **(Anon, 1998)**

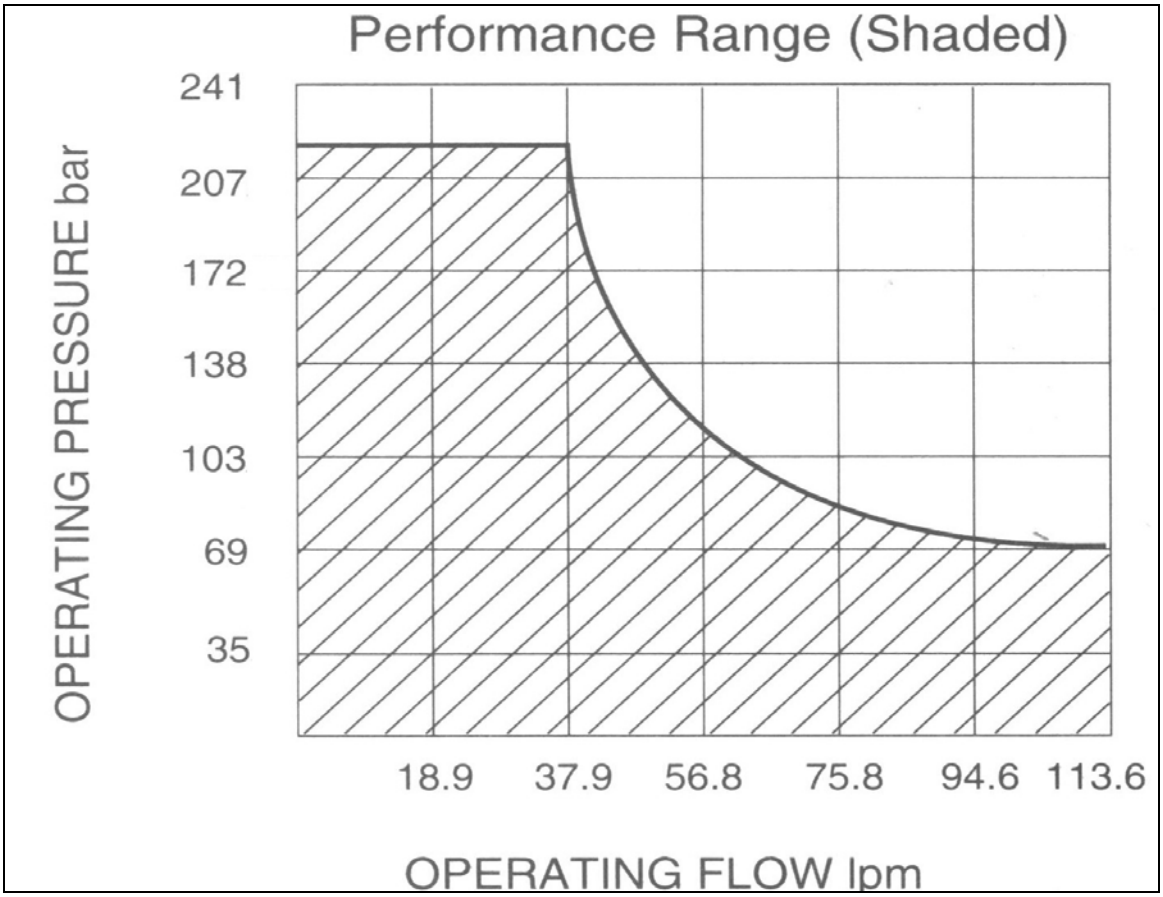

Figure 4.4 – Operating range for SV10-24 valve **(Anon, 1998)**

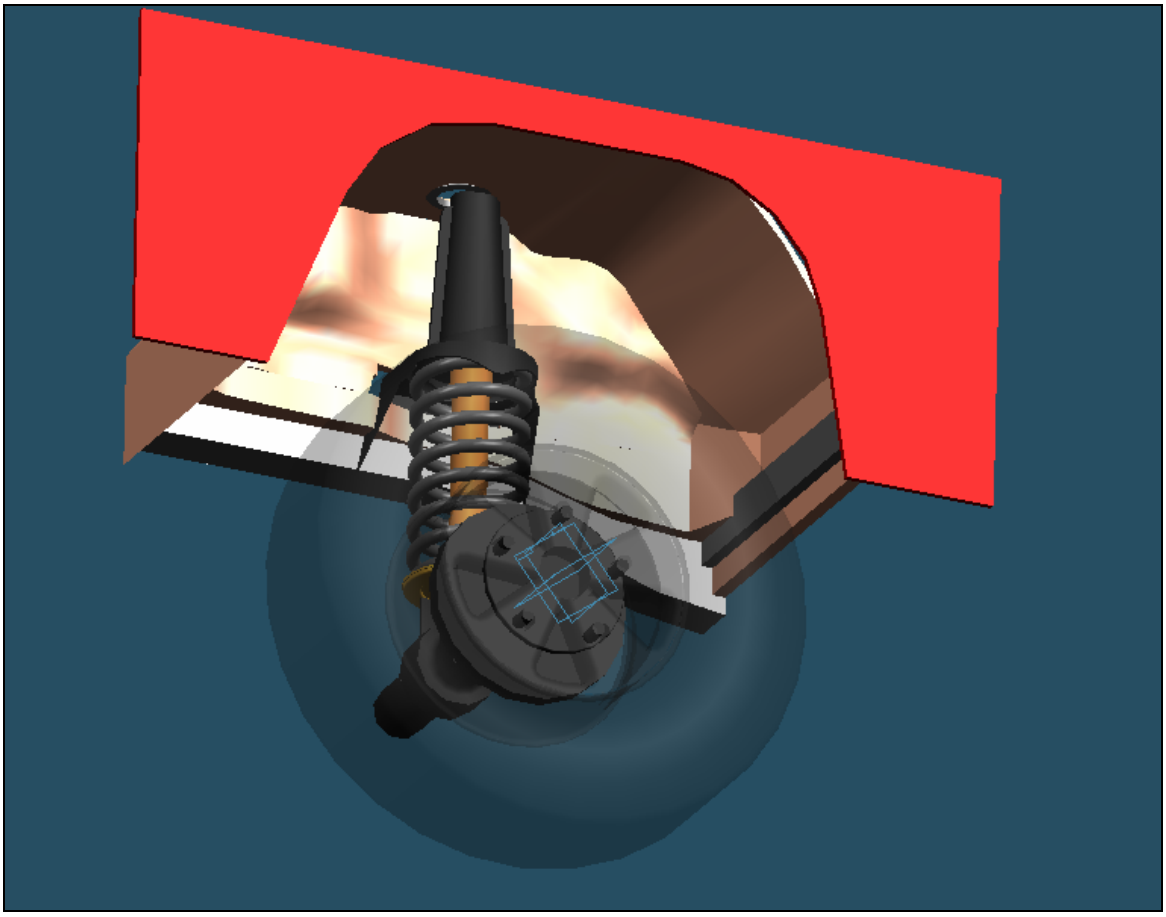

Figure 4.5 - Baseline left front suspension layout

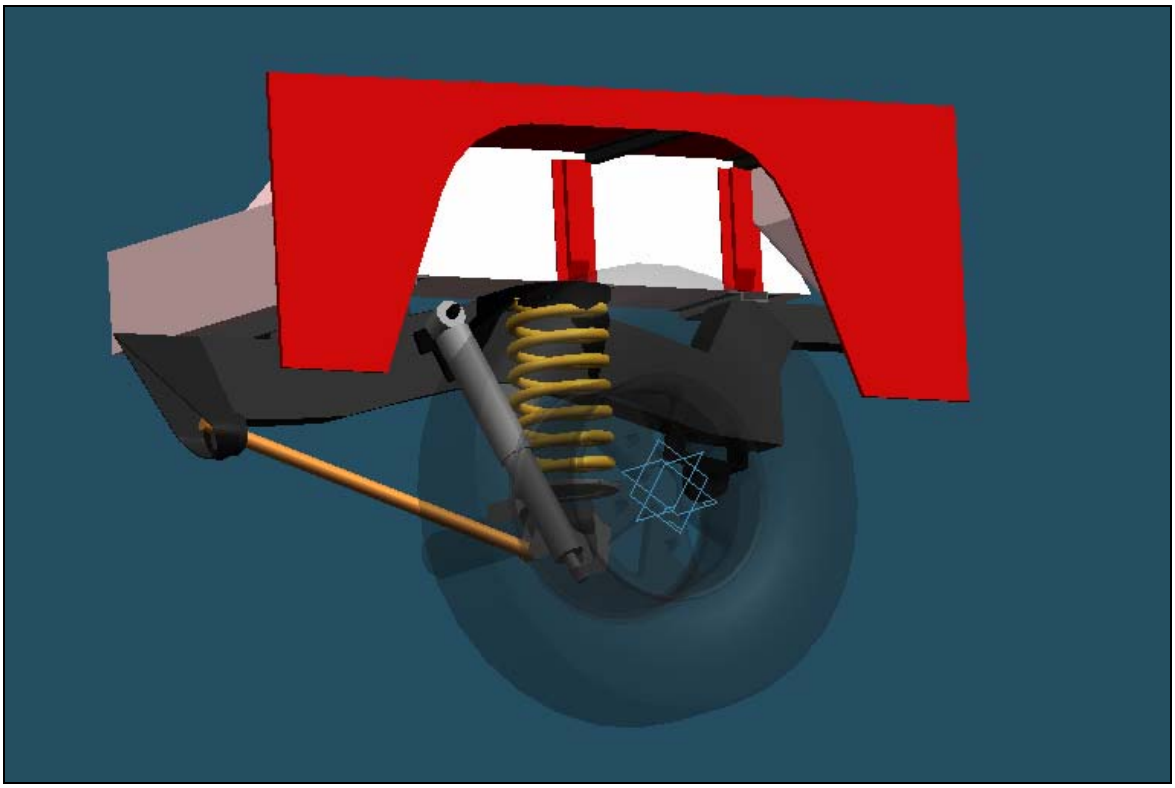

Figure 4.6 - Baseline left rear suspension layout

using a rod sealing arrangement with a triple seal system consisting of a TURCON STEPSEAL 2K, TURCON RIMSEAL and TURCON EXCLUDER 2 rod scraper.

During testing of the first prototype suspension system the force characteristics exhibited very high frictional behavior (hysteresis). This was traced to the off-center mounting arrangement on the first prototype that subjected the cylinder to a moment loading and caused high seal friction. The mounting arrangement on Prototype 2 was changed to be concentric with the cylinder. The new mounting arrangement eliminated the hysteresis encountered on the first prototype (see par 4.7.7. under test results).

On the prototype, provision is made for four pressure transducers (P_1 to P_4) to measure pressures in the system.

Two views of the Prototype 2 controllable suspension system are provided in Figures 4.8 and 4.9. Figure 4.8 shows an exterior side view and Figure 4.9 indicates a cross-sectional view. The suspension system is mounted to the axle and the chassis by means of a spherical bearing used axially. The spherical bearing, although normally intended for radial forces, is appropriately sized to handle the axial load. This bearing is used to ensure pure axial force loading on the suspension system and eliminates any moment loading.

Figures 4.10 and 4.11 depict the $4S_4$ unit fitted to the vehicle at the front and rear respectively.

It is concluded that the suspension system can be fitted in the available space although small changes to the vehicle may be required. The new suspension system is narrower than the coil spring and this may result in more interior space in the vehicle.

4.6 Manufacturing of $4S_4$ prototypes

The Prototype 2 controllable suspension system was manufactured according to detail design drawings. A photograph of the assembled unit is given in Figure 4.12. Figure 4.13 compares Prototype 2 to Prototype 1. Prototype 2 is considerably smaller than Prototype 1 in overall size and weight. Valve positions have been optimised to reduce size. The valve block requires very few external blanking plugs compared to the first prototype. The weight of the unit was reduced from 59 kg for Prototype 1 to 40 kg for Prototype 2. The mounting arrangement to the vehicle chassis has been modified considerably to remove the moment loading. On Prototype 2, the weight includes all the mounting brackets to the vehicle, while on Prototype 1 mounting brackets are not included in the quoted weight.

4.7 Testing and characterisation of the $4S_4$

The $4S_4$ Prototype 2 suspension was characterized on a test rig to obtain all the spring and damper characteristics as well as valve response times. A series of basic reliability tests were also performed to validate the choice of hydraulic seals and valves. The test rig consisted of a purpose designed test frame and a 100 kN SCHENCK hydropulse actuator (see Figures 4.14 to 4.18). The prototype suspension unit was instrumented with four pressure transducers to determine dynamic system pressures, with actuator force and actuator displacement also being measured. The switching signal to the valves was recorded for determining the valve response times. A linear potentiometer was installed on valve 3 to measure the valve plunger displacement.

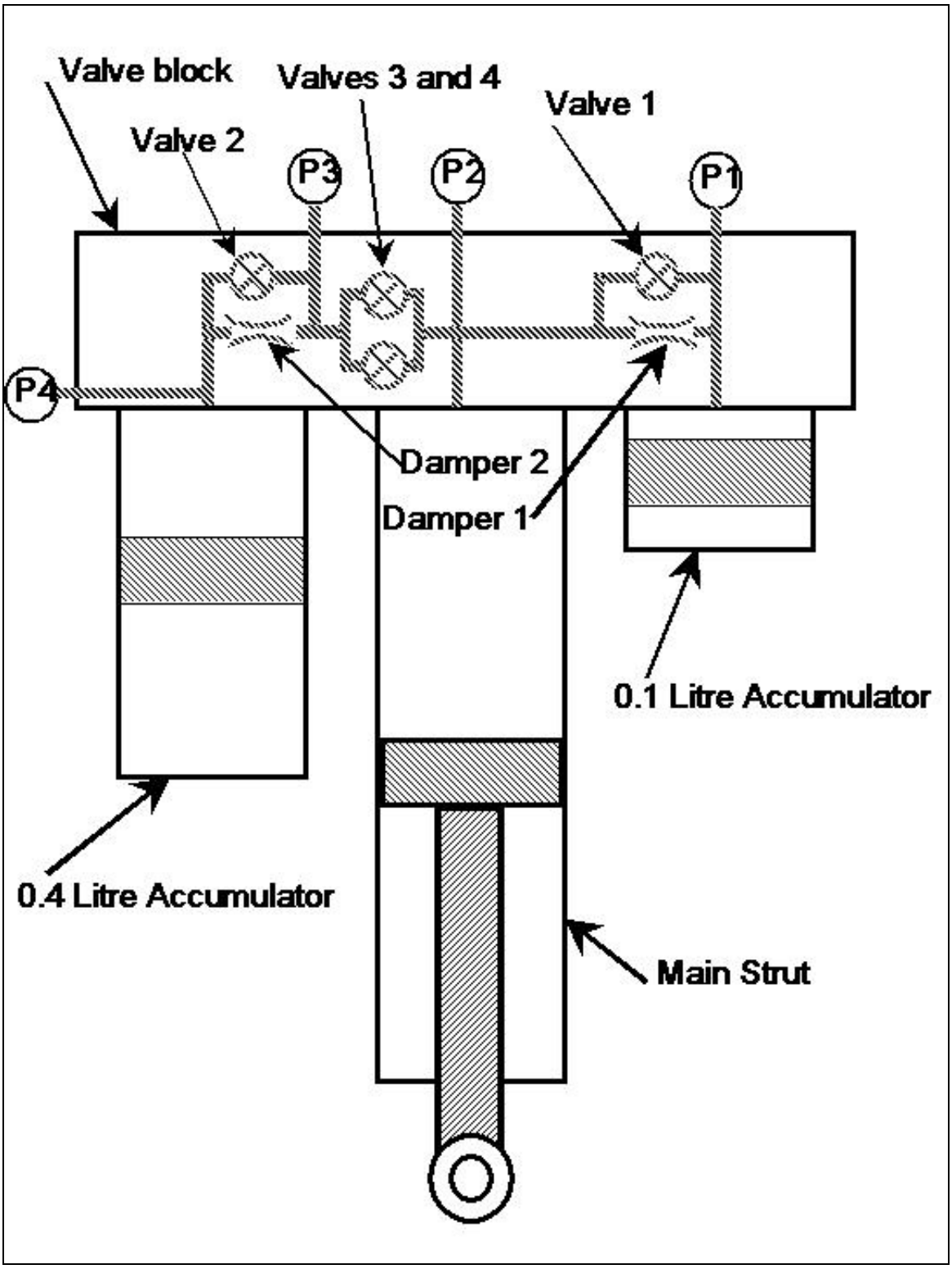

Figure 4.7 – $4S_4$ suspension schematic diagram

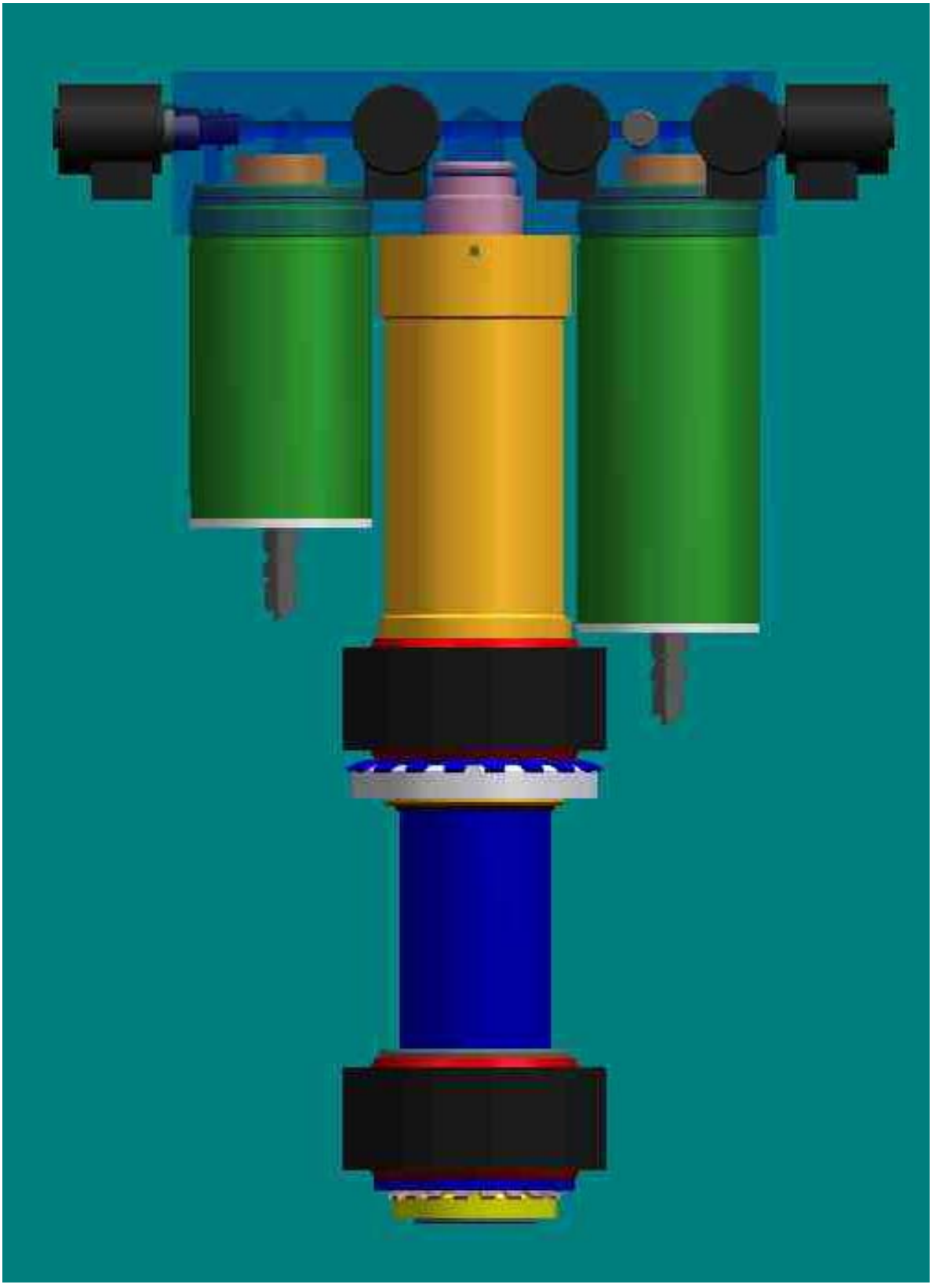

Figure 4.8 – $4S_4$ suspension system – exterior view

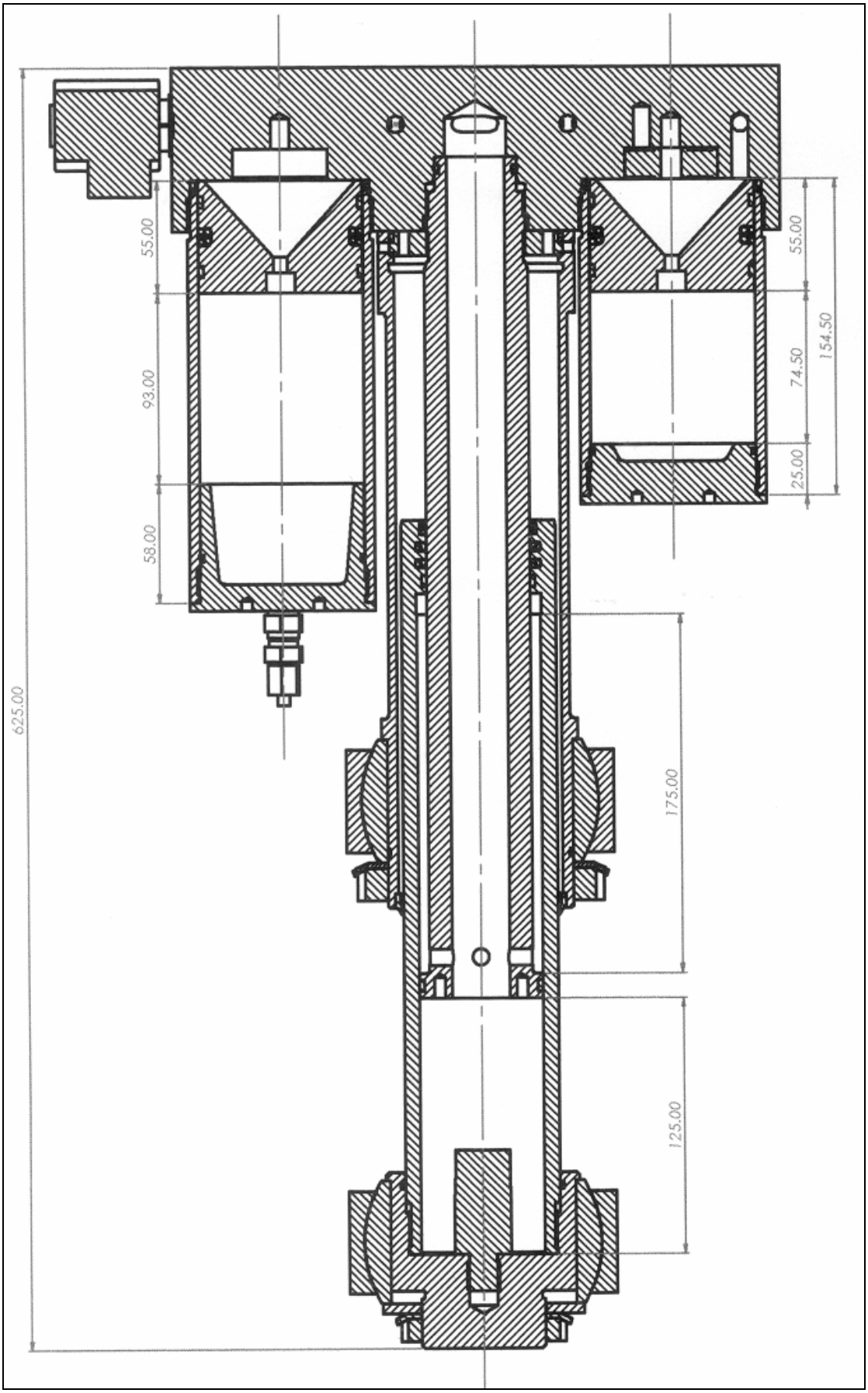

Figure 4.9 – $4S_4$ suspension system – cross sectional view

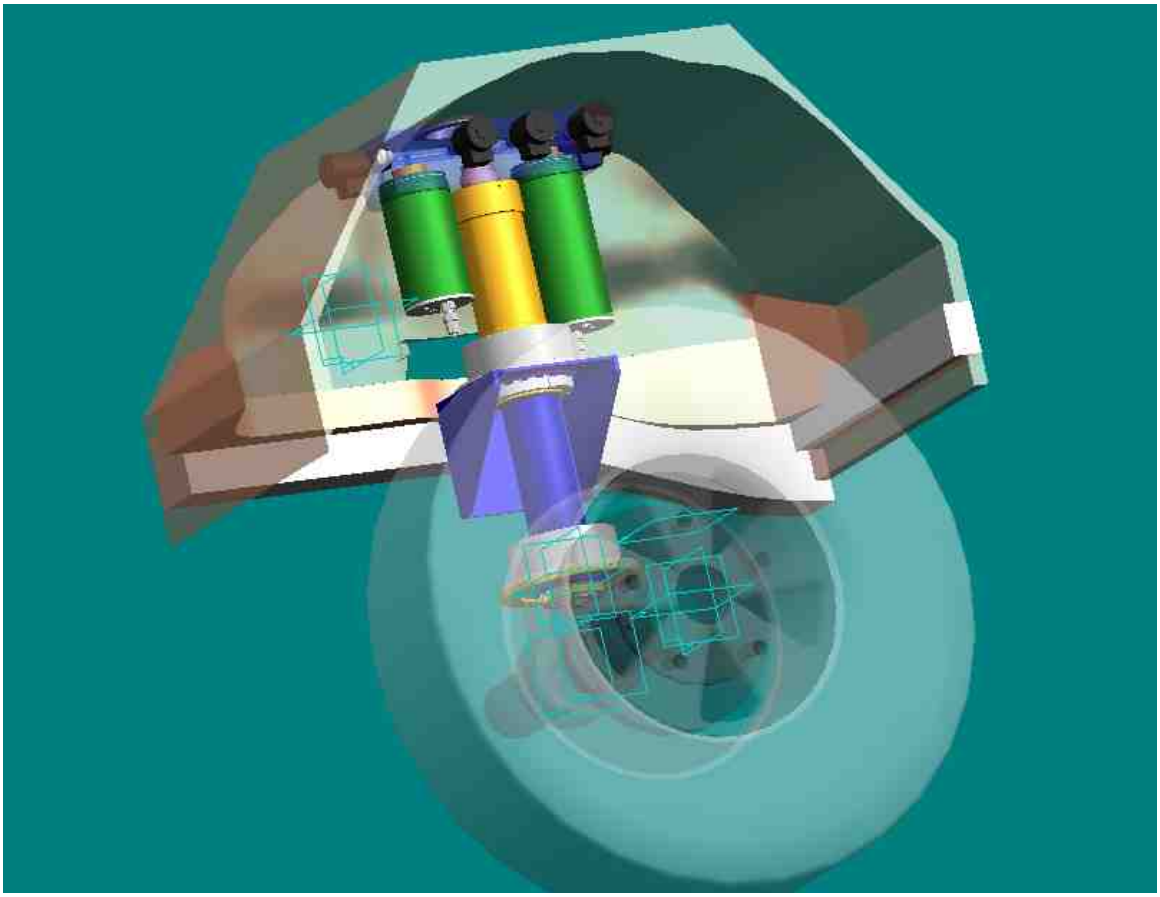

Figure 4.10 - Front suspension layout with $4S_4$ unit fitted

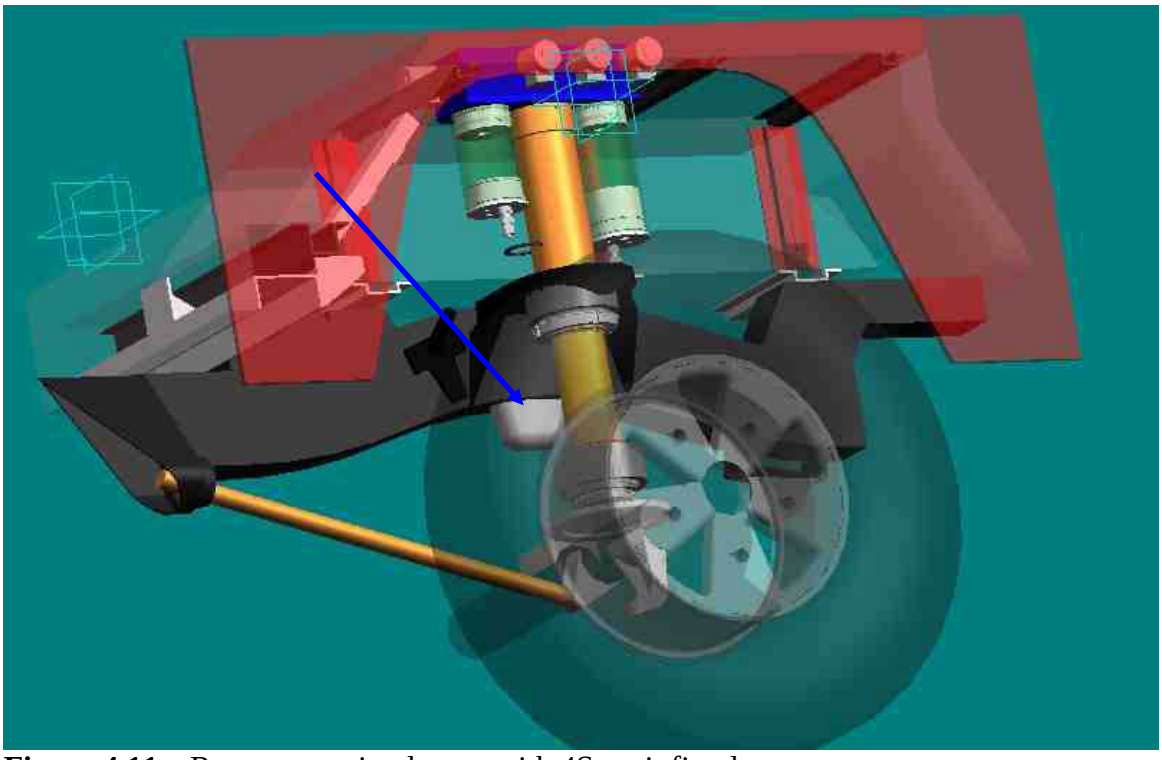

Figure 4.11 – Rear suspension layout with $4S_4$ unit fitted

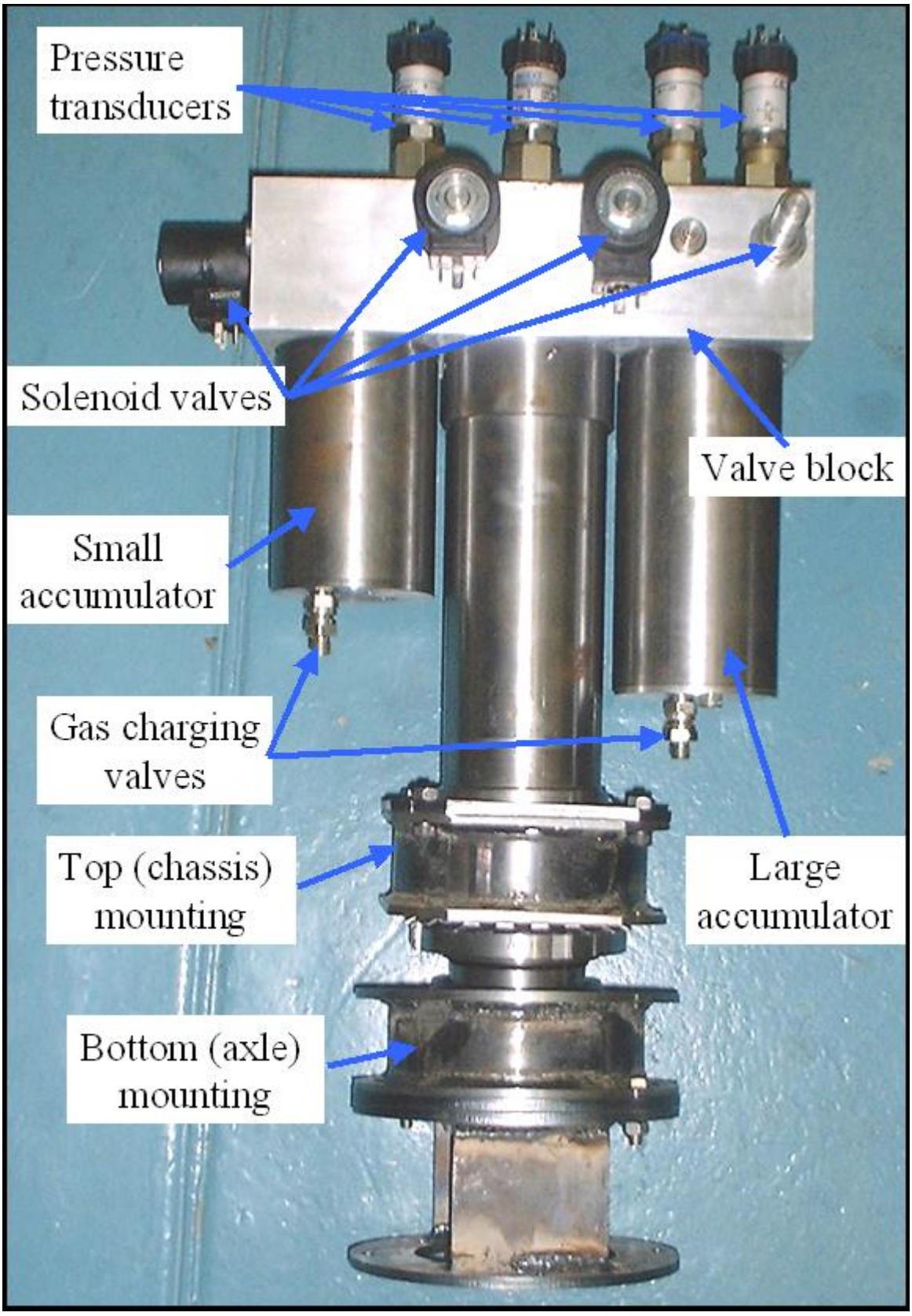

Figure 4.12 – $4S_4$ Prototype 2

Figure 4.13 - $4S_4$ Prototype 2 (left) compared to Prototype 1 (right)

4.7.1 Gas charging procedure

The spring characteristics are completely dependant on the volume of gas in each accumulator. It is therefore imperative that the gas charging procedure described below be strictly observed otherwise the spring characteristics will be in error.

i) During assembly of the suspension unit, both floating pistons must be pushed in until they touch the valve block.
ii) Move the piston rod to the maximum extended (rebound) position.
iii) Open all solenoid valves by connecting them to a suitable power supply.
iv) Fill the strut completely with oil. Tilt the strut slowly in different directions in an attempt to get rid of trapped air. If the unit seems to be full, let it stand for a few hours and top up frequently with oil. Slowly tilt the unit during each filling attempt. The unit should take at least 1.6 litres of Aeroshell Fluid 41.
v) Disconnect power to the valves.

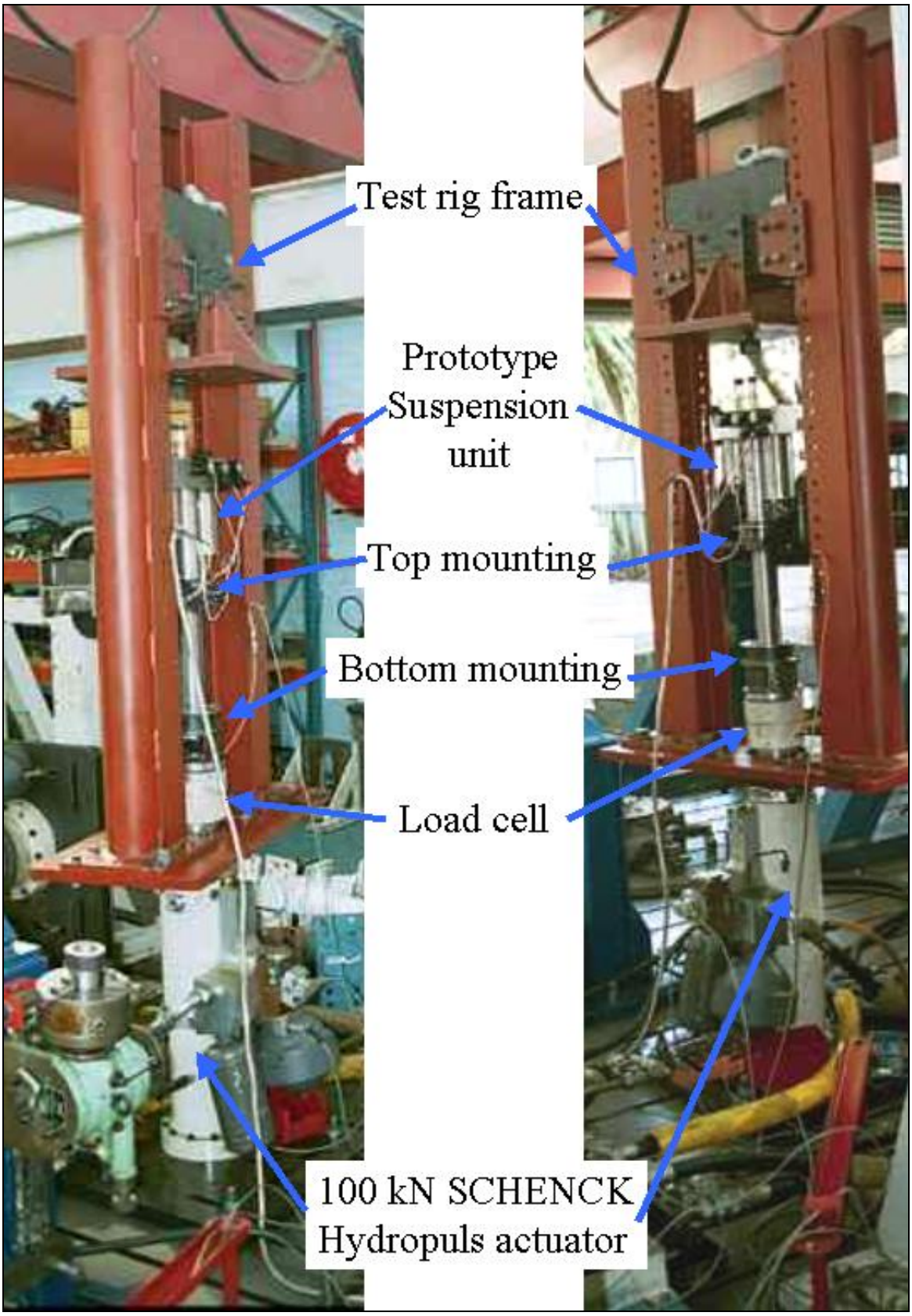

Figure 4.14 - $4S_4$ Prototype 2 on test rig

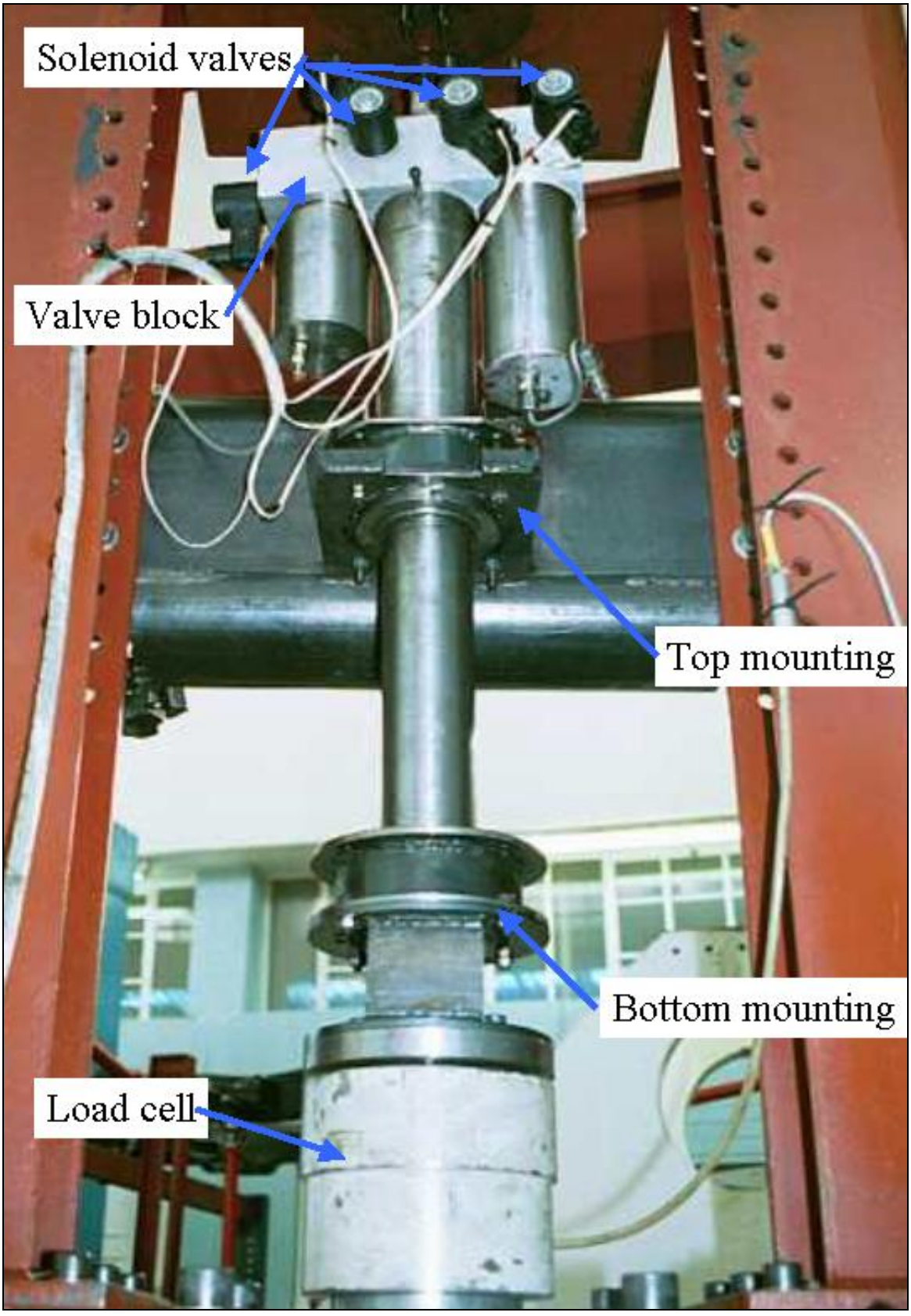

Figure 4.15 - $4S_4$ Prototype 2 on test rig

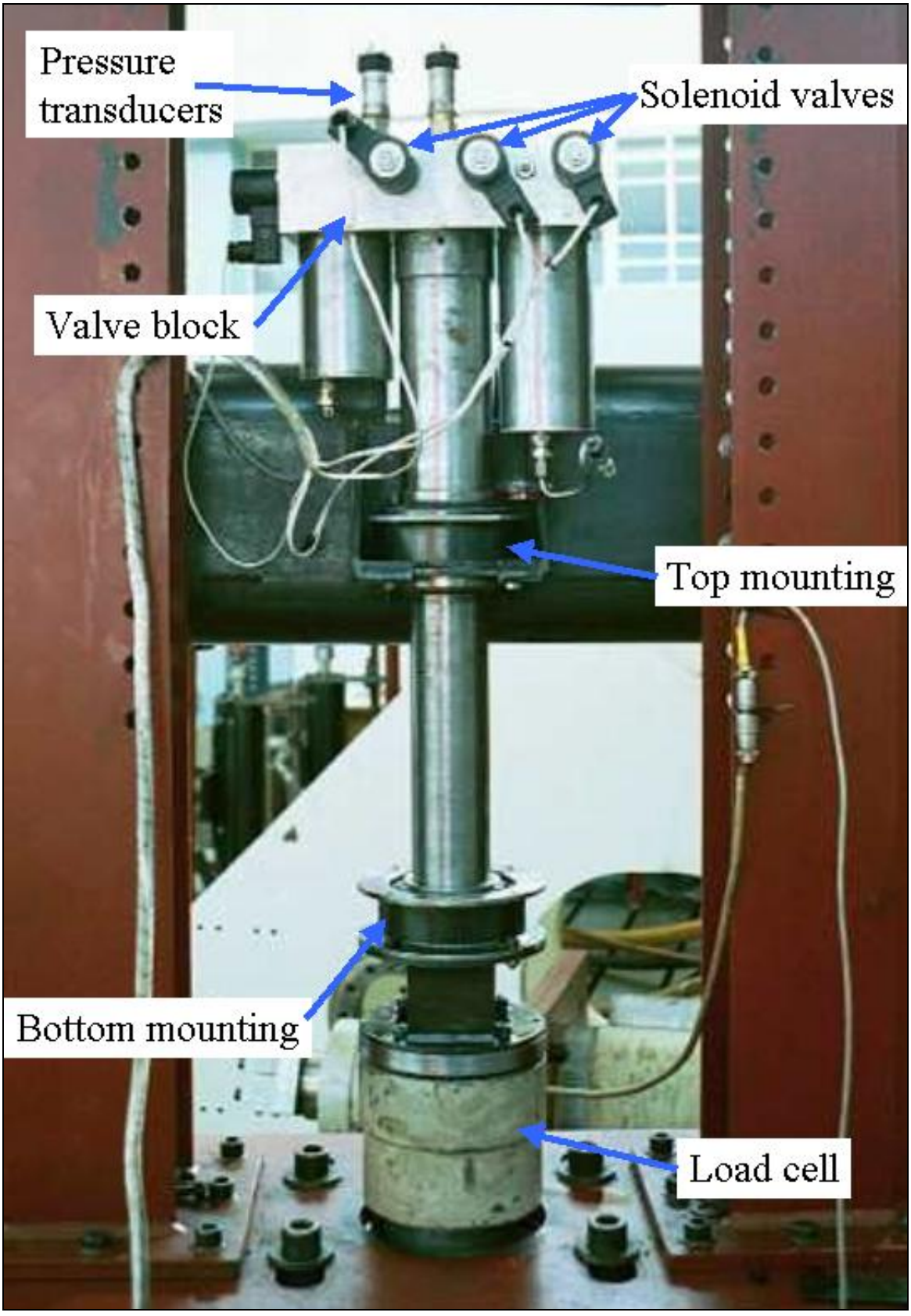

Figure 4.16 - $4S_4$ Prototype 2 on test rig

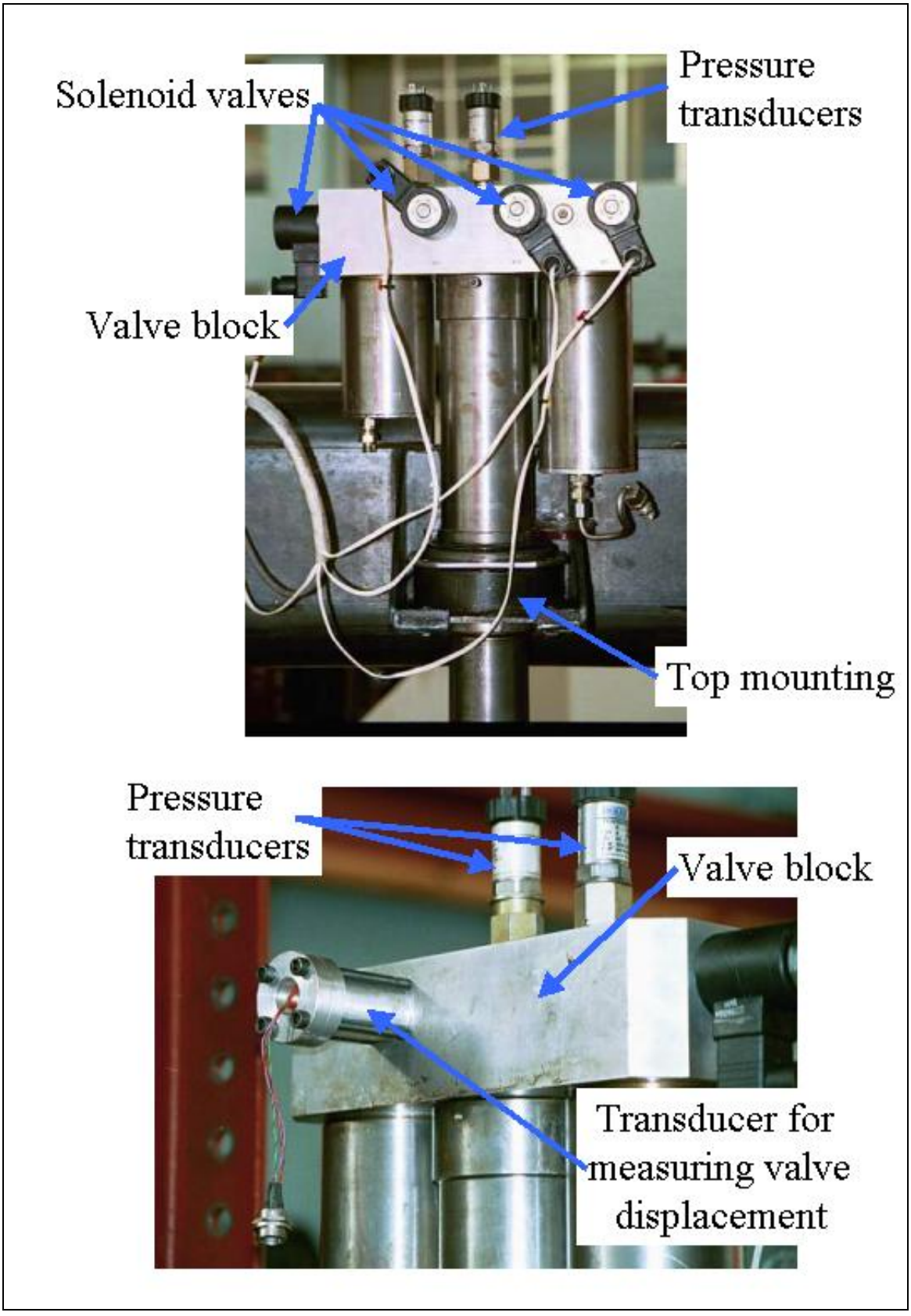

Figure 4.17 - $4S_4$ Prototype 2 on test rig

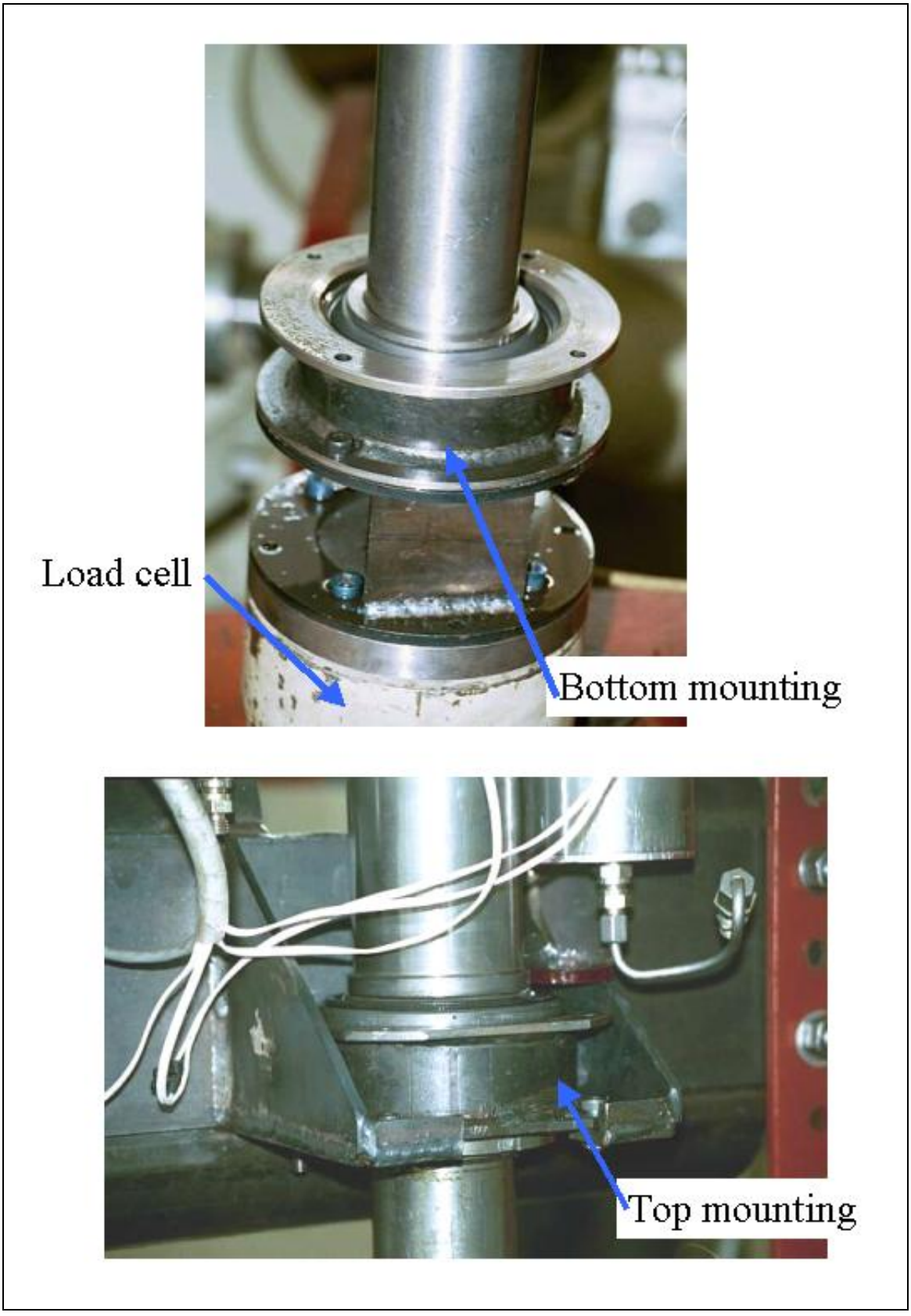

Figure 4.18 - $4S_4$ strut mounting to test rig

vi) Install the unit in the test rig.
vii) Reconnect the valves and apply power so that all the valves are open.
viii) Remove the M8 cap screws used to bleed off gas from the accumulators from the accumulator end caps.
ix) Slowly compress the unit to the maximum compression (bump) position, noting the force on the load cell whilst doing so.
x) If the force on the load cell starts increasing rapidly before maximum compression is reached, investigate the problem before continuing.
xi) When maximum compression is reached, measure the distance between the accumulator end caps and the floating piston through the gas bleed hole with a vernier. This distance should be 29 mm for the small (0.1 litre) accumulator and 62 mm for the big (0.4 litre) accumulator. The cavities in the accumulator end caps have been designed to result in the correct gas volumes in the maximum compressed positions when the floating pistons are resting against the end caps.
xii) If any of these two distances are greater than indicated, there is not enough oil in the strut. If this is the case, remove the highest blanking plug on the valve block. Extend the strut by about 10 mm. Fill the strut with more oil. Repeat steps (ix) to (xii) until the strut if filled completely. If there is too much oil in the strut, the excess can be drained off by removing the highest blanking plug and compressing the strut fully.
xiii) Once filled with oil, charging the accumulators with Nitrogen gas can begin.
xiv) Close the valves.
xv) Replace the gas bleed valve on the small (0.1 litre) accumulator.
xvi) Load gas into the small accumulator (about 1 MPa maximum).
xvii) Extend the strut by a distance of 40.8 mm by moving the actuator downwards.
xviii) Load more gas into the small accumulator until the required static spring force is reached on the actuator. For all the tests in this chapter, the accumulator was loaded to 7.8 kN (or 4 MPa). This should be done slowly to allow the gas to reach equilibrium temperature.
xix) Open all valves.
xx) Replace the gas bleed valve on the big (0.4 litre) accumulator.
xxi) Load some gas into the big accumulator.
xxii) Extend the strut by a further distance of 119.2 mm by moving the actuator downwards. This represents a total movement of 160 mm downwards.
xxiii) Load more gas into the big accumulator until the required static spring force is reached on the actuator. For all the tests in this chapter, the accumulator was loaded to 7.8 kN (or 4 MPa). This should be done slowly to allow the gas to reach equilibrium temperature.
xxiv) Check to make sure that there are no gas or oil leaks.
xxv) The unit is now ready for testing or vehicle installation.

4.7.2 Bulk modulus

Normally in hydraulic applications, the oil is assumed to be incompressible. In hydropneumatic suspension systems, ignoring the compressibility of the oil can result in significant errors. The compressibility effect is aggravated by the fact that there is always air present in the oil. Air is entrapped in the oil during filling due to mixing and diffusion. Air also gets trapped in channels in the valve block, behind seals and o-rings and in the

valves. One possible way of reducing this problem might be to remove air by using a vacuum pump. The current method of filling the unit is to pour oil slowly into the strut, giving enough time for air to escape. The strut is also moved slowly in all directions in an attempt to remove all the trapped air. This procedure may take several hours before all air bubbles disappear and even then there is a good possibility of air still trapped in the system. The total volume of oil required to fill the rear strut using this method was measured to be 1.6 litres.

The bulk modulus of the fluid is given by:

$$\beta = \frac{\Delta P}{\left(\frac{\Delta V}{V}\right)} \tag{4.1}$$

where:

β = Bulk modulus of the fluid [Pa]
ΔP = change in pressure of the fluid between two conditions [Pa]
ΔV = change in volume of the fluid between the same two conditions [m^3]
V = total volume of fluid in the system at atmospheric pressure [m^3]

To determine the bulk modulus of the oil in the strut, the accumulators are blocked with steel spacers so that the accumulator pistons cannot move (no gas in accumulators). The strut is then compressed slowly whilst the force and relative displacement is measured. Force and displacement is converted to pressure and volume by using the piston area (see Figure 4.19). The pressure initially stays almost constant until the spacers in the accumulators start compressing. At this point the accumulators become solid and only the oil is compressed. This assumes that the strut itself is incompressible which is a good assumption in this case.

The value for the bulk modulus measured on the strut is 1.368 GPa as shown in Figure 4.19. This compares favourably with typical values of bulk modulus of 1.4 GPa for hydraulic oil (**Poley, 2005**).

4.7.3 Thermal time constant

The thermal time constant is a measure of the heat transfer coefficient between a gas in a closed container and its surroundings **(Els and Grobbelaar, 1993)**. In the case of the hydropneumatic suspension system, it is determined experimentally by displacing the strut with a step input displacement at the highest possible velocity. During the step, the gas is compressed adiabatically (i.e. there is no time for heat transfer between the gas and its surroundings). The temperature will rise and then slowly return to the ambient value. On the other hand, in the case of a rebound step input, the gas will expand. The temperature will drop first and then rise to the ambient value. The time required for the temperature to change by 63%, between the initial value (immediately after the step) and final ambient value, is defined as the thermal time constant (τ).

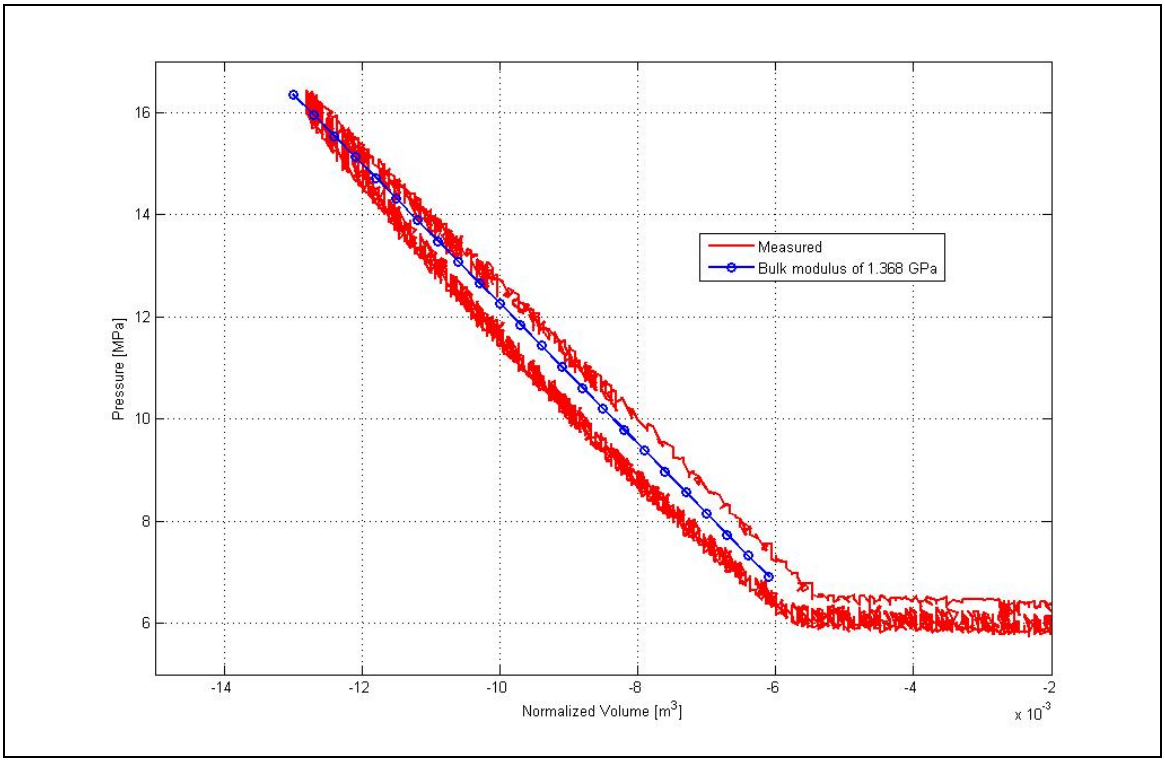

Figure 4.19 - Measured bulk modulus

Strictly speaking the thermal time constant is defined in terms of temperature. Measuring temperature fluctuation accurately at high speed is very difficult. If the ideal gas assumption is valid, then the time constant can be obtained from pressure or force measurements. The pressure in the strut is measured *vs.* time as indicated in Figure 4.20. The strut must be kept stationary both before and after the high-speed step input. The thermal time constant was measured with no damper packs in the system (i.e. free flow dampers). The experimentally determined thermal time constants for Prototype 2 are shown in Table 4.1 for three different test conditions. The values given for the soft spring are the combined time constant for both accumulators, while the stiff spring results are for the small accumulator only. The thermal time constants for compression and rebound compare well for each test, but the values depend significantly on the displacement of the step. **Els (1993)** however indicates that the analyses is fairly insensitive to the value of the thermal time constant and differences as large as 30% still result in acceptable predictions.

Table 4.1 – Thermal time constants

File name	Spring setting	Size of step input [mm]	P_{begin} [MPa]	P_{end} [MPa]	ΔP [MPa]	63% point [MPa]	τ [s]
TYD1 - Compression	Soft	25	5.07	4.91	0.16	4.97	10.1
TYD1 – Rebound	Soft	25	4.30	4.45	0.15	4.39	9.9
TYD2 - Compression	Soft	50	5.99	5.55	0.44	5.71	7.1
TYD2 – Rebound	Soft	50	4.11	4.42	0.31	4.31	7.1
TYD3 – Compression	Stiff	25	8.83	6.57	2.26	7.41	4.8
TYD3 - Rebound	Stiff	25	3.43	4.23	0.80	3.93	4.85

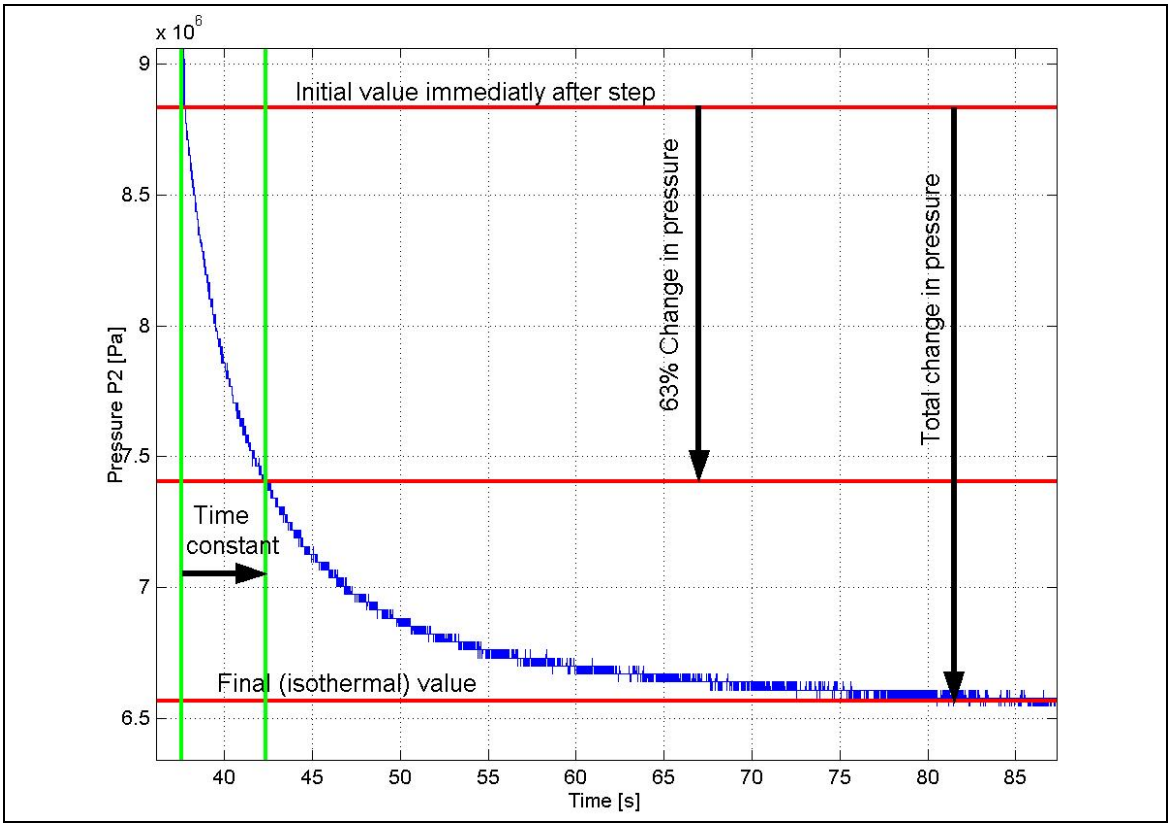

Figure 4.20 - Determination of thermal time constant

4.7.4 Spring characteristics

The two spring characteristics are determined by displacing the actuator slowly with a triangular wave input displacement with a frequency of 0.001 Hz or a period (duration) of 1000 s. This means that the strut is first compressed from the static position to maximum compression at a constant speed. The strut is then extended to the maximum rebound position, again at constant speed and finally returned to the static position at constant speed. This sequence is repeated for typically three cycles, although the graphs in the rest of this chapter only show data for typically one cycle. Figure 4.21 displays the soft spring characteristic measured for one complete compression and rebound cycle lasting 300 seconds. The measured value is compared to the predicted isothermal spring characteristic calculated for a static gas volume of 0.5 litres. Excellent correlation is observed. The small hysteresis loop in the measured characteristic can be attributed to heat transfer between the gas and the surroundings. This effect is well documented by **Els (1993)**. Other possible contributing factors are seal friction and hysteresis in the test frame.

Figure 4.22 indicates the stiff spring characteristic measured for a complete compression and rebound cycle. The displacement cycle starts in the static position, compresses the spring to -62 mm, extends the spring to +75 mm, compresses the spring again to -62 mm and then returns to the static position. This cycle lasts 1000 seconds. The measured value is again compared to the predicted isothermal spring characteristic, but in this case there is a significant discrepancy between measured and predicted results. The hysteresis loop in the measured characteristic can again be attributed to heat transfer between the gas and the surroundings, friction and hysteresis in the test frame. Further investigation indicated that the discrepancy in the stiff spring characteristic could partly be attributed to the

compressibility of the oil (usually deemed negligible). Figure 4.23 indicates a straight line corresponding to the bulk modulus of 1.368 GPa determined in paragraph 4.7.2. The compressibility is significant for the stiff spring characteristics and needs to be taken into account during spring calculations. The figure also indicates the very good correlation achieved when the spring characteristic is corrected using the bulk modulus. The correlation is however achieved with a static gas volume of 0.13 litres and not the 0.1 litres expected. Several sets of tests were performed on Prototype 2 where the damper configuration was changed. This meant that the unit had to be discharged and recharged every time. At the beginning of each new test series, the spring characteristics were measured. Significant variations in actual gas volume were found when measured characteristics were compared to predicted values. This re-iterates the fact that the oil filling and gas charging procedures are extremely important and still needs improvement to limit the errors due to static gas volume discrepancies.

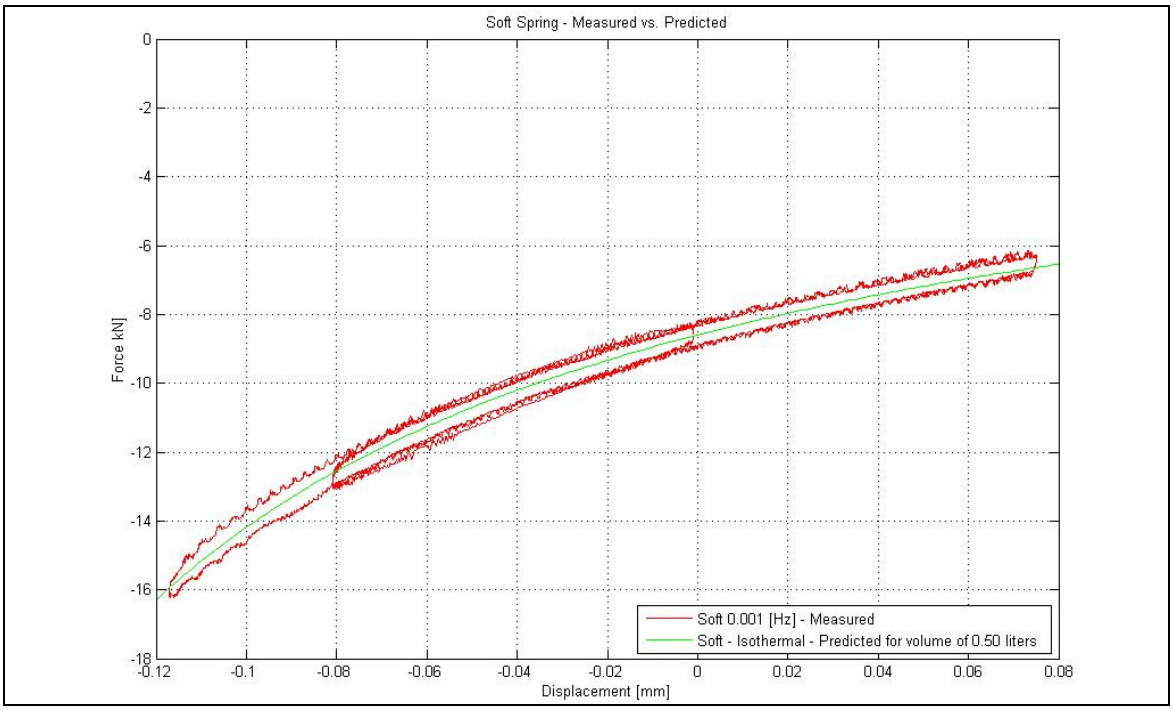

Figure 4.21 - Soft spring characteristic

Figure 4.23 indicates measured isothermal characteristics for both the soft and stiff springs.

4.7.5 Damping characteristics

The hydraulic damper characteristics of the suspension unit consists of different components, the most important of which are:

i) Pressure drops over valve block channels and ports
ii) Pressure drops over valves (partially and fully open)
iii) Pressure drops over hydraulic damper packs

These pressure drops are dependent on the flow rate through the various components. Measuring these characteristics on the prototype is very difficult because of all the

possible combinations and the fact that it is very difficult to isolate specific components to determine their individual contributions. In most instances it is impossible to measure or calculate the flow through a specific component as the flow is often split between the damper, the bypass valve, and the two accumulators. For these reasons the discussion that follows does not attempt to give exact values for individual components, but rather to give a better understanding of all the interactions and the orders of magnitude. This explains why most of the graphs indicate pressure drops against strut speed and not flow.

By closing off the large accumulator with valve 3 (see Figure 4.7), all the flow is forced into the small accumulator. The flow into the small accumulator can now be calculated by multiplying the speed with the piston area. Figure 4.24 indicates four different lines for the pressure difference (P_1–P_2) against flow. The data for "Valve block channel only" was measured on Prototype 2 with no damper packs installed in the unit, i.e. the only flow resistance was that of the valve block. "Valve block channel and valve" was measured with solid damper packs in the unit, i.e. with all oil flowing through the valve. Also indicated is the data measured by **De Wet (2000)** under steady state conditions on a hydraulic test bench, and the valve manufacturer's specification. All these values correlate exceptionally well, especially if taken into account the variation in test conditions and hydraulic oil used. Curve fits through the data are indicated in Figure 4.25. As expected the pressure drop is proportional to the square of the flow rate. Values for both flow directions are also very similar. These curve fits can be used in the mathematical model.

Figure 4.26 indicates the effect of a single valve in the V_3 position as well as for two identical valves in parallel. It is clear that the concept of two valves in parallel works very well as the pressure drop is significantly reduced. The ratio between the two graphs is not exactly a factor of two due to the fact that the ports and channels connecting the two valves in parallel are not identical.

The most important damper characteristic, as far as vehicle dynamics is concerned, is the force velocity relationship of the high damping and low damping characteristics respectively as measured using a triangular wave displacement input at various frequencies. Figure 4.27 indicates this relationship for the stiff spring with low damping (V_3 closed and V_1 open), stiff spring with high damping (V_3 and V_1 closed) as well as the soft spring with low damping (all valves open). The damper packs in the strut were sourced from standard Land Rover rear dampers. Also indicated on the graph is the baseline Land Rover Defender 110 rear damper characteristic, correctly scaled for the new application as explained below. The baseline graph is included as an indication of what could theoretically be expected in the case of the stiff spring with high damping. The baseline graph is scaled because the standard piston diameter is 35 mm and the piston diameter on Prototype 2 is 50 mm. For the same linear velocity, the flow in Prototype 2 will be higher than that on the baseline Land Rover damper by a factor of $(0.050)^2/(0.035)^2$ or 2.04. The force on Prototype 2 will also be higher than the force on the baseline Land Rover damper for the same pressure difference across the damper pack, also by a factor of 2.04. The Land Rover damper characteristic can therefore be scaled for Prototype 2 by multiplying the force by 2.04 and dividing the velocity by 2.04. It can be seen from Figure 4.27 that there is some discrepancy between the expected and measured characteristics. In the low speed region the Prototype 2 forces are lower than expected. This is attributed to leakage past the o-ring seals that mount the damper packs into the

cavity of Prototype 2. At higher speeds the Prototype 2 damping force is higher. This can be expected due to the extra flow losses through the valve block ports and channels.

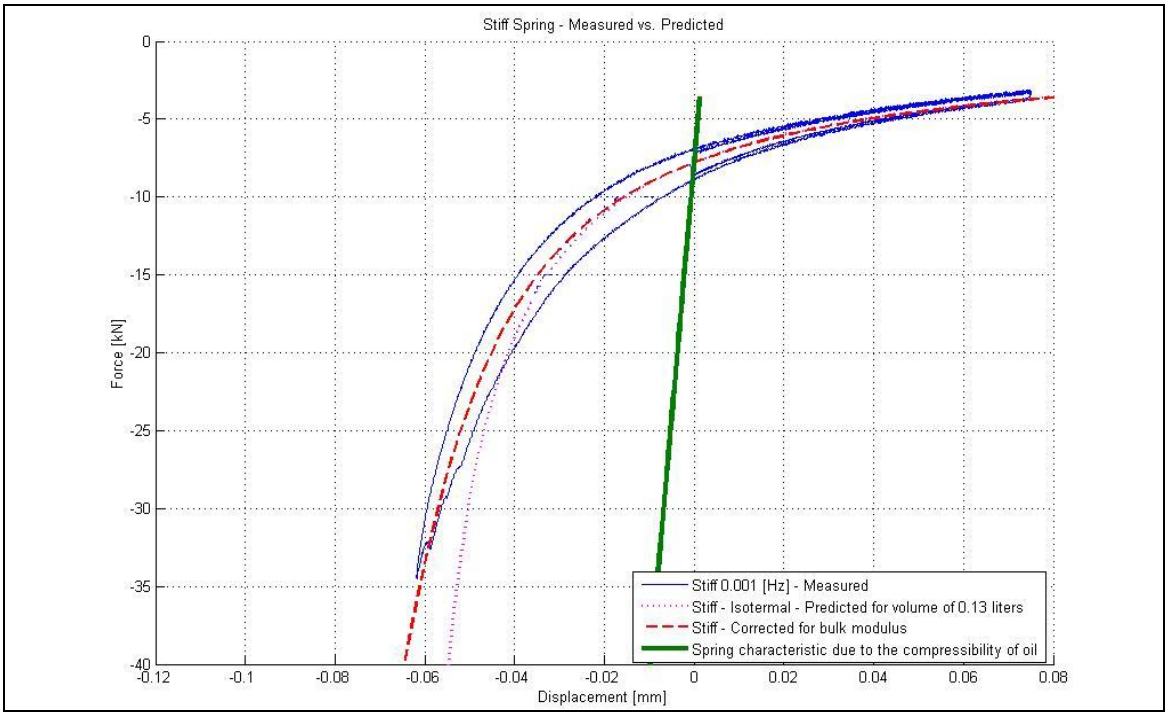

Figure 4.22 - Stiff spring characteristic

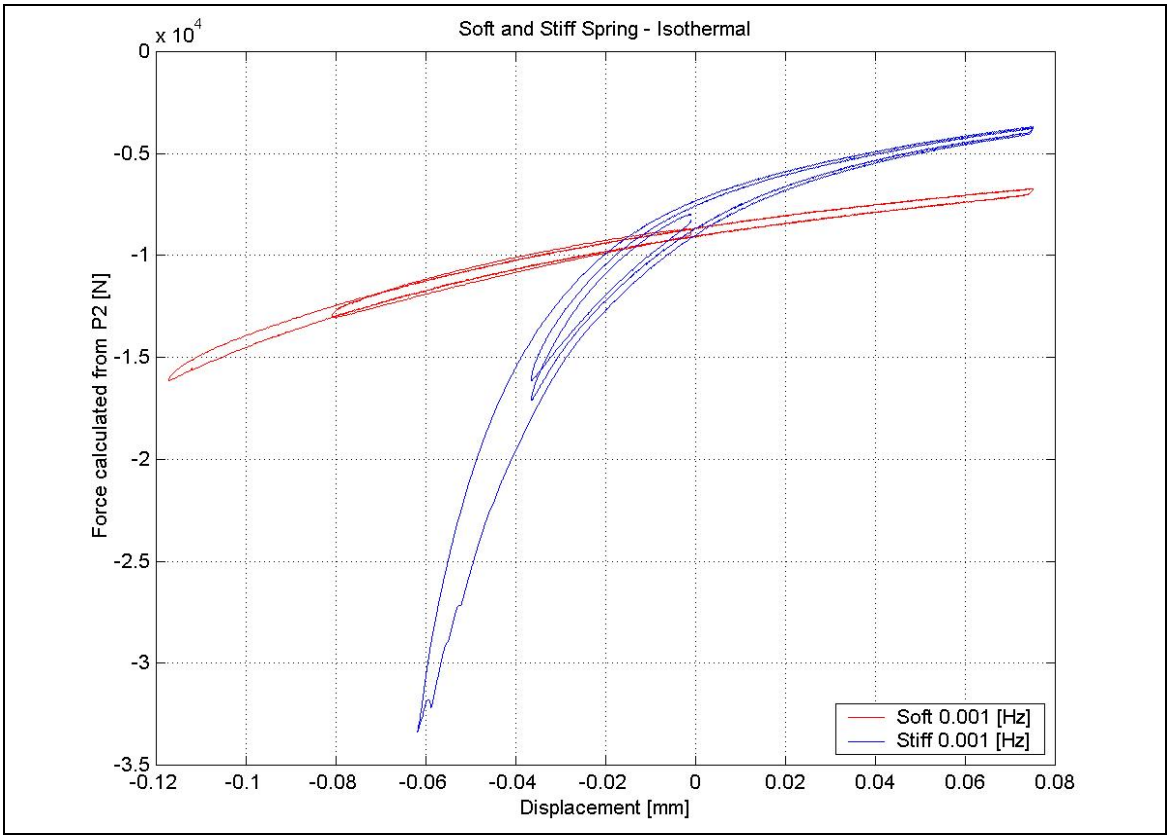

Figure 4.23 - Soft and stiff spring characteristics

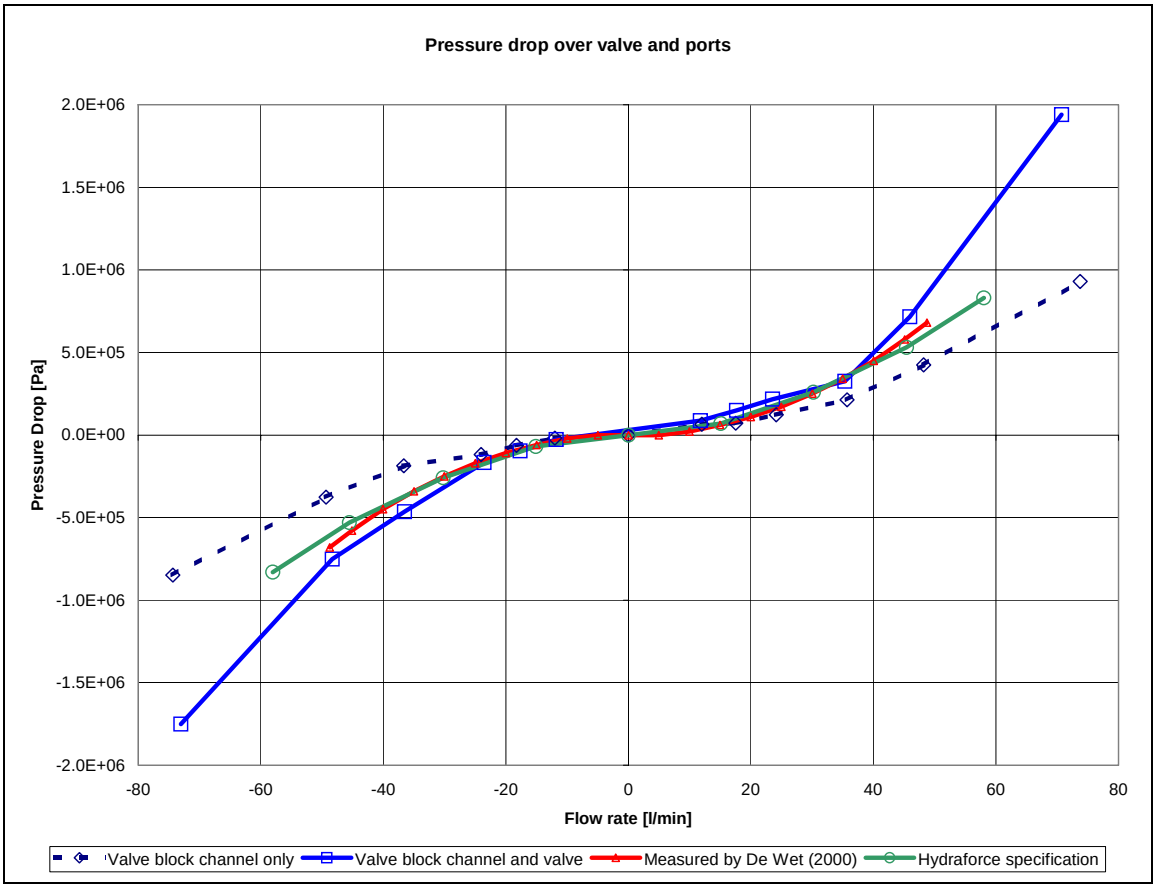

Figure 4.24 - Pressure drop over valve 1

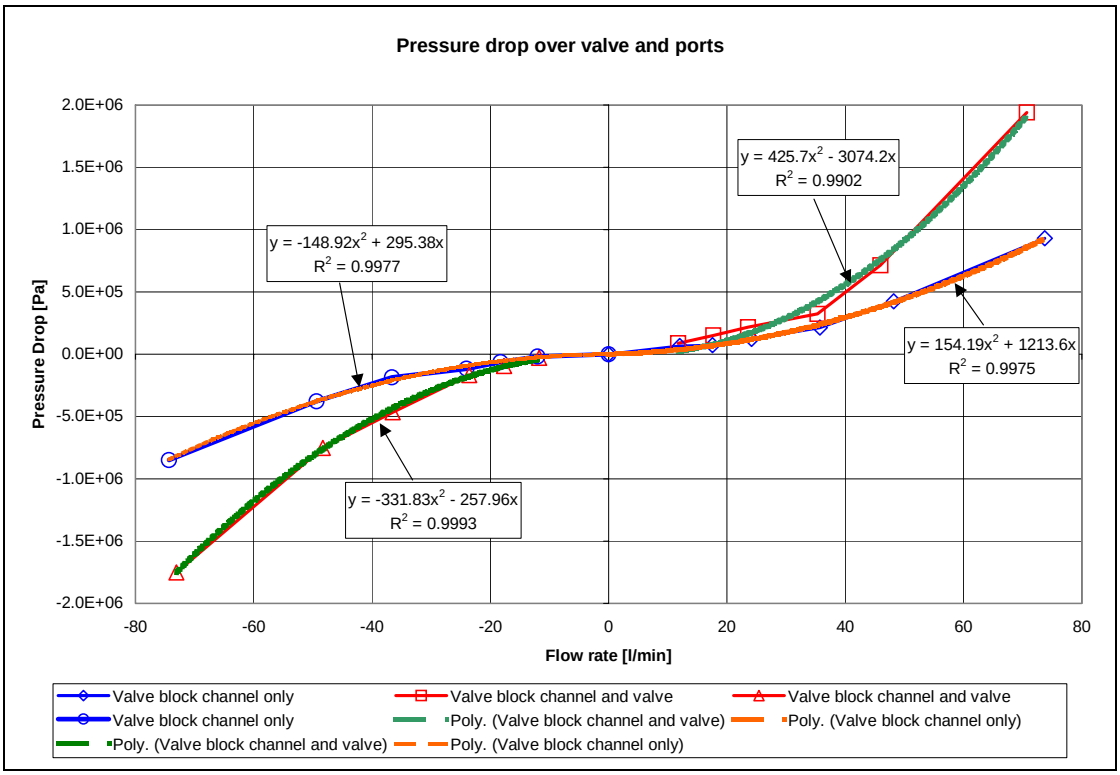

Figure 4.25 - Curve fits on pressure drop data

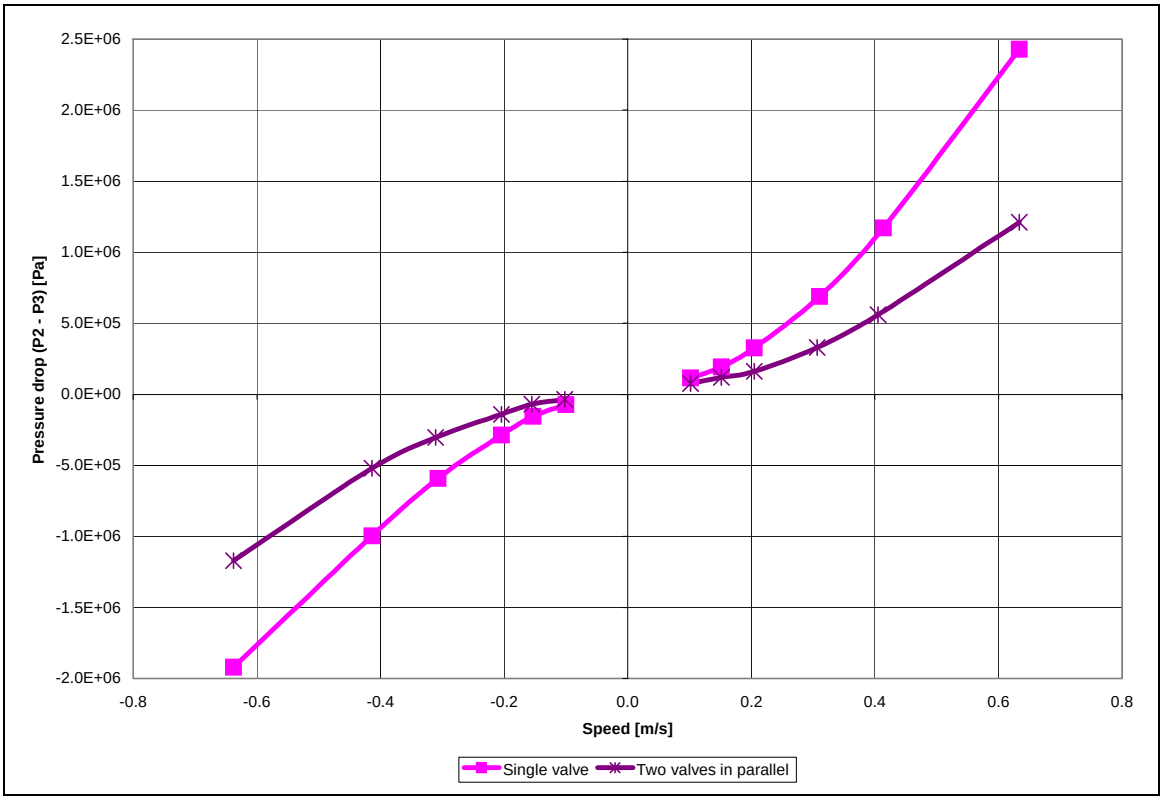

Figure 4.26 - Pressure drop over valve 3 (single valve *vs.* 2 valves in parallel)

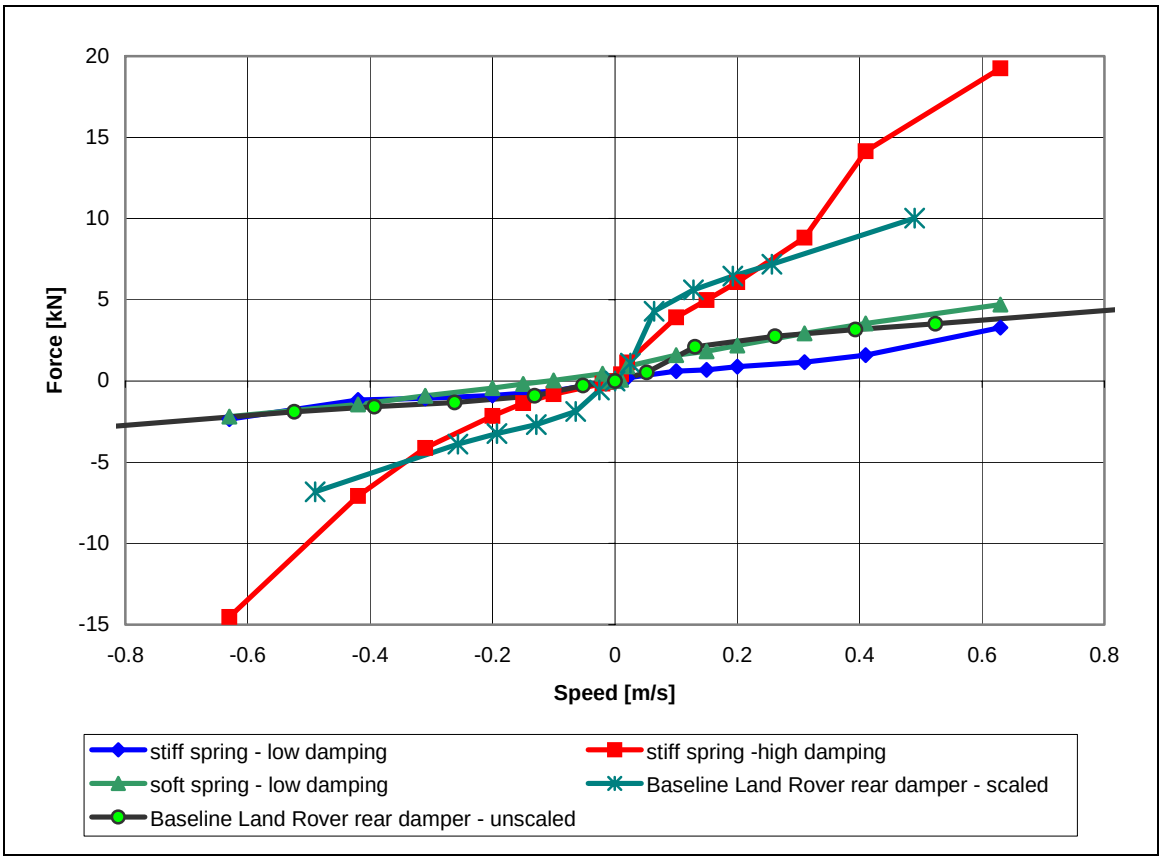

Figure 4.27 - Damper characteristics for Prototype 2

4.7.6 Valve response times

Valve response times are very important for predicting the transient response of the system to valve switching. A typical trend of pressure drop over the valve *vs.* time is shown in Figure 4.28. The solenoid switching signal is indicated on the same graph. To obtain the valve response time, the initial pressure difference (before switching) and the final pressure difference (after the transient response has died away) is determined. Two values (represented by horizontal lines) are calculated representing a 5% change and a 95% change in pressure difference respectively. This is done in order to define the switching points more precisely as the exact moment where the change occurs is very difficult to determine. The time from the solenoid switching signal to the 5% change point is defined as the initial delay. This is the time required for the solenoid to build up enough force so that the valve plunger starts moving. The time between the 5% and 95% point is defined as the transient response time of the valve and represents the time required from the initial plunger movement until the valve is fully open. The total valve response time is the sum of the initial delay and the transient response time as indicated in Figure 4.28.

The valve response times were measured for all 4 four valves. The damper orifices were blocked so that all the flow was channelled through the valves. The valve response time was measured by closing the respective valve, compressing the strut until the required pressure difference was obtained, and then opening the valve. This resulted in flow through the valve until the pressure in the system stabilized. The procedure was repeated in the opposite direction, e.g. closing the valve and extending the strut before opening the valve.

Figures 4.29 and 4.30 give the valve response time (initial delay, transient response time and total response time) as a function of pressure drop across the valve for Prototypes 1 and 2 respectively. Prototypes 1 and 2 were both fitted with the same valves, although Prototype 1 used 24 Volt solenoids. This was changed to 12 Volt solenoids on Prototype 2 to be compatible with the test vehicle's electrical system.

The valve response time is to some extent dependant on the system **(Janse van Rensburg, Steyn and Els (2002)**. All four valves in Prototype 2 are fitted in different positions in the valve block with the result that the channels to these valves are all different. Valve response times are also dependent on the pressure difference across the valve as can be seen in the figure. The valve response time varies from 40 to 100 milliseconds over the pressure range of interest and is acceptable for the current application.

4.7.7 Friction

The isothermal spring characteristic was determined by slowly compressing the spring through its operating range whilst recording force, displacement and pressure. Figure 4.31 indicates the spring force against spring displacement for the soft spring on Prototype 1. Two curves are shown namely the force measured by the load cell, and the force calculated from the pressure data. The measured force shows unacceptable levels of hysteresis, while the force calculated from the pressure measurement gives the expected characteristic.

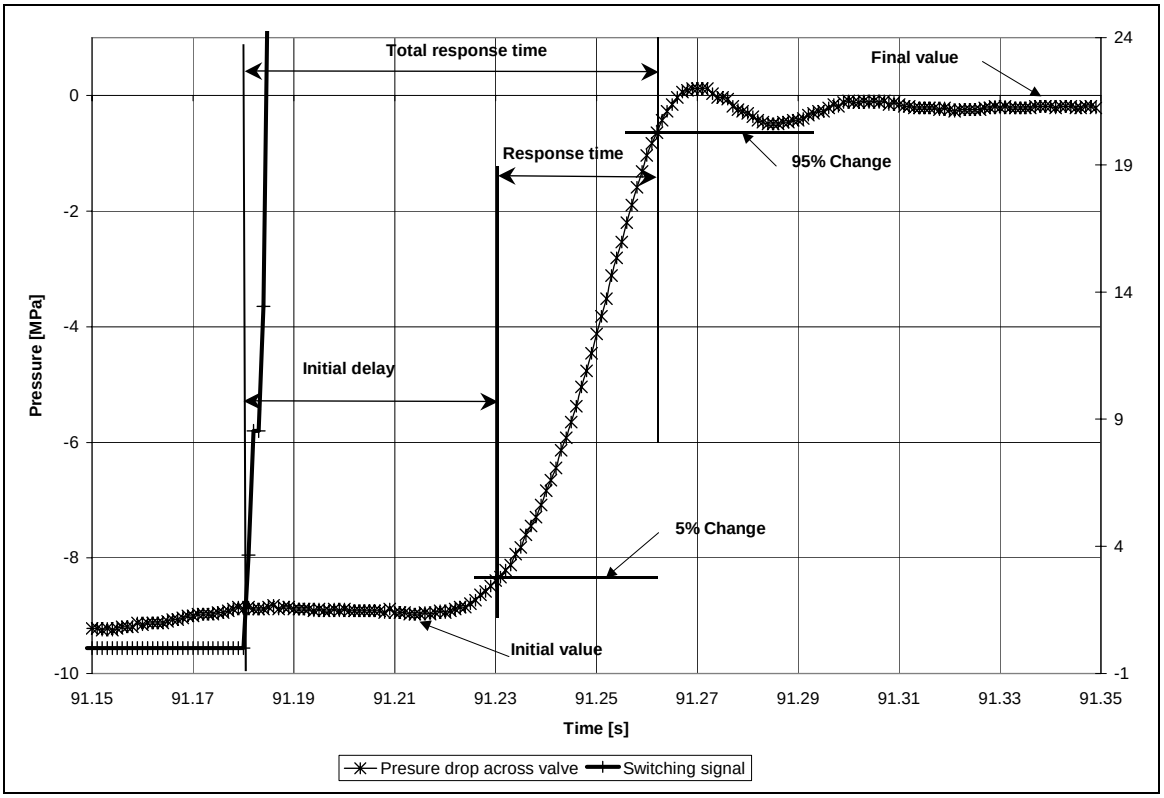

Figure 4.28 - Explanation of valve response time definitions

During initial assembly of the unit, it was found that the main cylinder could be moved easily by hand, while the accumulator pistons had to be moved using compressed air. There was no way to move the accumulator pistons by hand. The hysteresis was therefore attributed to seal friction (stick-slip) in the accumulator seals. After considerable research, two new accumulator pistons were designed and manufactured using wear rings combined with a state-of-the-art accumulator seal (Turcon AQ Seal5) with negligible stick slip. The original design used a fairly basic seal layout with a double o-ring and back-up ring system.

After testing the more advanced sealing concept in the suspension system, it was found that the hysteresis had improved only marginally. Careful investigation traced the problem to the bending moment applied to the main cylinder due to the offset of the chassis mounting arrangement used on Prototype 1. This results in a high side force between the main cylinder and the piston, causing unacceptable friction and wear.

Figures 4.32 to 4.35 illustrate that friction in Prototype 2 is very low and should not cause any serious problems. Friction may however degrade the vibration isolation of the system for small road inputs.

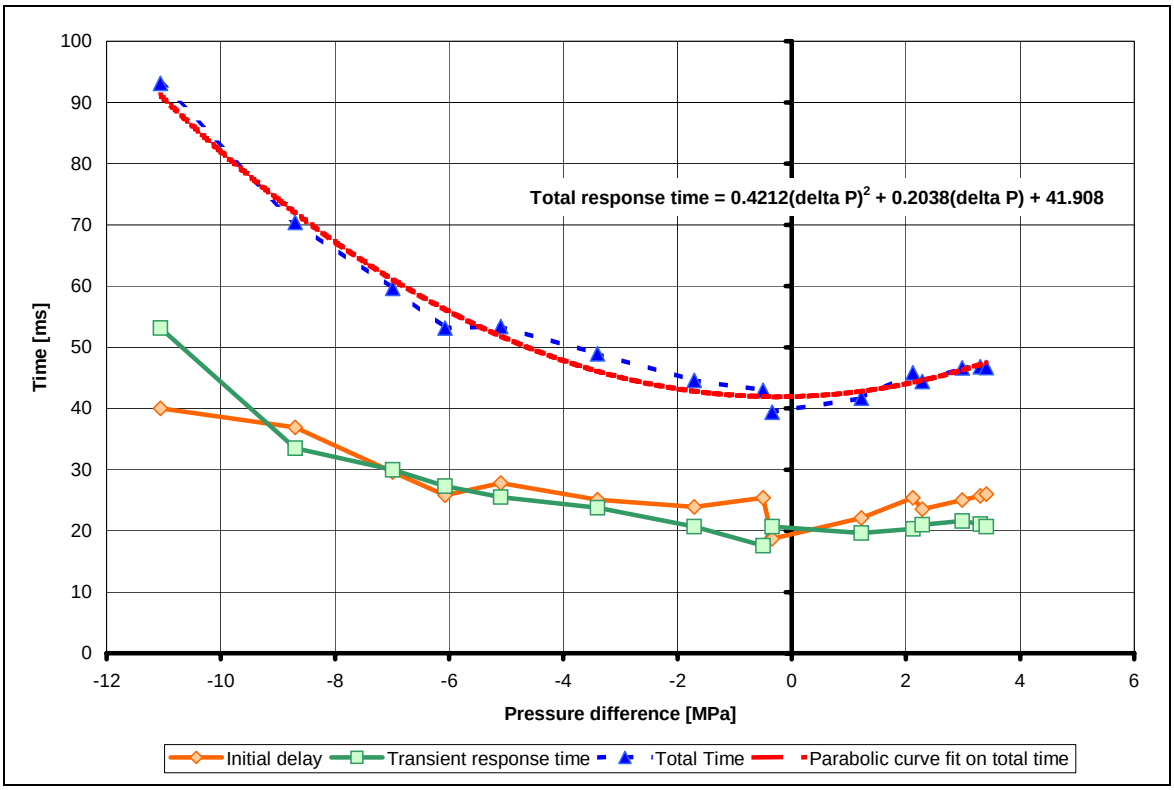

Figure 4.29 - Valve response time for Prototype 1

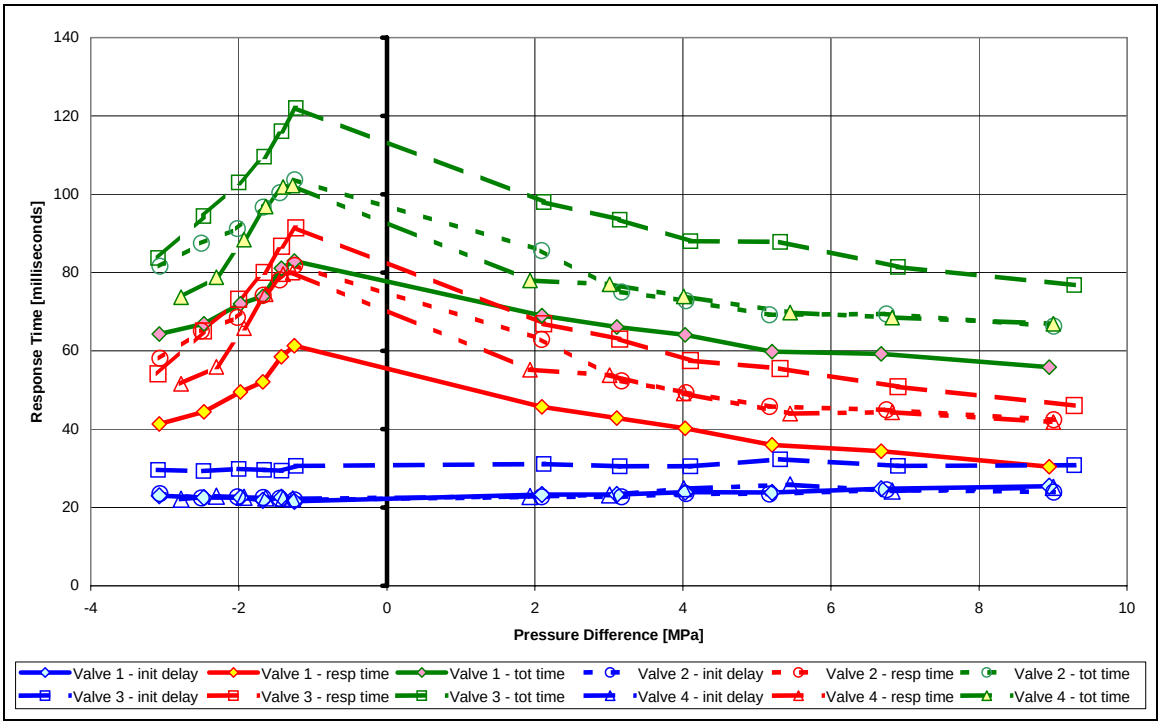

Figure 4.30 - Valve response time for Prototype 2

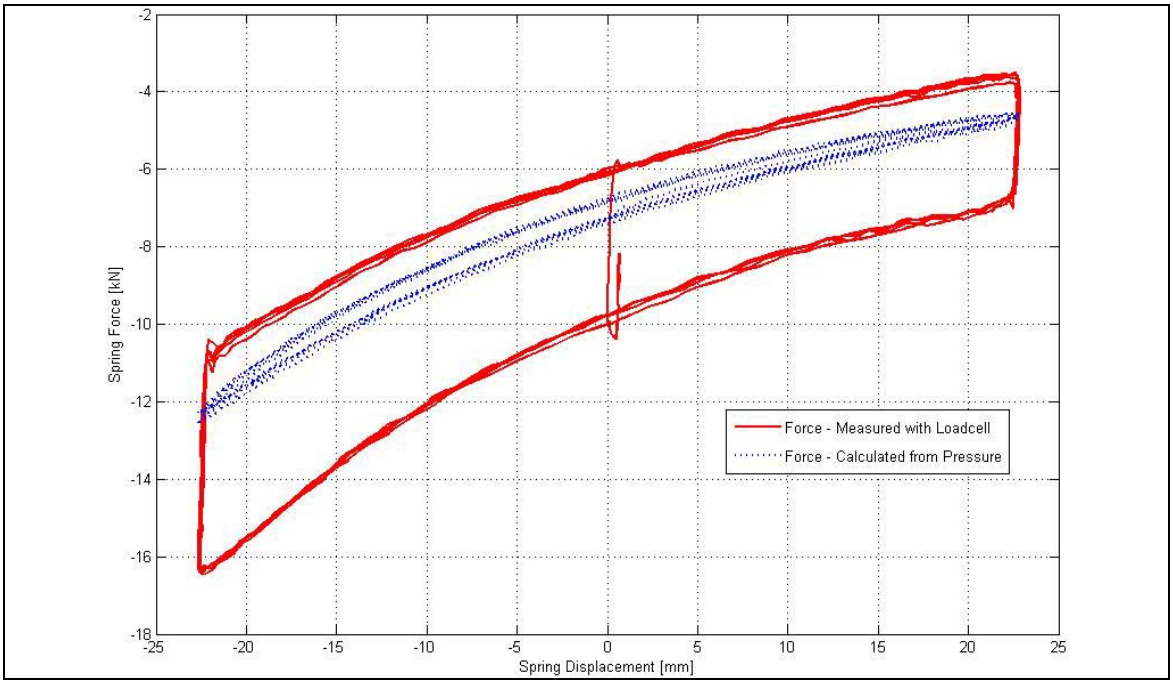

Figure 4.31 - Hysteresis problem on Prototype 1

4.8 Mathematical model

A SIMULINK® model of the suspension unit was developed by **Theron (Theron and Els, 2005)**. This model takes the deflection rate of the suspension unit as input and employs simple fluid dynamics theory in an iterative manner to calculate the flow rates from each accumulator to the cylinder. Iteration takes place until pressure balance in the parallel branches is established. The model then calculates the pressure in the two accumulators by solving the energy equation for an ideal gas in an enclosed container (**Els and Grobbelaar, 1993**) and time integrating the flow rates to determine the gas volumes in the two accumulators. The model renders the dynamic force generated by the suspension unit as output.

Physical tests have been performed on Prototype 2, where the spring characteristics, damper characteristics and valve dynamics have been measured. These tests were described in previous paragraphs. Generally, good correlation exists between the results of the SIMULINK® model and the experimental data measured in the laboratory on the prototype suspension unit. A number of aspects, where the model or the quantification of its parameters needs improvement, were identified.

The aim was to develop a mathematical model that can be used in vehicle dynamic simulations and to investigate suitable control strategies for semi-active switching of the spring and damper.

4.8.1 Modelling philosophy

In developing a mathematical model, a tension force in the unit is considered positive, while a compressive force is negative. Any extension of the unit relative to a reference state is considered as a positive (relative) displacement and compression of the unit as

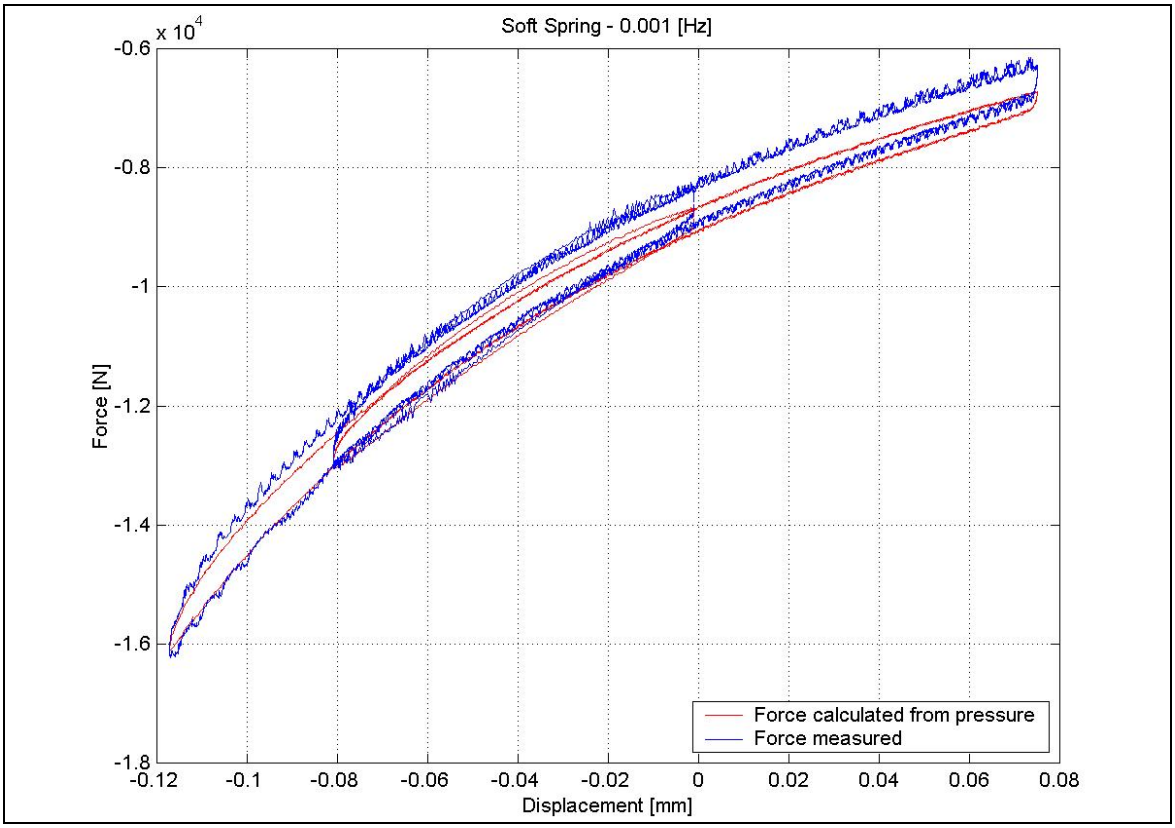

Figure 4.32 - Effect of friction on soft spring at low speeds

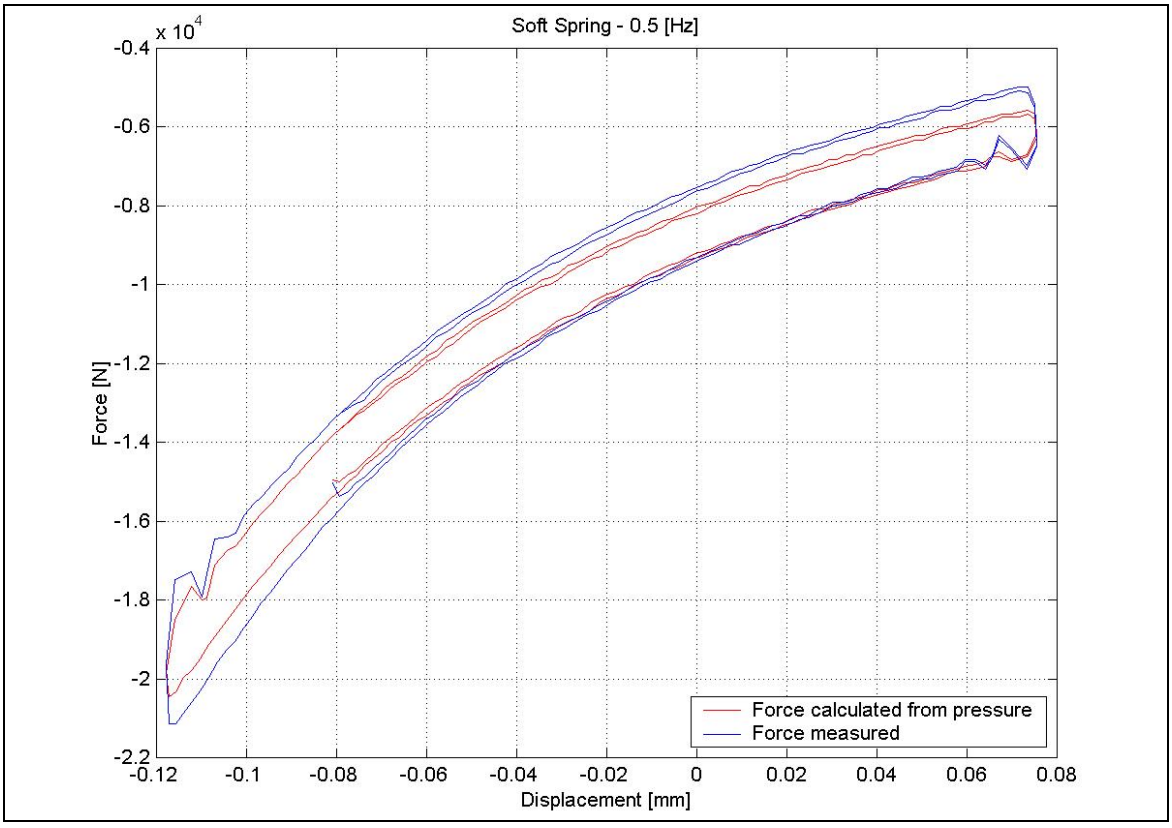

Figure 4.33 - Effect of friction on soft spring at high speeds

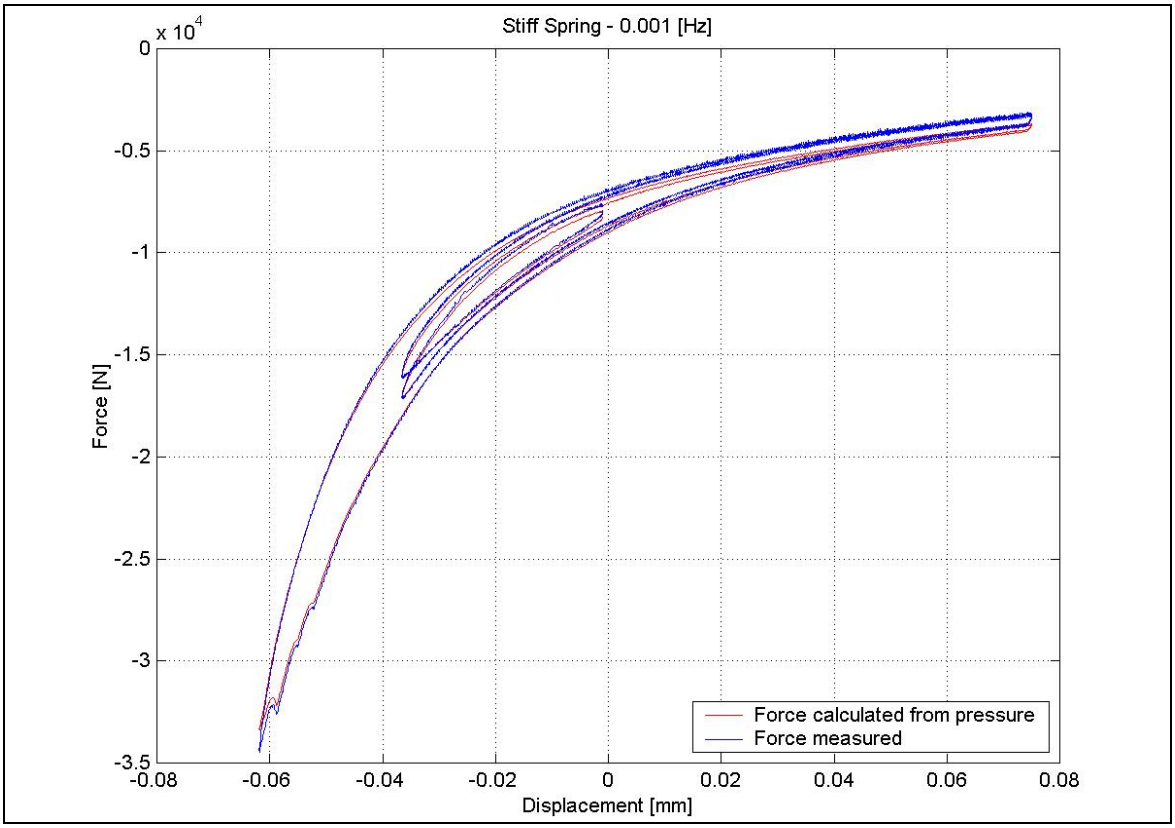

Figure 4.34 - Effect of friction on stiff spring at low speeds

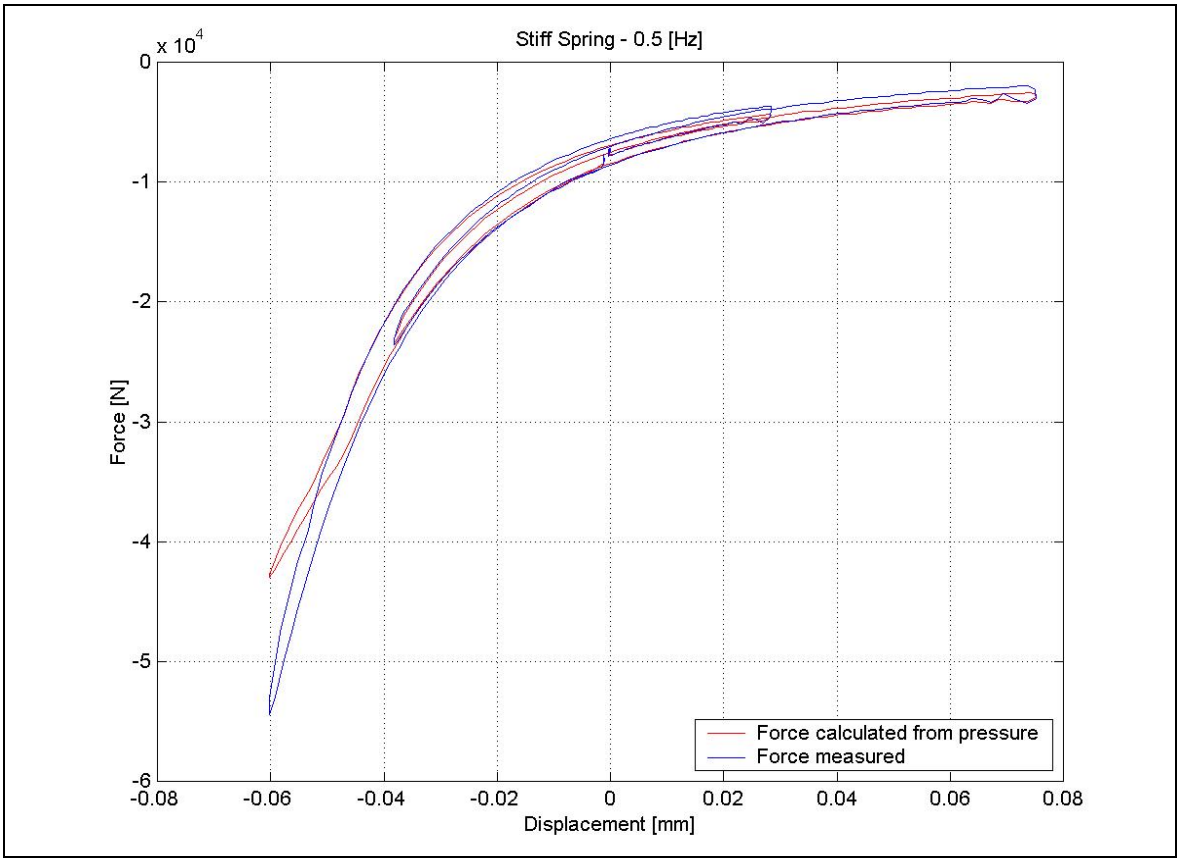

Figure 4.35 - Effect of friction on stiff spring at high speeds

negative displacement. An extensional speed is considered positive and a compression speed as negative.

For the purposes of vehicle dynamics simulation a mathematical model of this unit is required that calculates the combined spring-damper force for a certain set of valve settings and a given state of displacement and speed. One may therefore consider the force of the suspension unit as the output of the model and the valve settings of the three valves and the displacement and speed of the unit as the inputs to the model, where the model calculates the output for given inputs. This calculation is typically performed within a time step in a simulation run and is repeated for each time step.

The working principle of the suspension unit is discussed in paragraph 4.2. Figure 4.7 indicates the various pressures, dampers and valves in the suspension system. The output force of the unit is essentially directly related to the pressure P_2 in the main strut cylinder. This pressure depends on the pressures in the two accumulators, the flow through and corresponding pressure drops over the two dampers with corresponding channels and the valve switching. The pressure in the accumulators depends on the volume of oil in the accumulators, which is related to the displacement of the suspension unit and the state of valve 3. An alternative way of looking at the volume of oil in the accumulators is to realise that this is determined by the flow history, i.e., these volumes may be determined by integrating the flow rates in the two main branches of the system. Using this approach makes the mathematical model independent of the displacement of the unit as an input. This is indeed the approach that was used in modelling the unit. The input to the model of the suspension unit is therefore, in addition to the three valve switch signals, only the extensional speed $\dot{x}$ of the unit. From this the volume flow rate $q = A\dot{x}$ into the main strut cylinder, of cross sectional area A, can directly be calculated. The flow rates in the two branches are taken as q_i, $i = 1,2$, for the branch associated with accumulator i, positive in the direction from the accumulator towards the main strut.

4.8.2 Pressure dependent valve switching

It is assumed that the electric signals with which the various valves are switched changes instantaneously from low to high values, or vice versa. When this happens, valve and other dynamics prevent immediate pressure and flow changes. These dynamic effects are not currently modelled mathematically, but are taken into account empirically. The valve response time was defined and determined in paragraph 4.7.6 (Figures 4.29 and 4.30). The parabolic curve indicated in Figure 4.29 (although determined for Prototype 1) was subsequently employed in the mathematical model with respect to all three valves and for both prototypes.

Wherever the state of the valve is taken into account in the model, a fraction f_i between zero and one is used, where the subscript $i = 1,2,3$ indicates the valve number. For switching on the valve (electric signal going from low to high, valve going from closed to open) $f_i = 0$ before the electrical signal switches, $f_i = 0.05$ at half the valve response time after the electrical signal switches, $f_i = 0.95$ at the valve response time and $f_i = 1$ after 1.5 times the valve response time. In between these time points a piecewise cubic Hermite interpolation is used to calculate the fraction. For switching off the valve the same type of interpolation is used on the reversed sequence.

4.8.3 Pressure drop over dampers and valves

Due to the complexity of possible dampers that may be used in the suspension unit, it was decided to use table look-up techniques to get the pressure drop over the damper for a given flow rate through the damper. Quite often the pressure-flow characteristics display significant hysteresis. For now the table look-up procedure employed does not provide for possible hysteresis. The pressure drop over the damper was measured, with the by-pass valve both open and closed, for various positive and negative flow rates in a practically realistic range. This measured data was used to establish a high damping and a low damping damper curve, corresponding to the by-pass valve being closed and open, respectively. These curves are used in the table look-up procedure for both dampers 1 and 2, since they currently are identical and their by-pass valves are also identical. The fact that the internal passages in the valve block for the two dampers at this time are not identical is neglected in the model.

For a certain flow rate q_i the pressure drop over damper i with $i = 1,2$, is calculated as $\Delta P_{di} = f_i \Delta P_{doi} + (1 - f_i)\Delta P_{dci}$, where ΔP_{dci} is the pressure drop interpolated at q_i from the high damping graph of damper i, while ΔP_{doi} is the pressure drop interpolated at q_i from the low damping graph of damper i.

When valve 3 is fully open ($f_3 = 1$), the pressure drop over valve 3, ΔP_{v3}, is calculated using an experimentally determined loss factor and the flow q_2. When the valve is opening ($0 < f_3 < 1$, f_3 increasing), a value ΔP_{v3o} is calculated in exactly the same way as ΔP_{v3} above, but the actual pressure drop over the valve is taken as $\Delta P_{v3} = f_3 \Delta P_{v3o} + (1 - f_3)\Delta P_{v3i}$, where ΔP_{v3i} is the pressure drop over the valve before the switching started. When the valve is closing ($0 < f_3 < 1$, f_3 decreasing), on the other hand, the actual pressure drop over the valve is taken as $\Delta P_{v3} = f_3 \Delta P_{v3o} + (1 - f_3)\Delta P_{v3e}$, where ΔP_{v3e} is the pressure drop over the valve calculated for the scenario where all variables are at their current values except $q = q_1$ and $q_2 = 0$, i.e., as if valve 3 is fully closed.

4.8.4 Flow and pressure calculation

The mathematical model is essentially based on the assumption that the hydraulic fluid is incompressible. In the simulation, however, the compressibility of the fluid is taken into account as a refining correction in the calculation of the gas volumes in the accumulators. This correction is based on the various major volumes of fluid in the system, each at its respective pressure, and the bulk modulus of the hydraulic fluid (see paragraph 4.7.2).

Whenever valve 3 is closed, the system can be modelled as a third order non-linear state space system; otherwise a fourth order non-linear state space system with an algebraic constraint is obtained. These two alternative situations will now be considered separately.

i) Valve 3 closed

When valve 3 is closed, $q = q_1$ and $q_2 = 0$, due to the assumed incompressibility of the hydraulic fluid. Let the volume of gas in accumulator i be V_{gi}. The rate of change in the gas volume in accumulator 1 is

$$\dot{V}_{g1} = q_1 \ . \tag{4.2}$$

The pressure P_{accui} in the accumulator i is calculated using the ideal gas law

$$P_{accui} = m_i R T_i / V_{gi} = R T_i / v_i \ , \tag{4.3}$$

where: m_i is the mass of gas with which the accumulator is charged, $R = 296.797$ is the gas constant for Nitrogen, $v_i = V_{gi} / m_i$ is the specific volume and T_i is the absolute temperature of the gas in the accumulator. ($P_{accui} = P_1$ for accumulator 1 and $P_{accui} = P_4$ for accumulator 2.) T_i is calculated by solving the following differential equation, as suggested by **Els (1993)** and **Els and Grobbelaar (1993)**:

$$\dot{T}_i = \frac{T_{i0} - T_i}{\tau_i} - \frac{T_i}{c_v}\left(\frac{\partial P_{accui}}{\partial T_i}\right)_v \dot{v}_i \tag{4.4}$$

where T_{i0} is the initial gas temperature, in this taken as the ambient temperature, τ_i is the thermal time constant of the accumulator and c_v is the specific heat at constant volume of the gas. The thermal time constant is taken at experimentally determined values of 4.8 seconds for both accumulators (see paragraph 4.7.3). Calculating the gas temperature in this way means that if the gas is suddenly compressed, the model calculates the pressure rise along an adiabatic compression curve, while the temperature rises. However, if the gas is subsequently allowed to cool down, the model allows the pressure to drop to the value indicated by the isothermal compression curve.

From equation (4.3) it follows that

$$\frac{\partial P_{accui}}{\partial T_i} = \frac{R}{v_i} \ . \tag{4.5}$$

Substituting this in equation (4.4) renders

$$\dot{T}_i = \frac{T_{i0} - T_i}{\tau_i} - \frac{T_i R}{c_v V_{gi}} q_i = f_{Ti}(T_i, V_{gi}, q_i) \ , \tag{4.6}$$

where the $f_{Ti}(T_i, V_{gi}, q_i)$ on the right hand side indicates that $\dot{T}_i$ is a function of the variables T_i, q_i and V_{gi}. Equation (4.6) is non-linear due to the appearance of the product of these variables.

Since $q_2 = 0$, there is no change in the gas volume in accumulator 2. The pressure in this accumulator may however still change, as the gas temperature may change. The third order system is thus defined by the three differential equations, equation (4.2) and equation (4.6) for $i = 1,2$. Within a simulation time step, in addition to these three differential equations, various other variables are calculated (for example, the accumulator pressures with equation (4.3)). There are, however, no algebraic equations that need to be solved simultaneously with the three differential equations, and the solution is therefore fairly straightforward.

Once q_1 for the current time step has been calculated, the pressure P_2 in the main strut cylinder is calculated by calculating ΔP_{d1} as described in section 4.8.3 above, and then $P_2 = P_1 - \Delta P_{d1}$. With P_2 known the output of the model is simply calculated by multiplying this pressure with the negative of the main strut cross sectional area.

ii) Valve 3 open, opening or closing.

When valve 3 is partially or fully opened, the flow rate q_2 is no longer zero. Due to the assumed incompressibility of the hydraulic fluid, $q = q_1 + q_2$. The rate of change in gas volume in accumulator 1 is still given by equation (4.2), while the rate of change in the gas volume in accumulator 2 is

$$\begin{aligned} \dot{V}_{g2} &= q_2 \\ &= q - q_1 \end{aligned} \tag{4.7}$$

In this case, however, an additional algebraic equation needs to be solved simultaneously with the differential equations. This equation may be considered as a constraint that needs to be satisfied, namely that the pressure P_2 in the main strut cylinder calculated along two different paths must be the same. Let P_{21} be the pressure in the main strut cylinder, calculated along the branch connecting this to accumulator 1 as outlined in section 4.8.4(i) above (which for a given flow rate q_1 is also valid in this case). P_{21} is therefore a function of the flow rate q_1 and the pressure P_1. The pressure P_1, by equation (4.3), is a function of T_1 and V_{g1}. Therefore $P_{21} = P_{21}(q_1, T_1, V_{g1})$. In a similar way the pressure P_{22} in the main strut cylinder, calculated along the branch connecting this to accumulator 2, may be calculated, by first calculating ΔP_{d2} and ΔP_{v3} at flow rate $q_2 = q - q_1$, as described in section 4.8.3 above. Then, $P_3 = P_4 - \Delta P_{d2}$ and $P_{22} = P_3 - \Delta P_{v3}$. The pressure P_4 is a function of T_2 and V_{g2}, therefore, $P_{22} = P_{22}(q, q_1, T_2, V_{g2})$. The algebraic constraint may then be written as:

$$0 = P_{21}(q_1, T_1, V_{g1}) - P_{22}(q, q_1, T_2, V_{g2}) \ . \tag{4.8}$$

Also, whereas equation (4.6) is still valid for accumulator 1, for accumulator 2 the flow rate q_2 needs to be substituted with $q - q_1$, so that the system dynamics may be summarized in the following non-linear state space representation:

$$\begin{bmatrix} 1 & 0 & 0 & 0 & 0 \\ 0 & 1 & 0 & 0 & 0 \\ 0 & 0 & 1 & 0 & 0 \\ 0 & 0 & 0 & 1 & 0 \\ 0 & 0 & 0 & 0 & 0 \end{bmatrix} \begin{bmatrix} \dot{T}_1 \\ \dot{T}_2 \\ \dot{V}_{g1} \\ \dot{V}_{g2} \\ \dot{q}_1 \end{bmatrix} = \begin{bmatrix} f_{T1}(T_1, V_{g1}, q_1) \\ f_{T2}(T_2, V_{g2}, q, q_1) \\ q_1 \\ q - q_1 \\ P_{21}(q_1, T_1, V_{g1}) - P_{22}(q, q_1, T_2, V_{g2}) \end{bmatrix}, \tag{4.9}$$

with input variable q and state variables T_1, T_2, V_{g1}, V_{g2} and q_1. The flow rate q_1 is not truly a state variable, but it is convenient to consider it as such in order to write the four differential equations and the algebraic constraint in a single equation as above.

The matrix on the left of equation (4.9) is often called a mass matrix. This equation is an example of a so-called differential-algebraic equation, as the mass matrix is singular. This singularity is clearly caused by the algebraic constraint.

4.8.5 Implementation in SIMULINK®

As mentioned above, the aim of this research was to develop a mathematical model of the suspension unit, to be used in vehicle dynamic simulations. It was decided earlier to use the ADAMS® program for the vehicle dynamics simulation. A very convenient way to interface a mathematical model like that of the suspension unit as described above with an ADAMS model of a larger system (in this case the vehicle and its suspension system components other than the suspension units) is to implement the mathematical model in the SIMULINK environment. ADAMS can be linked to MATLAB® SIMULINK sub-programs. For this reason the mathematical model was implemented in SIMULINK.

MATLAB provides a solution scheme for differential-algebraic equations and as a consequence SIMULINK has the ability to model algebraic constraints. Solution of the differential-algebraic equation, equation (4.9), using this functionality has been unsuccessful thus far. The mathematical model was however implemented successfully in SIMULINK by, within each time step, first calculating the valve fractions f_i, $i = 1,2,3$, based on the pressure drops over the valves at the end of the previous time step and then enforcing the algebraic constraint using a Newton-Raphson type iteration to find the values of q_1, q_2, P_2 and P_3. After these values have been calculated, T_1, T_2, V_{g1} and V_{g2} are calculated by solving the four first order differential equations contained in equation (4.9). Lastly P_1 and P_4 are calculated using equation (4.3). During the Newton-Raphson type iteration the values of P_1 and P_4 at the end of the previous time step are used. This iteration is performed in a MATLAB s-function that is called by the SIMULINK program. Once P_2 is calculated, the output force of the suspension unit for the current time step may be calculated as $F = -P_2 A$ and the program may move on to the next time step. It should be noted that the friction between the piston and the cylinder walls and the piston rod and its bushing is neglected in the calculation of F.

4.8.6 Validation of the mathematical model

The model of the suspension unit has been validated by comparing its predicted force output with forces measured on the Prototype 2 unit in a SCHENCK Hydropulse hydrodynamic testing machine under displacement control.

During testing on the hydrodynamic testing machine, the displacement feedback signal and resulting force as measured with a load cell were recorded. In addition to these two signals, the signals from the four pressure transducers measuring pressures P_1 to P_4 and the electric command signals for switching the valves were also recorded. All these signals were filtered to prevent aliasing, digitised and stored on disc.

Comparing the load cell force and the pressure P_2 measurements clearly showed that the error made in the model by neglecting the friction on the sliding parts of the unit and taking the output force of the unit as $-P_2A$, is not insignificant but generally quite small. There is a second reason, other than friction, for the difference between the load cell force and $-P_2A$, especially in situations of oscillation at high frequency. During vehicle simulation, the inertial properties of the piston and piston rod should be combined with those of the unsprung mass, so that the associated dynamic effects are taken into account by the ADAMS model, rather than the SIMULINK model. The output of the SIMULINK model should therefore be the suspension unit output force before the inertial effect of the piston and piston rod has been taken into account. The load cell, however, measures the suspension unit net output force after accelerating this mass. It is therefore prudent, in the comparison of the mathematical model with the measured results, to compare the output of the model in terms of measured and calculated $-P_2A$ values. In the discussion that follows all reference to measured force should be understood to mean force calculated from the measured pressure P_2 and thus neglects friction.

Since the mathematical model does not accept a displacement time history as input, but rather the extensional speed time history, the measured displacement signal first had to be differentiated with respect to time. It was always possible to bring the displacement signal back to its initial value at the end of a test run. The differentiation was therefore performed by transforming the whole displacement time history of a test run to the frequency domain using a Fast Fourier Transform (FFT), then multiplying the resultant double sided complex spectrum with $j\omega$, setting all values corresponding to frequencies above a chosen low pass filter cut-off frequency and below the negative of this cut-off frequency to zero and lastly back transforming the signal to the time domain using the inverse FFT. (In this $j=\sqrt{-1}$ and ω is the circular frequency.) This procedure not only performs the differentiation but also realizes a low pass filter with very sharp cut-off properties and no magnitude and phase distortion below the cut-off frequency. During vehicle simulation this differentiation of the displacement is not required, since the ADAMS model directly calculates the required speeds.

To first test the spring properties without the influence of the dampers the suspension unit was cycled through a triangular wave displacement at low speed, as indicated in Figure 4.36. This figure also shows the output force of the suspension unit, as calculated from the measured pressure P_2, for the case of stiff spring and low damping properties. Figure 4.37 shows the comparison between the measured and SIMULINK calculated time histories for this case, for the pressure in the active accumulator, P_1, and the main strut, P_2. Even though the nominal gas volume of accumulator 1 at the static wheel load was designed to be 0.1 litres, during this simulation it was adjusted to 0.135 litres, in order to obtain what was considered an acceptable correlation between the measured and calculated results. This adjustment is to some extent justified due to the fact that the volume calculation during design did not take into account some small cavities and screw thread inside the accumulator, and it was also determined that it is rather difficult to fill the suspension unit with oil without trapping small pockets of air inside the unit. The volume of accumulator 1 could have been adjusted to an even higher value, to get an even closer correlation between the measured and calculated results at the peak at 100 seconds in Figure 4.37, but there also was evidence that valve 3 was prone to leak at a high

pressure differential, which may have caused a reduced pressure during the measurement. The force-displacement graph obtained during the test that produced Figure 4.37 is shown in Figure 4.38, once again comparing the measured and calculated results. This test was repeated with a high damping setting and essentially the same results were obtained, as expected, since the very slow speed renders very small damping.

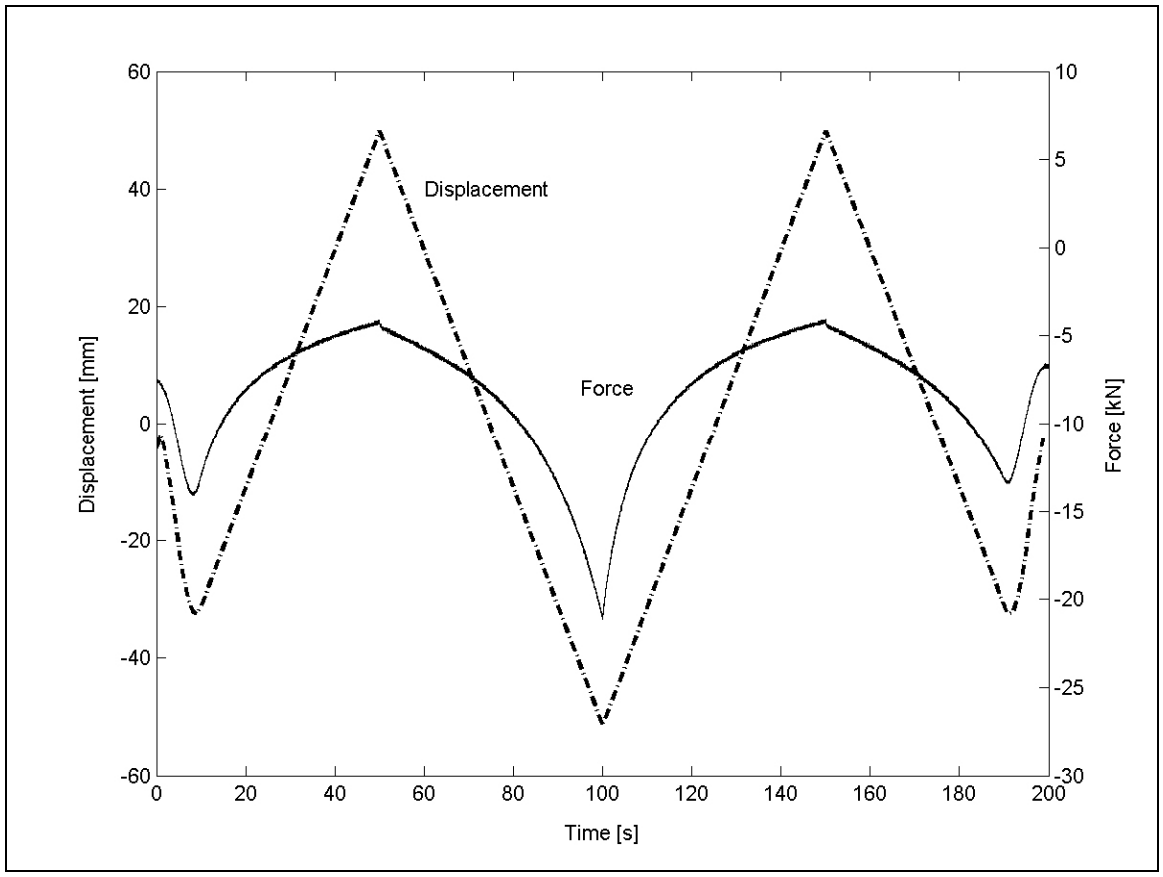

Figure 4.36 – Measured input and output: stiff spring and low damping at low speed

Next a similar test was conducted but at considerably higher speeds, to generate a significant damping effect. The input displacement and output force for a stiff spring and low damping setting is shown in Figure 4.39. The comparison between the measured and calculated time histories for this case, for P_1 and P_2, are shown in Figure 4.40 and the force-displacement graph obtained during this test in Figure 4.41. The correlation between measurement and calculation displayed in Figure 4.40 is generally good, except at the high-pressure peaks. The calculated force-displacement graph shows an interesting figure eight shape, which was not observed in the measurement nor any other simulation result. When evaluating the force-displacement graphs generated by the simulation, one needs to bear in mind that the model does not yet provide for hysteresis in the damping properties. This may account for the strange curve calculated and displayed in Figure 4.41.

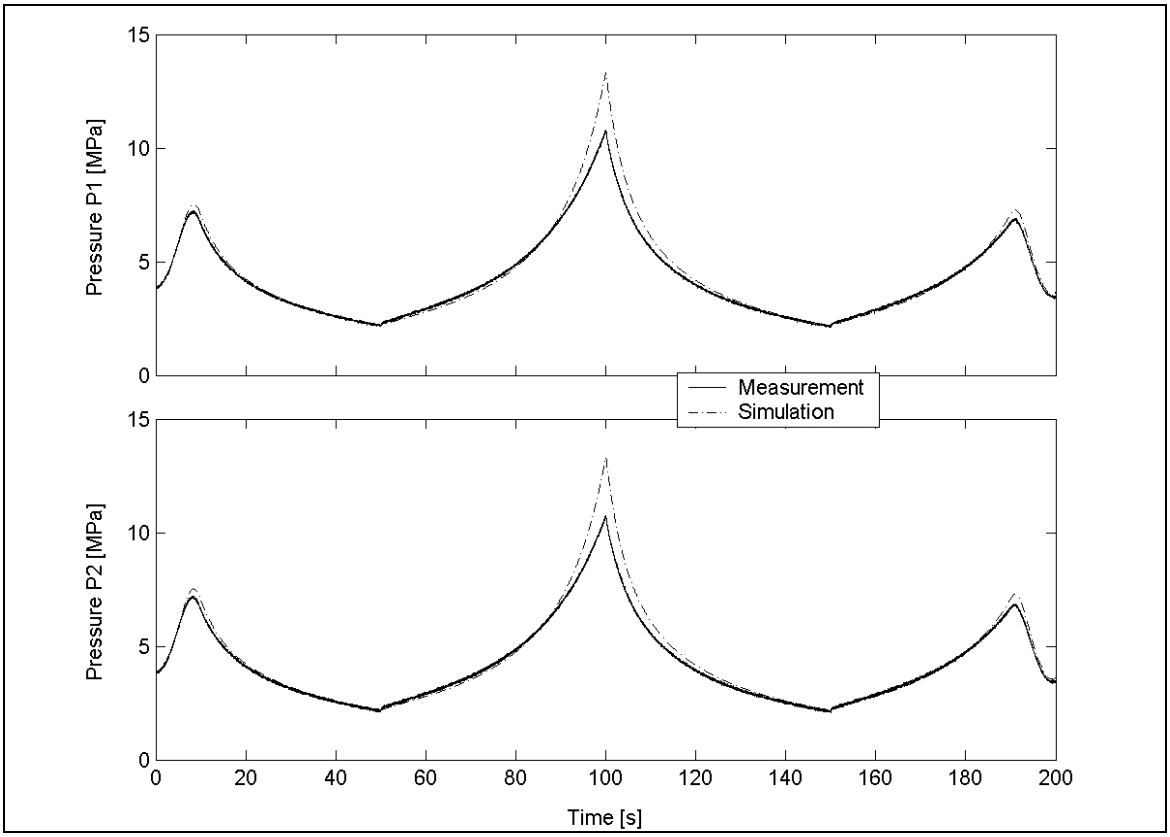

Figure 4.37 – Comparison between measured and calculated values of P_1 and P_2: stiff spring and low damping at low speed

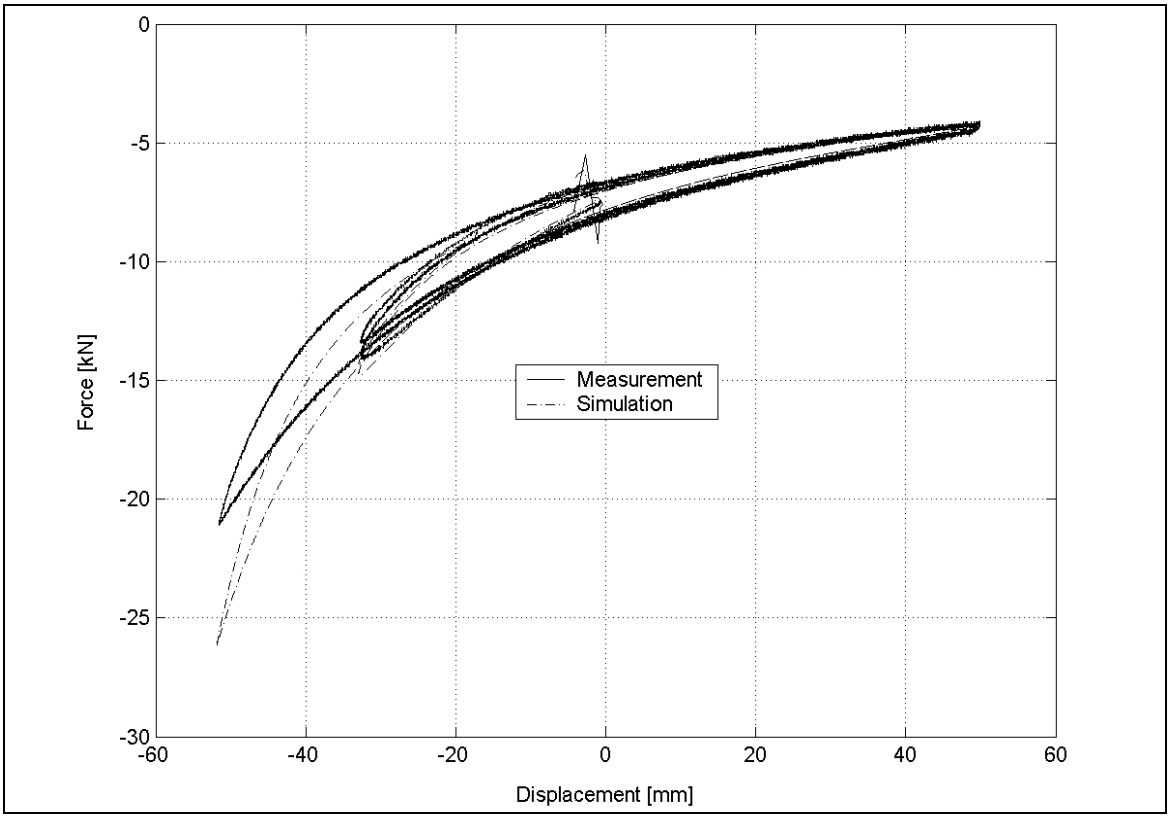

Figure 4.38 – Comparison between measured and calculated force-displacement curve: stiff spring and low damping at low speed

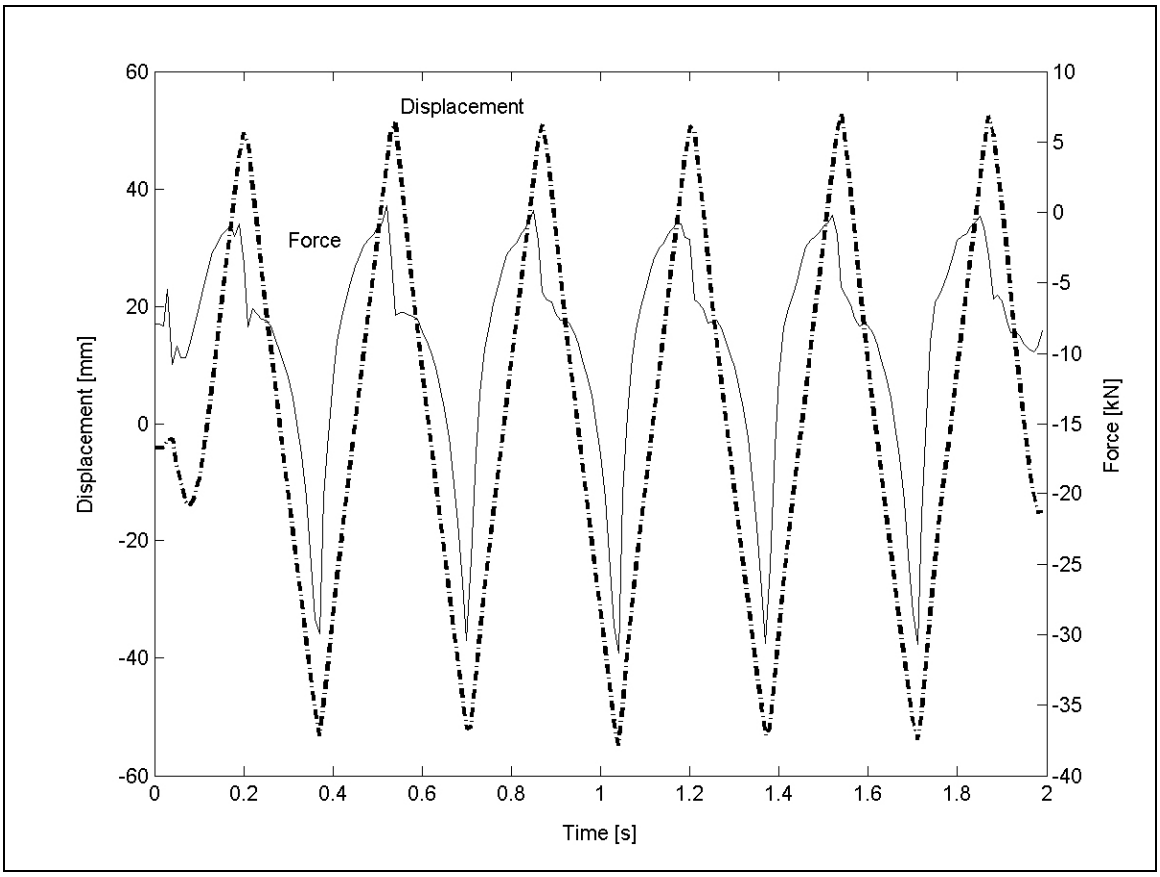

Figure 4.39 – Measured input and output: stiff spring and low damping at high speed

A third stiff spring low damping test was performed at a slightly lower speed but a higher displacement stroke, as indicated in Figure 4.42. The comparison between the measured and calculated time histories for this case, for P_1 and P_2, are shown in Figure 4.43 and the force-displacement graph obtained during this test in Figure 4.44. The simulation indeed indicated significantly higher pressures to accompany the higher displacement input, but the measured pressures failed to reach the high values as expected. The clear kink in the measured force-displacement graph in Figure 4.44 near –50 mm displacement is seen as a clear indication of leakage, at high differential pressure, through valve 3.

Next the same kind of test as shown in Figure 4.39 was performed, only now with high damping (i.e., high stiffness and high damping, triangular displacement excitation at high speed). The input displacement and measured force time histories are shown in Figure 4.45. It is clear that the output force is clipped at about zero Newton, and the reason for this is that the pressure cannot drop very far below zero Pascal (atmospheric pressure) because at lower pressures the oil starts to boil preventing further pressure drop. In any case, the pressure cannot drop below zero absolute, which would correspond to a positive output force of merely 196 N. The time histories of the pressures P_1 and P_2 are shown in Figure 4.46. The SIMULINK model has been constructed such that pressure P_2 will only drop to zero. It is seen that while P_2 is dropping, the model follows the measurement quite well into the saturation at zero. The model, however, recovers from this more quickly that the actual physical unit. This causes the calculated pressure to start rising significantly earlier on the compression stroke than the measured pressure. After a

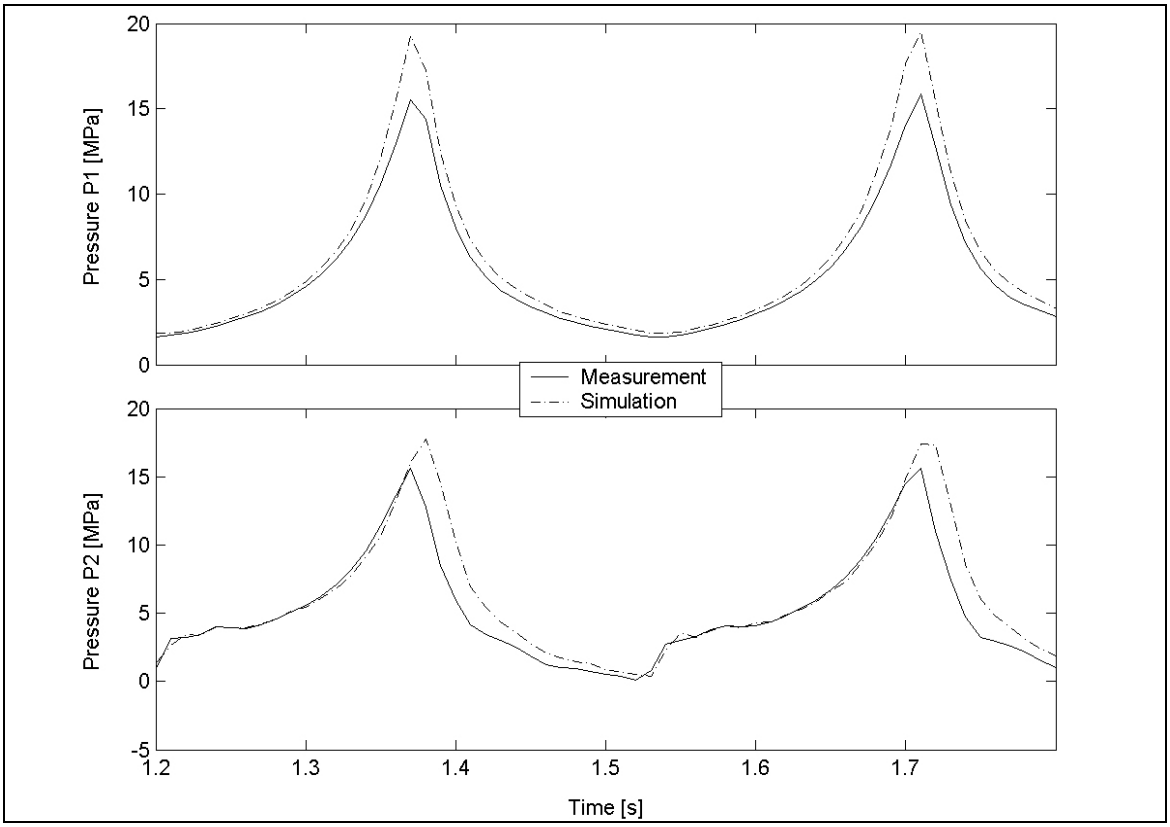

Figure 4.40 – Comparison between measured and calculated values of P_1 and P_2: stiff spring and low damping at high speed

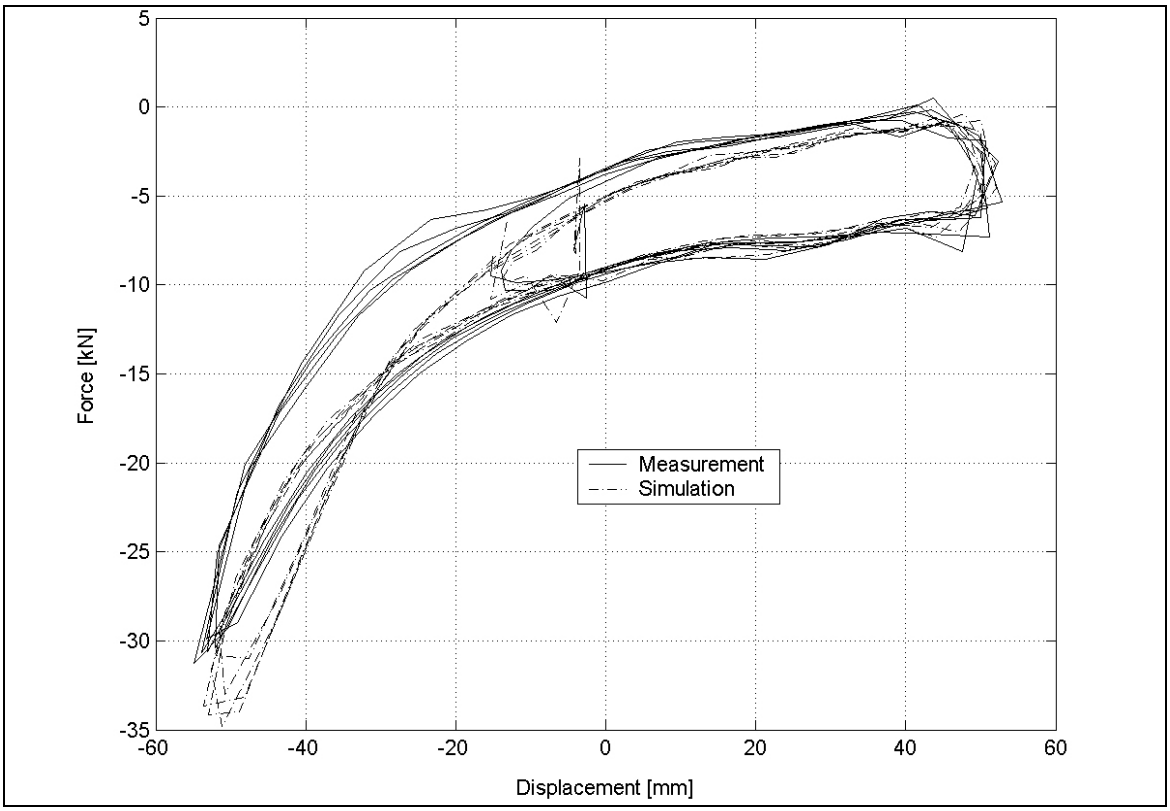

Figure 4.41 – Comparison between measured and calculated force-displacement curve: stiff spring and low damping at high speed

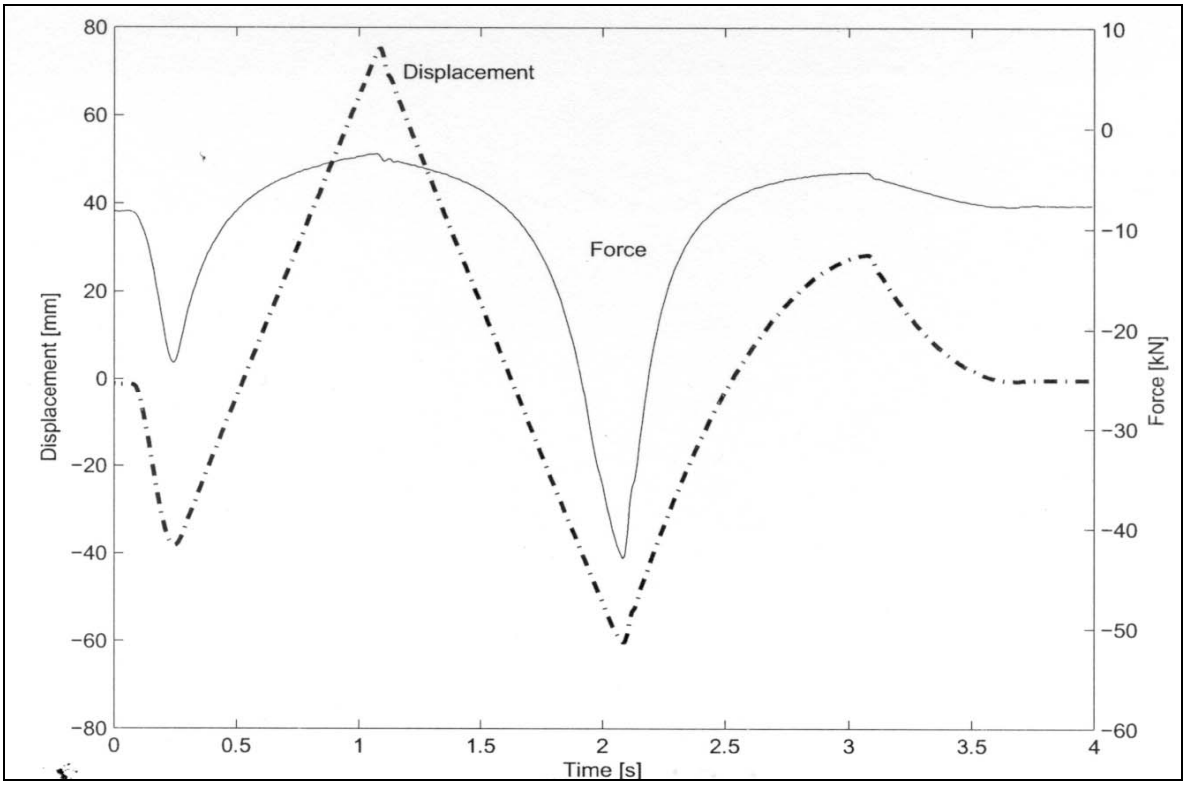

Figure 4.42 – Measured input and output: stiff spring and low damping at high speed, larger displacement stroke

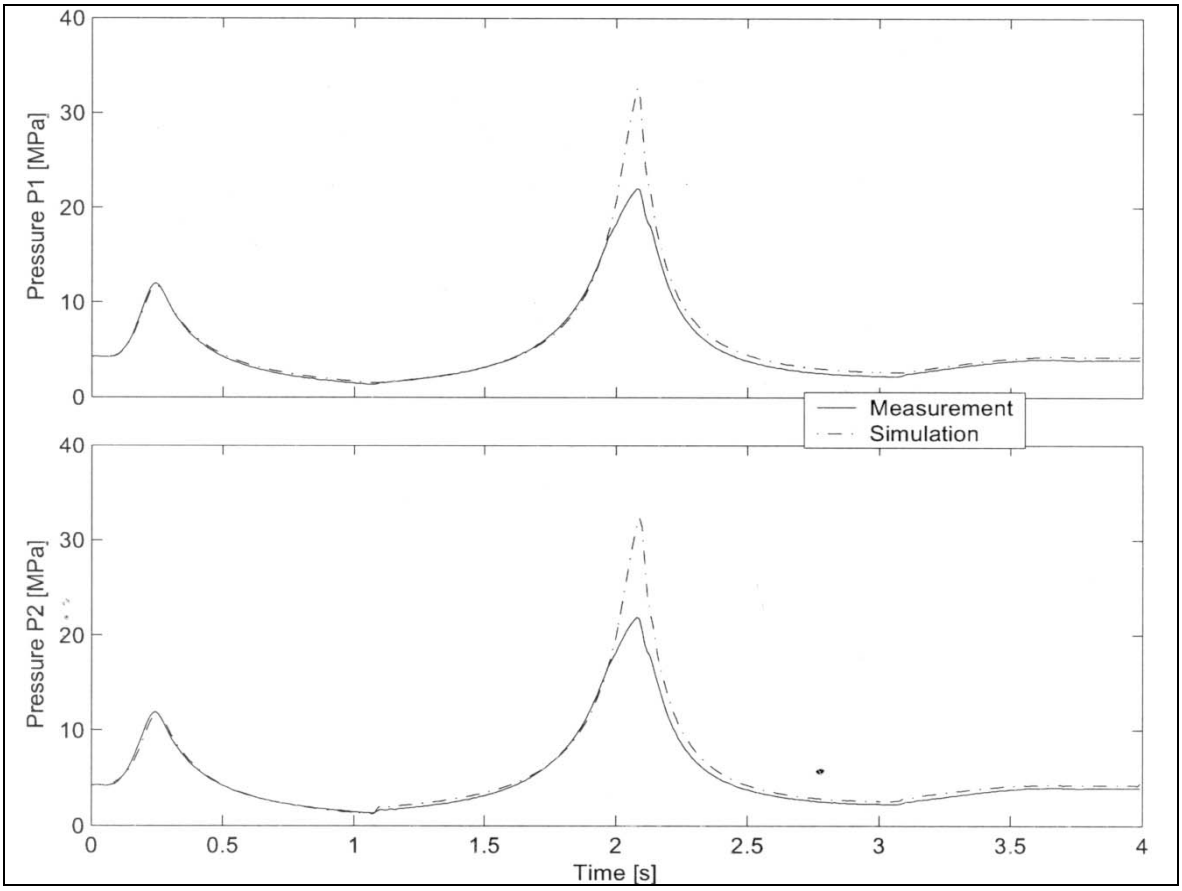

Figure 4.43 – Comparison between measured and calculated values of P_1 and P_2: stiff spring and low damping at high speed, larger displacement stroke

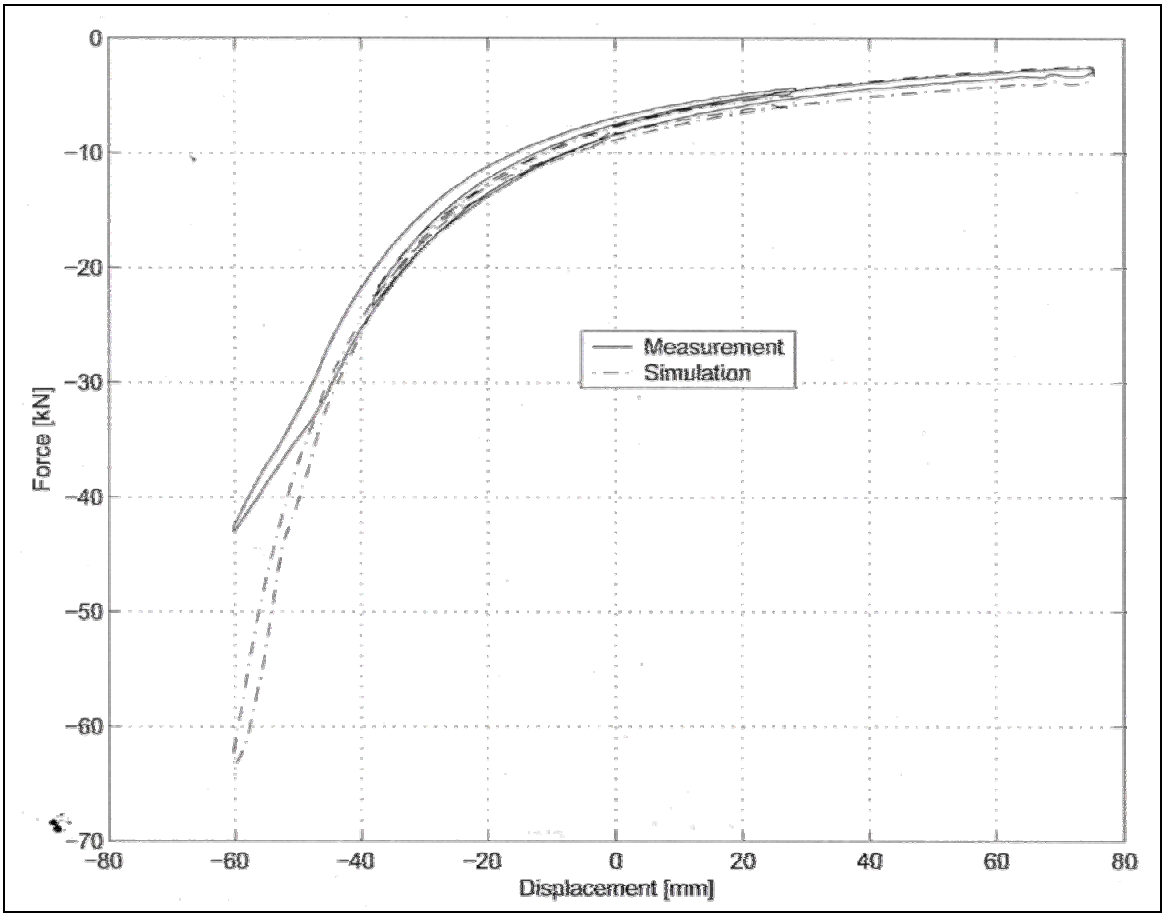

Figure 4.44 – Comparison between measured and calculated force-displacement curve: stiff spring and low damping at high speed, larger displacement stroke

delay, the calculation and the measurement meet up again with good correlation until this is repeated in the next cycle. One possible explanation for this delay is that in the physical unit some boiling of the oil at low pressure occurs, a phenomenon that is not provided for in the SIMULINK model. Oil vapour caused by boiling and suspended in the oil is expected to cause a delay in pressure rise on compression. In this case, during the low-pressure part of the P_1 cycle, the correlation between simulation and measurement is not as good as observed in the results discussed earlier. This may be related to the suspected boiling of the oil. The poor correlation in both the P_1 and P_2 results is not of serious concern, as the situation where the suspension unit is subjected to a prescribed high speed rebound that can cause P_2 to drop to zero, even though easy to create on a test bench, is highly unlikely with the unit installed in a vehicle, even under rough road conditions. There is simply no downwards pull on the wheel available to cause such a condition. The force-displacement graph generated for this test is shown in Figure 4.47.

Whereas all the results discussed above pertain to stiff spring scenarios, with valve 3 closed, the more complicated part of the model corresponds to the soft spring scenario. Figure 4.48 shows input displacement and output force measured for a soft spring and low damping case, at low speed. Figure 4.49 shows the comparison of the measured and calculated time histories of the two accumulator pressures P_1 and P_4, while Figure 4.50 shows the same for the pressures P_2 and P_3. The force-displacement curve is shown in

Figure 4.51. In this case the gas volumes of accumulator 1 and 2 during the simulation were taken as 0.135 and 0.4 litres, respectively. Correlation is generally acceptable.

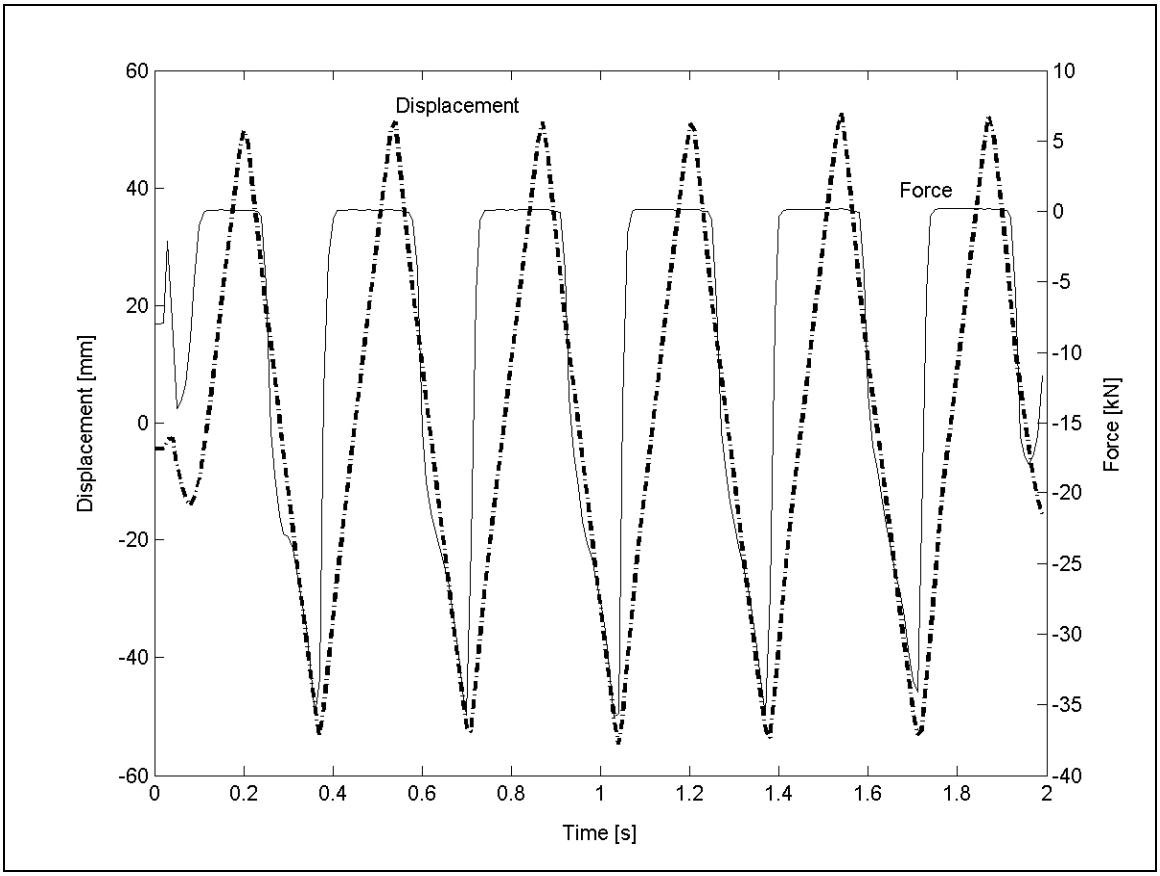

Figure 4.45 – Measured input and output: stiff spring and high damping at high speed

Next the above test was repeated at high speed, the displacement input and measured force output shown in Figure 4.52. The comparison of the measured and calculated time histories of P_1 and P_4 for this case is shown in Figure 4.53 and that of P_2 and P_3 in Figure 4.54, with the force-displacement curve in Figure 4.55. Once again the correlation is generally acceptable.

Lastly, a test was performed on the suspension unit wherein it was compressed some distance in the stiff spring mode, then kept at this displacement for a while, after which valve 3 was opened and the pressures in the system allowed to equalize. Valve 3 was then closed again and the unit was then further compressed. This was repeated twice after which the unit was extended in a similar stepwise manner. This procedure, referred to herein as the incremental compression test, is well illustrated in Figure 4.56, which shows the time histories of the input displacement, the measured output force and the switch signal for valve 3. The switch signal is not plotted against a specific scale; it merely indicates when the valve is open (high) or closed (low). This whole test was conducted with a low damping setting. The measured and calculated time histories of the pressure in the two accumulators are shown in Figure 4.57, while the time histories of P_2 and P_3 are shown in Figure 4.58. In this case the gas volumes of accumulator 1 and 2 during the simulation were taken as 0.111 and 0.4 litres, respectively. The change in the volume of accumulator 1 may be justified by the fact that the suspension unit was emptied of both gas and oil, and then refilled, between this test and the test described earlier. With these

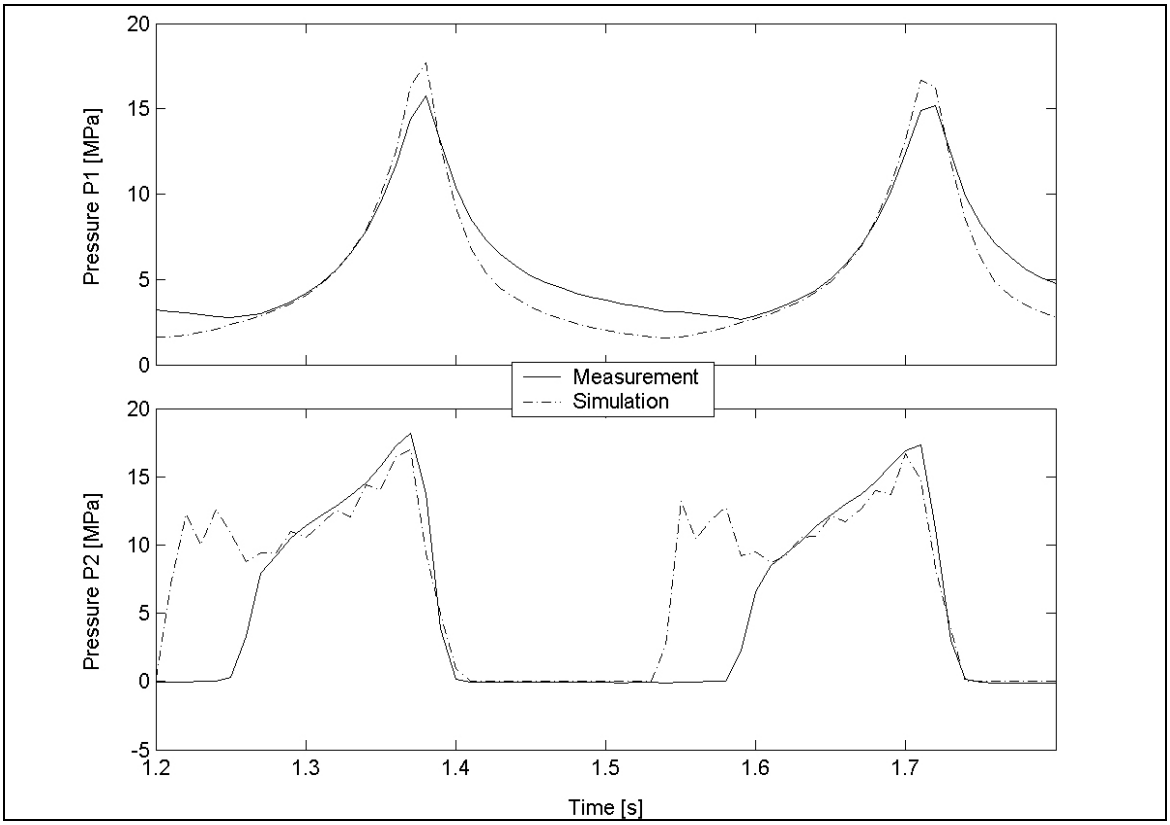

Figure 4.46 - Comparison between measured and calculated values of P_1 and P_2: stiff spring and high damping at high speed

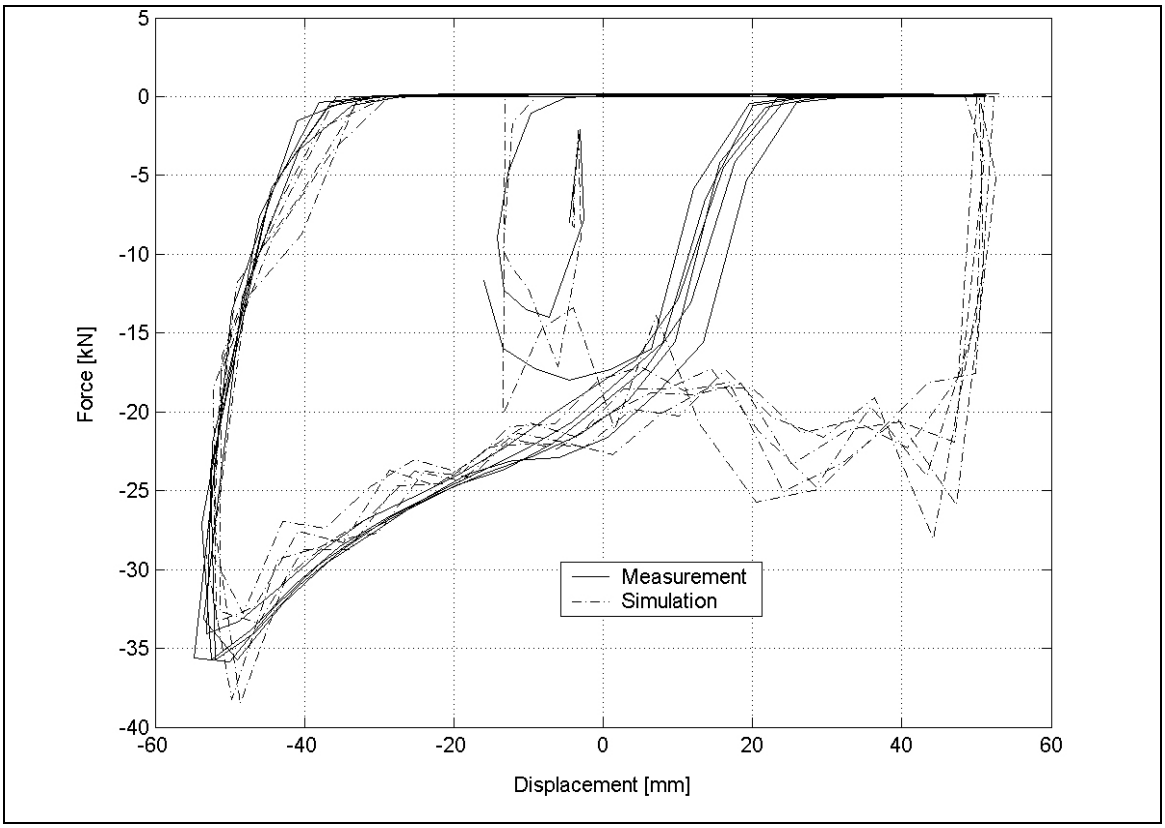

Figure 4.47 – Comparison between measured and calculated force-displacement curve: stiff spring and high damping at high speed

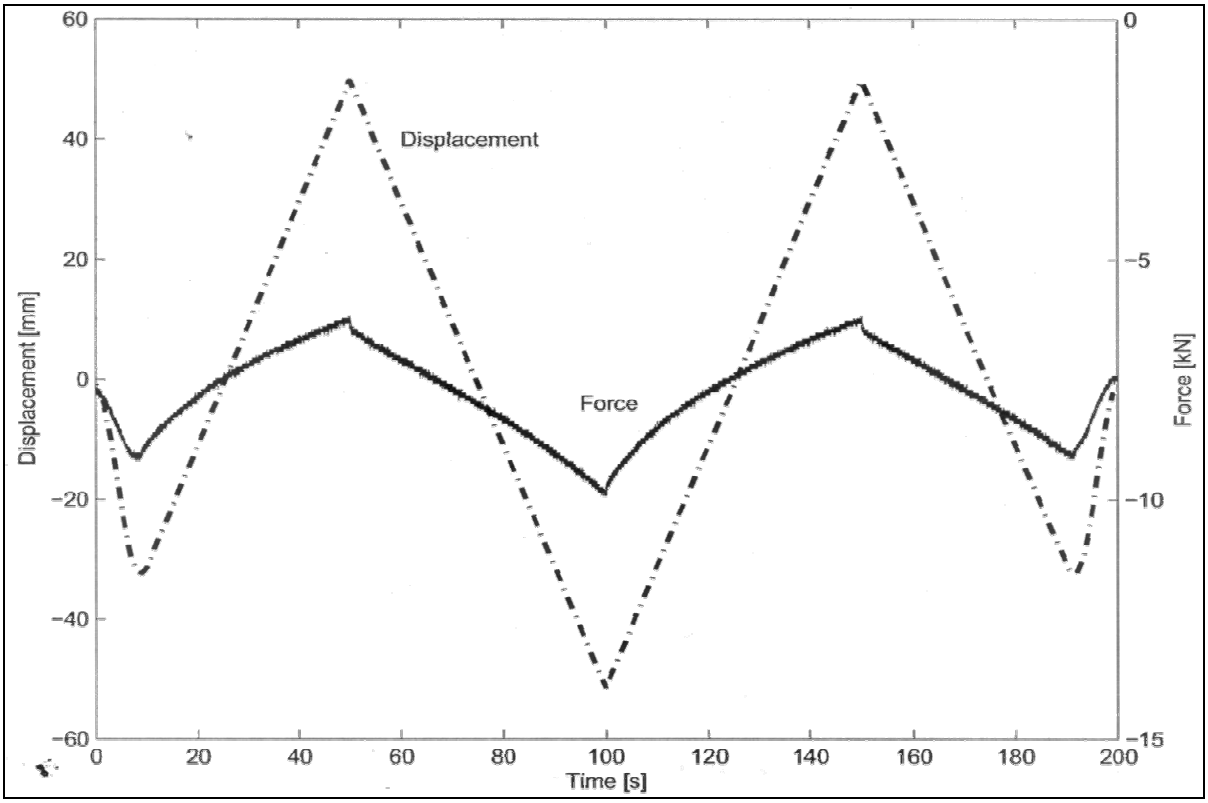

Figure 4.48 - Measured input and output: soft spring and low damping at low speed

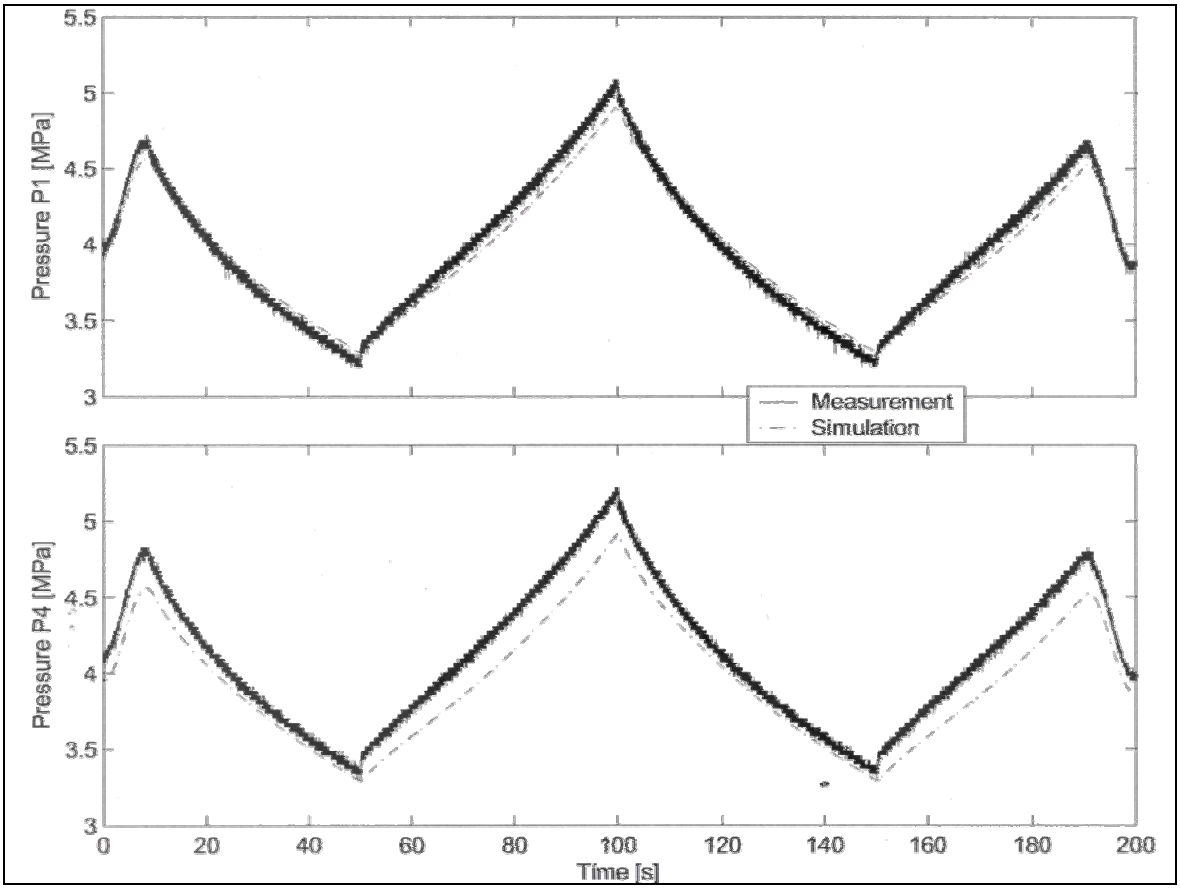

Figure 4.49 – Comparison between measured and calculated values of P_1 and P_4: soft spring and damping at low speed

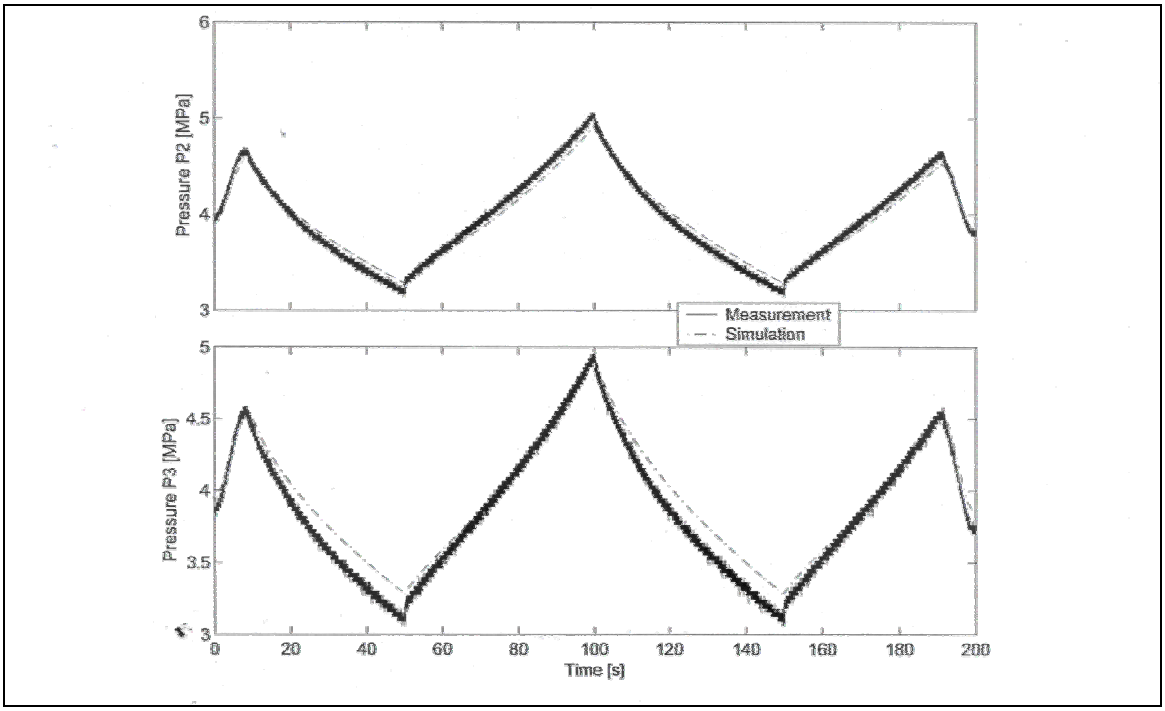

Figure 4.50 – Comparison between measured and calculated values of P_2 and P_3: soft spring and low damping at low speed

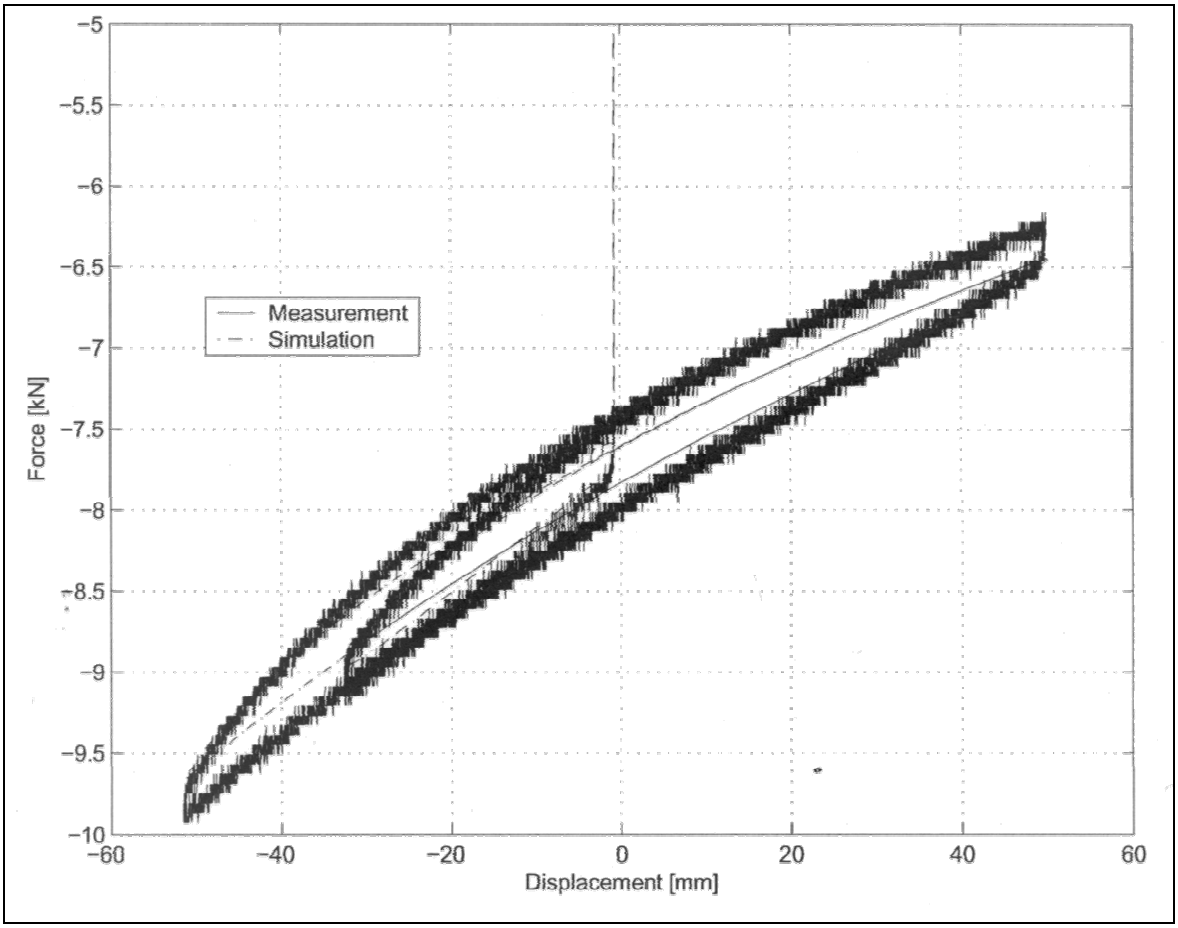

Figure 4.51 - Comparison between measured and calculated force-displacement curve: soft spring and low damping at low speed

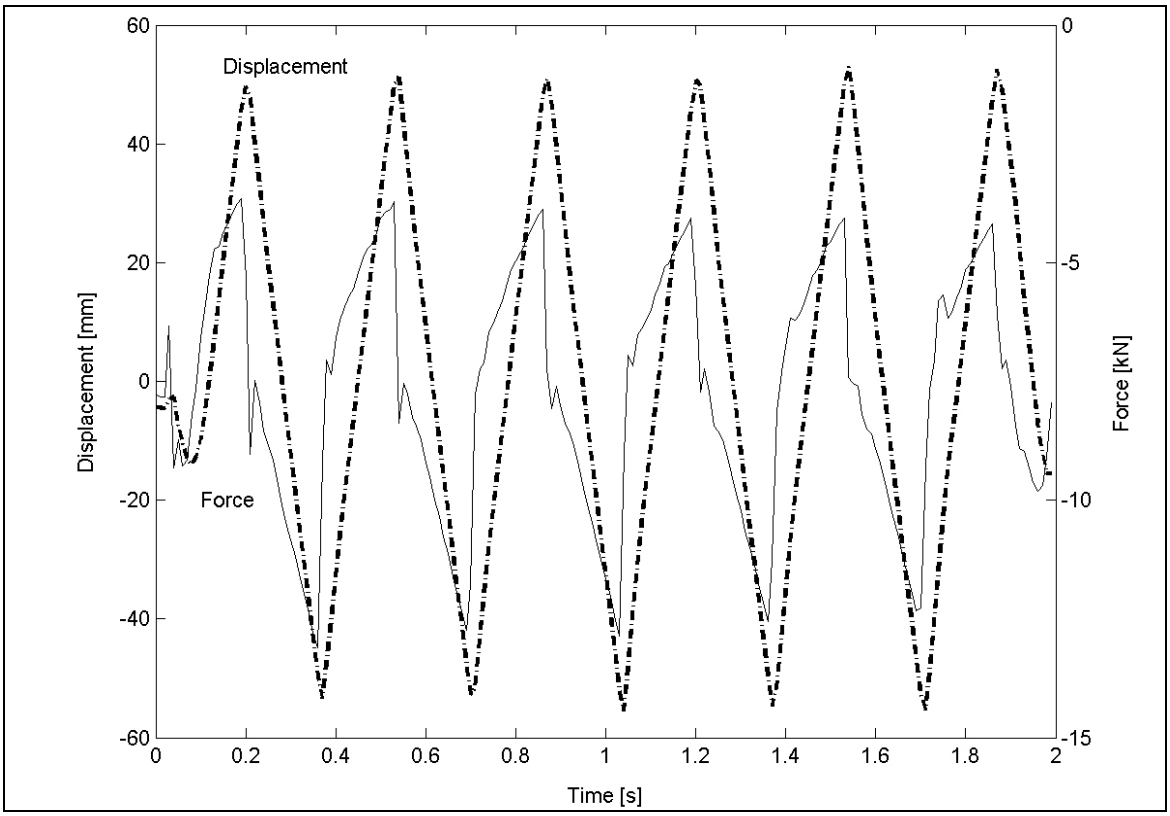

Figure 4.52 - Measured input and output: soft spring and low damping at high speed

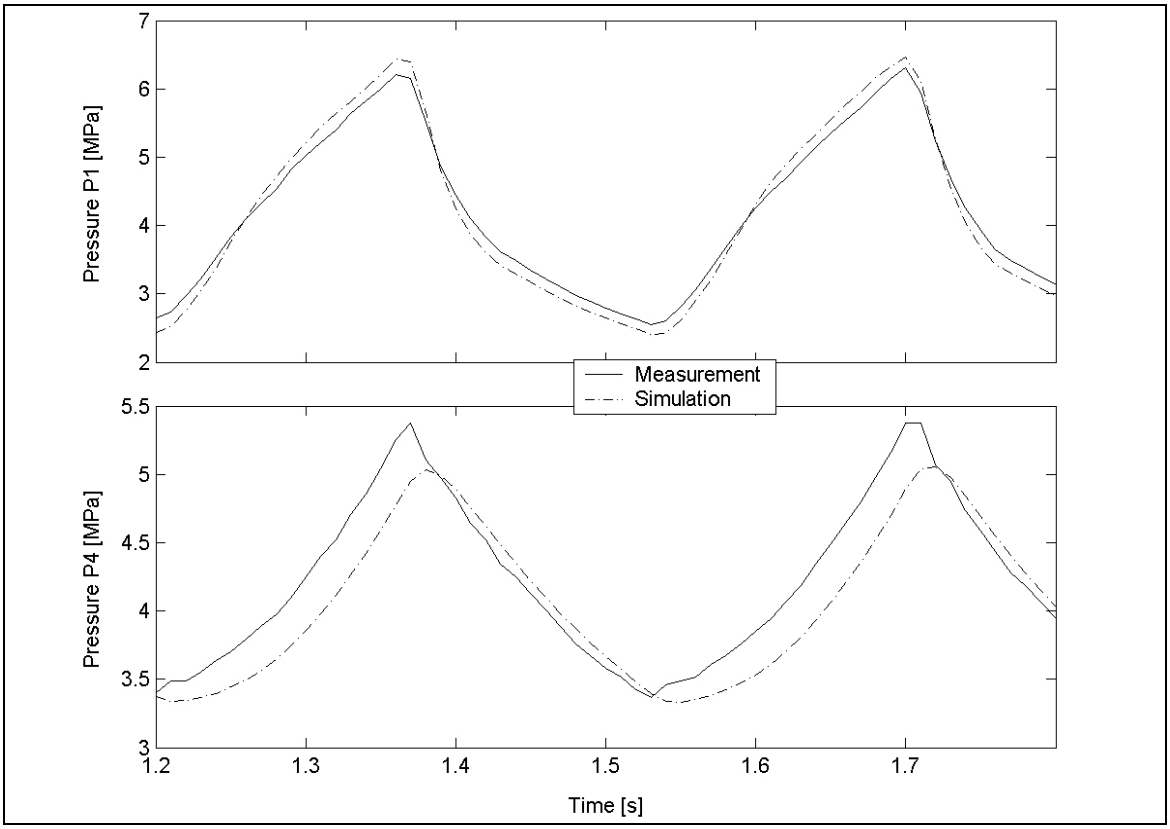

Figure 4.53 – Comparison between measured and calculated values of P_1 and P_4: soft spring and low damping at high speed

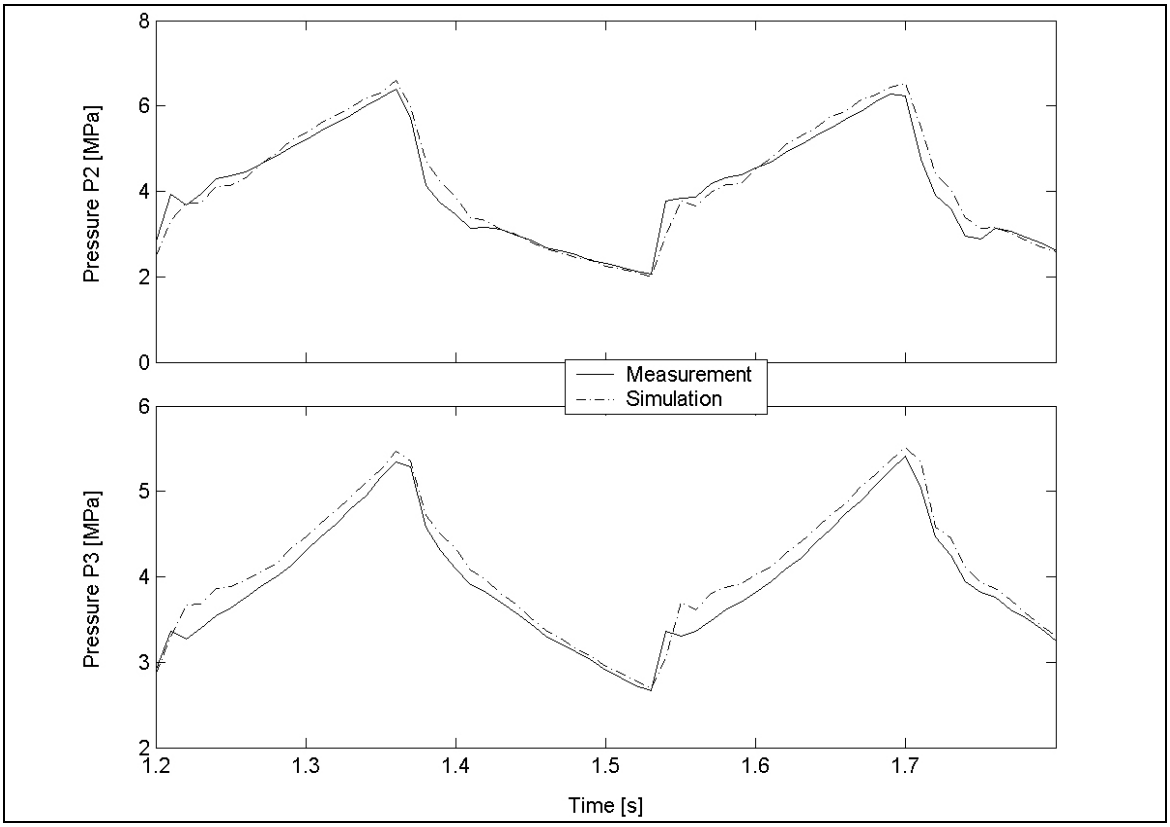

Figure 4.54 – Comparison between measured and calculated values of P_2 and P_3: soft spring and low damping at high speed

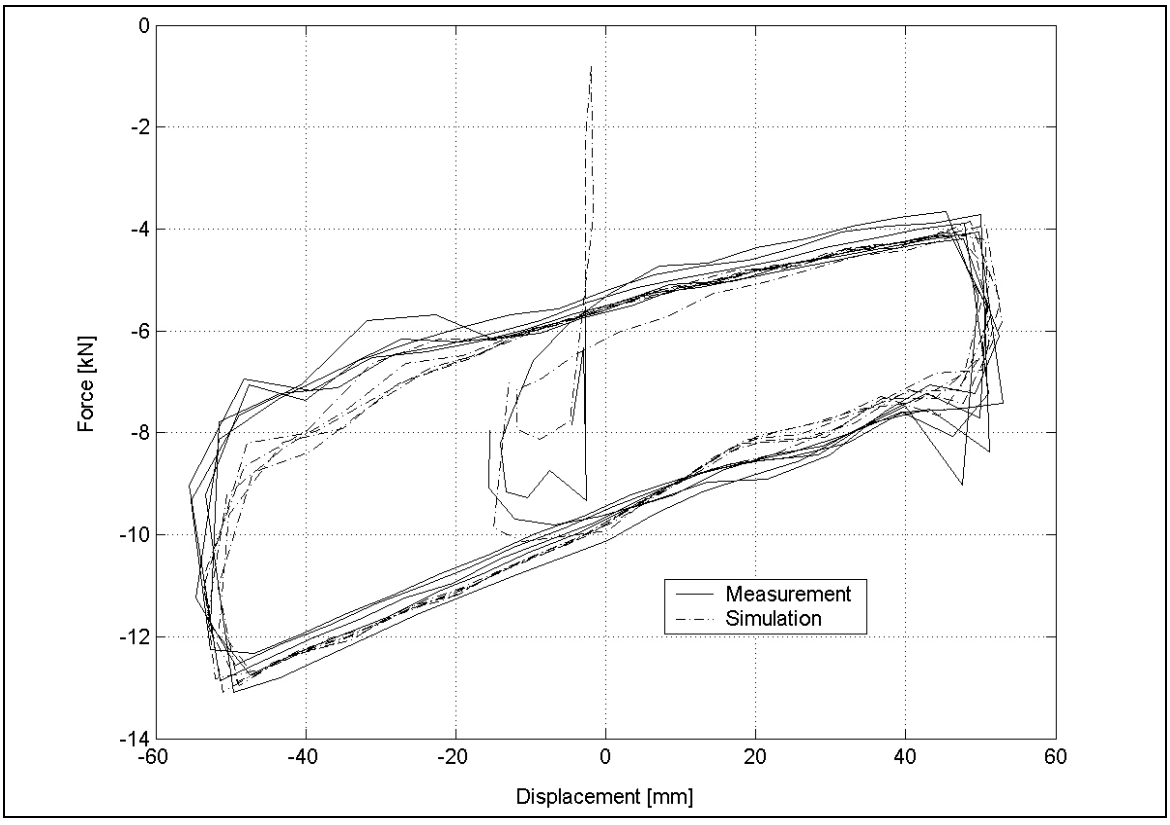

Figure 4.55 – Comparison between measured and calculated force-displacement curve: soft spring and low damping at high speed

settings, the only correlation that does not seem good is that between the measured and calculated time histories of P_4. It should however be realized that while valve 3 is closed, P_3 and P_4 should practically be identical, as there is no flow through damper 2 or its by-pass valve. If the measured values of P_4 and P_3 from Figures 4.49 and 4.50 are compared, during the first second, when valve 3 is indeed closed, it is seen that the P_4 pressure transducer reads a pressure slightly higher that the P_3 transducer, by the same amount as the difference in the measured and calculated P_4 values in Figure 4.57. If based on this observation it is assumed that an offset was present in the P_4 measurement, the correlation between the measurement and the simulation result may be considered as very good. The measured and calculated force-displacement graphs for this test are shown in Figure 4.59. This figure also shows a very good correlation between measurement and simulation.

It is also worth noting that the slow drop in pressure P_1 right after achieving the local peaks at the end of the compression strokes in Figure 4.57, just before valve 3 is opened, is predicted quite well by the model. Since the displacement input does not vary in this period, it is evident that the cooling of gas in accumulator 1 causes this pressure drop. This effect is captured adequately in the model by the use of equation (4.4).

Since the displacement of the suspension unit is not taken as an input in the mathematical model, it is necessary to check that the displacement of the unit that would be mandated by the solution of the differential equations like equation (4.2) does in fact correspond to the actual displacement experienced by the unit. During all the tests described in this section this was in fact checked and the correlation was exceptionally good. At this time it is proposed that a similar check should be incorporated in an implementation of the SIMULINK model within an ADAMS simulation of vehicle dynamics.

To date no measurement was done to specifically validate the way that the pressure dependent valve switching was implemented in the mathematical model.

4.9 Conclusion

A prototype four-state semi-active hydropneumatic spring-damper system ($4S_4$) has been designed, manufactured, characterised on a test rig and modelled mathematically.

The design meets all the initial specifications and can be fitted to the proposed test vehicle without major modifications to the test vehicle.

The manufactured prototypes (Prototypes 1 and 2) have been extensively tested and characterised on a SCHENCK hydropulse actuator. Although several problems have been identified on Prototype 1, these have been adressed and eliminated on Prototype 2. Prototype 2 meets all the dynamic requirements.

A mathematical model of the suspension unit was developed and implemented in SIMULINK. Agreement between the model predictions and the measurements was generally good. Some aspects where the model or the quantifying of its parameters need improvement were identified. In particular, the tests to date clearly identified the need for an accurate method of quantifying the mass of gas loaded into the two accumulators.

Further work will be done on testing the model within simulations of a full vehicle equipped with these suspension units.

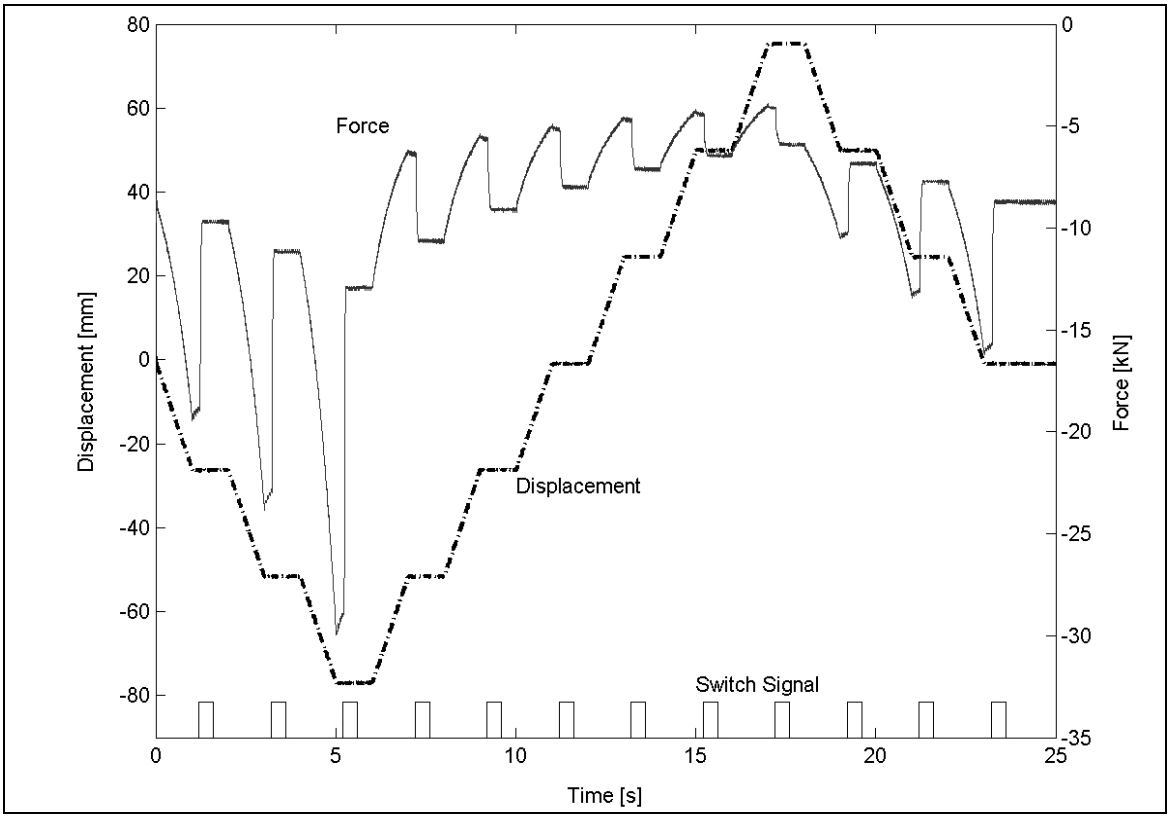

Figure 4.56 – Measured input and output, and valve 3 switch signal: incremental compression test with low damping

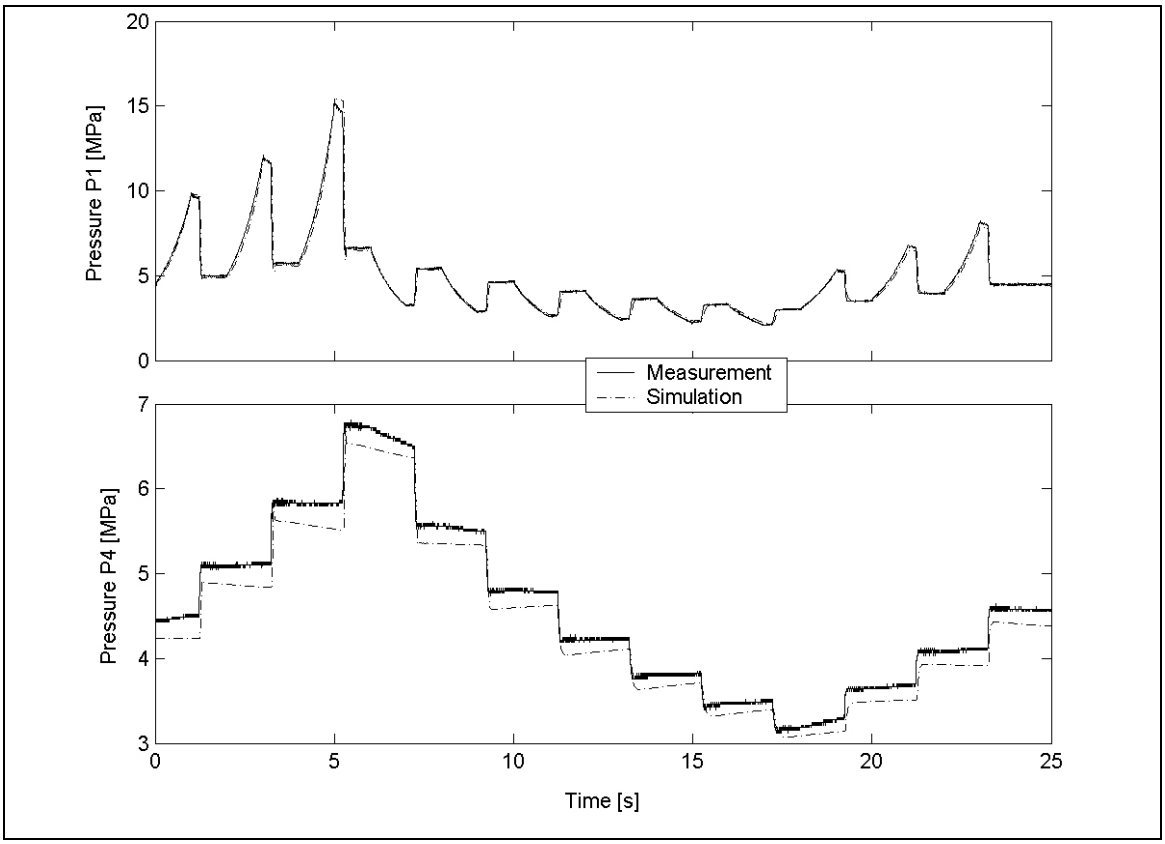

Figure 4.57 – Comparison between measured and calculated values of P_1 and P_4: incremental compression test with low damping

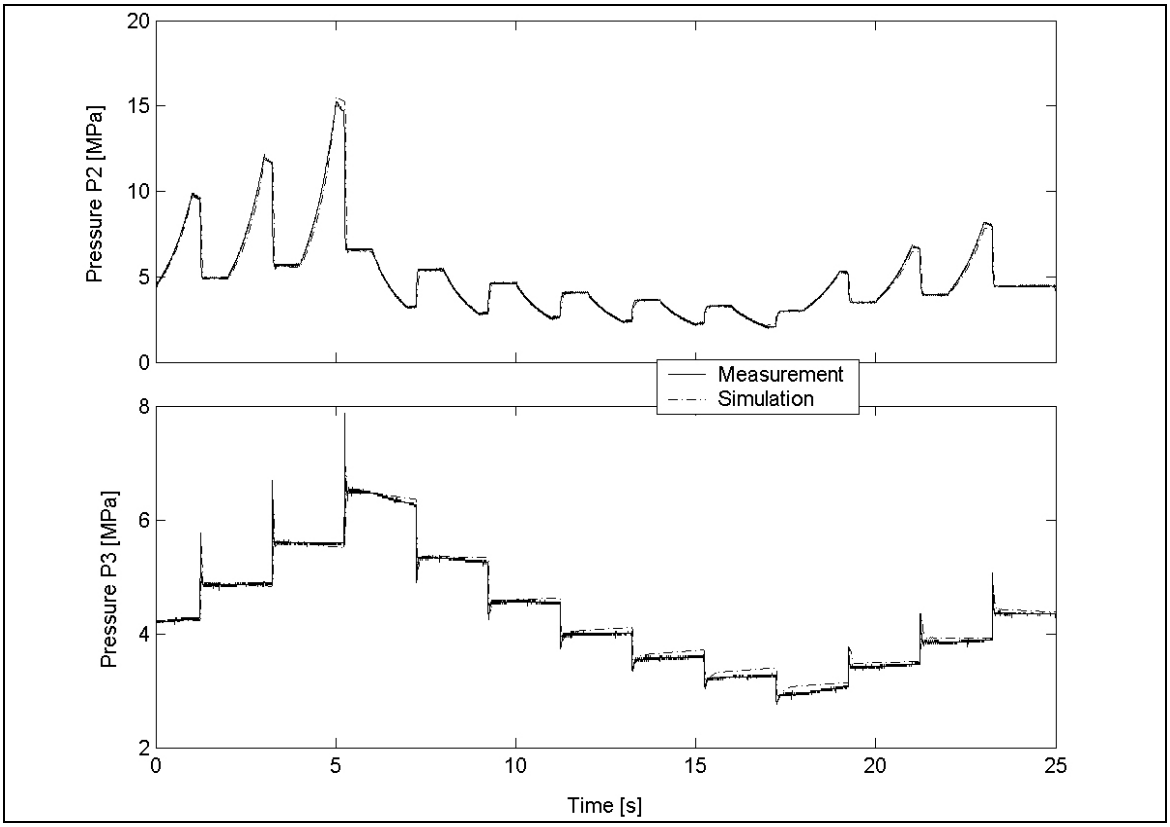

Figure 4.58 – Comparison between measured and calculated values of P_2 and P_3: incremental compression test with low damping

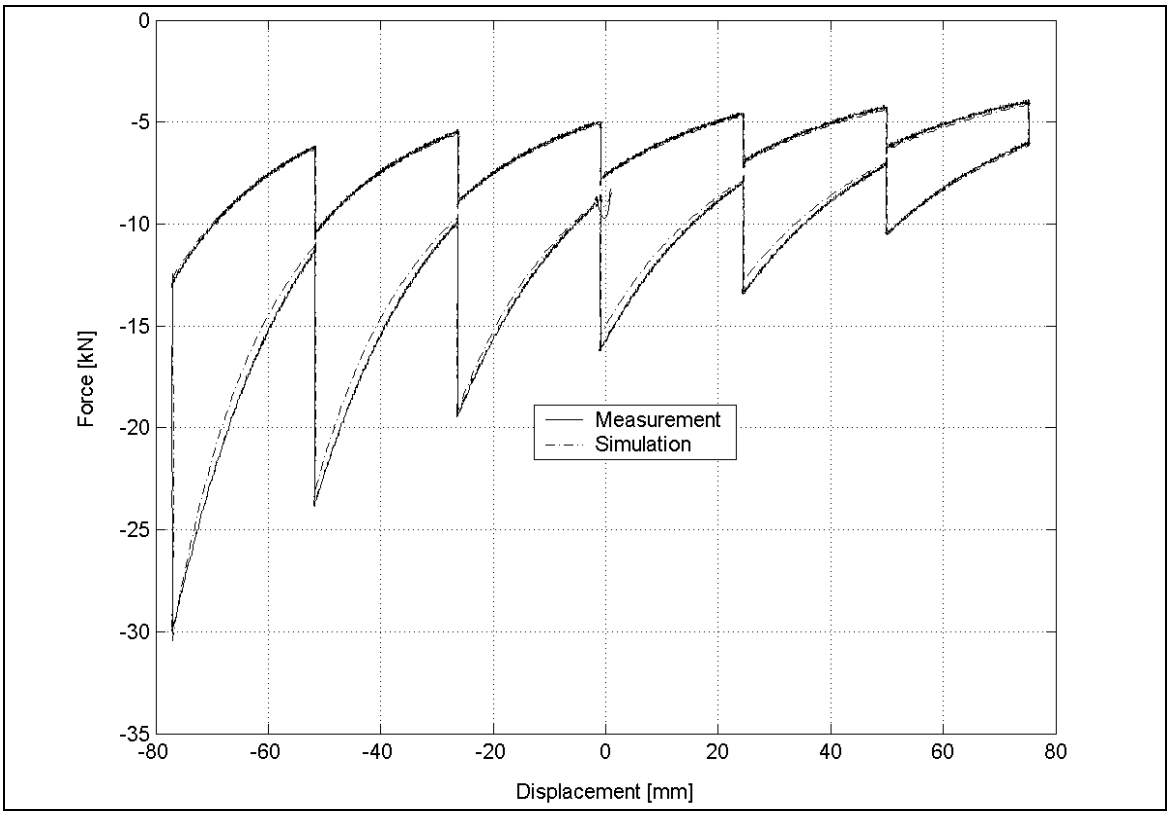

Figure 4.59 – Comparison between measured and calculated force-displacement curve: incremental compression test